THE COAGULATION OF WASTEWATER USING BIOWASTE MATERIALS AS COAGULANTS

Submitted in fulfilment of the requirements for the degree of:

Master of Engineering in the Department of Chemical Engineering,

Green Engineering Research Group,

Faculty of Engineering

and the Built Environment

at Durban University of Technology

Londiwe Zikhona Ngomane

Supervisors: Dr Thembisile Patience Mahlangu

Dr Emmanuel Kweinor Tetteh

Prof. Sudesh Rathilal

Date: November 2024

Preface

This research was conducted under the supervision of Dr Thembisile Patience Mahlangu, Dr Emmanuel Kweinor Tetteh, and Prof. Sudesh Rathilal under the Green Engineering research group at Durban University of Technology, Chemical Engineering Department. The experiments were analyzed in the Chemical Engineering Department of the Faculty of Engineering and the Built Environment at DUT.

Declaration

I, Londiwe Zikhona Ngomane the undersigned candidate declares that

i. The research reported in this dissertation, except where otherwise indicated, is my original work.

ii. This dissertation has not been submitted for any degree or examination at any other university.

iii. This dissertation does not contain other persons' data, pictures, graphs or other information, unless specifically acknowledged as being sourced from other persons.

iv. This dissertation does not contain other persons' writing, unless specifically acknowledged as being sourced from other researchers. Where other written sources have been quoted, then:

a) their words have been re-written, but the general information attributed to them has been referenced;

b) where their exact words have been used, their writing has been placed inside quotation marks, and referenced.

v. Where I have reproduced a publication of which I am an author, co-author or editor, I have indicated in detail which part of the publication was actually written by myself alone and have fully referenced such publications.

vi. This dissertation does not contain text, graphics or tables copied and pasted from the Internet, unless specifically acknowledged, and the source being detailed in the dissertation and in the References sections.

Londiwe Zikhona Ngomane Signature: Date …15/11/2024…

Dr Thembisile Patience Mahlangu Signature: Date: 26 February 2025

Dr Emmanuel Kweinor Tetteh Signature: Date: ……

Prof. Sudesh Rathilal Signature Date: 28 February 2025

Acknowledgements

Praise to the most high God, my Lord and Saviour Jesus Christ. His grace, mercy, and guidance has led me through this journey. I would also like to thank my supervisor, Dr T.P Mahlangu, whose mentorship, encouragement, support and guidance have been unmatched throughout my master's project. I would also like to thank my co-supervisor, Dr E.K Tetteh, for the support, guidance and many opportunities that not only helped me grow academically but also as a person. I would also like to express my gratitude to my co-supervisor, Prof S Rathilal, for all the guidance, motivation and support. I would not have been able to complete my work without my supervisors and for that, I am eternally grateful.

I would also like to acknowledge and thank the Green Engineering Research Group (GERG) for their support throughout this research. I would like to specifically thank Nqobile Mkhize, Devona Sathiyah, Nokubonga Mjoli and Lindokuhle Ngema, who have become my brothers and sisters. Thank you for all the emotional support and motivation. I would also like to thank my seniors in the GERG, Nomthandazo Sibiya-Dlomo, Siphesihle Khumalo and Dr Ivan Madondo, for patiently guiding me throughout my project. I would also like to acknowledge the entire Department of Chemical Engineering, the technicians and all of the postgraduates who helped me during my research. In addition, I would like to thank Durban University of Technology for the financial assistance through the DUT scholarship program.

To my husband, Mr Zamile Mthembu, thank you for always making life easier for me, and for your unconditional love, support and understanding. Thank you for letting my dreams be your dreams. Finally, I would like to thank the Mthembu family and the Ngomane family. Thank you for always pushing me to be better, for the prayers and for your words of motivation and encouragement, especially my mother-in-law Mrs Bongekile Mthembu. Thank you to everyone who had a hand in the completion of my research.

Dedication

This dissertation is dedicated to my mother, Mrs Nokuthula Ngomane; thank you for the constant prayers, motivation and encouragement and my late father, Mr Msuli Samson Ngomane; thank you for all the love and the teachings you gave me; I am the woman I am today because of you. I love you, Daddy.

Abstract

In recent years, there has been a growing societal, governmental, and industrial concern about chemical and biological contamination of water. Numerous domestic and industrial operations generate wastewater that contains undesirable toxic contaminants. Chemical coagulants (aluminium and iron-based salts) effectively pre-treatment water and wastewater via coagulation and flocculation. Nevertheless, accumulating these chemical coagulants in the form of sludge and metal oxides significantly affects the environment, as well as human and aquatic life. Against this background, along with biowaste generation and the desire to meet the United Nations Development Goal on Clean Water and Sanitation (UN SDGs#6,9 and 12). Addressing chemical coagulant challenges with alternative solutions, such as using biowaste as coagulants, comes in handy. Therefore, this study aimed to examine the potential of banana peel, eggshell, and seashell powder as substitutes for traditional coagulants in water and wastewater treatment. The biowaste materials (banana peel, eggshell and seashell) underwent calcination at 400°C- 800°C for 2 -3 hours.

Scanning electron microscopy (SEM), energy dispersive X-ray (EDX), Brunauer Emmett Teller (BET), Fourier transform infrared spectroscopy (FTIR), and X-ray diffraction (XRD) were used to analyse the morphology, elemental composition of the structure, the pore surface area, the functional and molecular properties and the crystal structure, respectively. The overall analysis demonstrated the calcination of the engineered biochar was successful. Among the samples, the calcined banana peel was found to have the highest BET surface area of 4.3889 m^2/g, and the peeks on the XRD showed that calcined banana peels have the presence of calcium and potassium. The observed functional groups included O-H, C-O and C-H groups. This was followed by a feasibility study via the coagulation process using the calcined and uncalcined bio-coagulants. The results affirmed that these bio-coagulants are suited for wastewater treatment. In the preliminary studies, the removal efficiencies for turbidity and chemical oxygen demand (COD) were over 80% between the 0.8 – 8 g/L dosage range.

The response surface methodology (RSM) was used for the optimisation process with an input variable coagulant dosage (1 g/L – 6 g/L), mixing speed (30 rpm – 150 rpm), mixing time (2 min – 15 min), and settling time (20 min – 120 min) and colour, turbidity and COD removal as responses. The Box-Behnken design response model had a correlation factor (R^2) of over 0.9 at 95% confidence level. The optimum conditions were 1.6963 g/L (coagulant dose),

119.796 min (settling time), 2.25 min (mixing time), and 30 rpm (a mixing rate), achieving a removal efficiency of 92.39% COD removal, 99.77% Turbidity removal and 104.59 % colour removal at a desirability performance of 100%.

The optimum conditions were then validated with various bio-coagulants for the removal of the physiochemicals (COD, Turbidity, and colour) and other emerging contaminants such as phenol, phosphate, nitrate, and ammonia. The response model's predicted results were in total agreement with the experimental results, with less than 5% deviation. In addition, the calcined seashells had the best removal efficiency, with over 80% removal for phenol, phosphate, and ammonia and under 60% removal for nitrates. The findings of this research show that bio-coagulants (eggshells, seashells and banana peels) have valuable potential to be substituted for conventional coagulants in the water sector. Therefore, exploring if their economic and environmental viability for water and wastewater treatment is feasible for adaptation and implementation by policy makers and stakeholders is recommended.

Research outputs

This is to confirm that, the candidate (**Ngomane L.Z**,) is the author and presenter of the following manuscripts: who conducted the experiments, analysed the data, and wrote the manuscripts under the guidance of the supervisors.

Planned publications:

1. **Ngomane L.Z**, Mahlangu T.P, Tetteh E.K, and Rathilal S. Coagulation treatment for the removal of colour, turbidity and COD using banana peels, eggshells and seashells as coagulants. (under preparation, submission by April 2024)
2. **Ngomane L.Z**, Mahlangu T.P, Tetteh E.K, and Rathilal S. The optimisation of the coagulation process with the aid of a predictive model: kinetics and isotherm model evaluation (under preparation for submission by April 2024)
3. **Ngomane L.Z**, Mahlangu T.P, Tetteh E.K, and Rathilal S. The removal of phosphate, nitrate, phenol and ammonia using bio-waste materials as coagulants (under preparation for submission by May 2025).

Conference presentations and proceedings:

1. **Ngomane L.Z**, Sibiya N.P, Amo-Duodu G, Tetteh E.K, Mahlangu T.P, Chollom M.N and Rathilal S. Modified and unmodified banana peels as biosorbent for heavy metal removal from water: Characteristics and cost-benefits analysis. 2nd Sustainable Bioenergy and processes Conference (SBP2022, Dec. 12-14, 2022, Cape Town (SA). (Presenter)

2. **Ngomane L.Z**, Kraai S.A and Xaba S. Rainwater storage and treatment using bio-waste materials. Next Generation City Action, UIA 2023 World Congress of Architects. 2nd-6th July 2023, Copenhagen, Denmark. (Presenter)

3. **Ngomane L.Z**, Khumalo S, Mahlangu T.P, Tetteh E.K, and Rathilal S. 2023. The Preparation and Characterization of Banana Peels, Eggshells, and Seashells for The Treatment of Wastewater. Proceedings of 39th JOHANNESBURG International Conference on “Chemical, Biological and Environmental Engineering” (JCBEE-23) Nov. 16-17, 2023. Birchwood Hotel & OR Tambo Conference Centre, Johannesburg,

International Institute of Chemical. Biological & Environmental Engineering, Available: https://doi.org/10.17758/IICBE5.C1123025.

Awards:

1. Best oral presentation PG student, platinum award (FEBE) 2023
2. DUT Envision 2030 International awards: Research based business award
3. DUT MICA Minning innovation challenge (2nd place).

Table of Contents

List of tables

List of figures

Nomenclature

ANOVA	Analysis of variance
a.u	Arbitrary unit
BBD	Box-Behnken design
BET	Brunauer-Emmett-Teller
BP	Banana peel
CBP	Calcined banana peel
CES	Calcined eggshell
COD	Chemical oxygen demand
CSS	Calcined seashell
EDX	Energy-Dispersive X-ray
ES	Eggshell
FTIR	Fourier-Transform Infrared Spectroscopy
NTU	Nephelometric turbidity units
PAC	Poly-aluminium chloride
rpm	Revolution per minute
RSM	Response surface methodology
SANS	Southern African National Standards
SEM	Scanning Electron Microscopy
SS	Seashell
WHO	World Health Organisation
XRD	X-ray Diffraction Analysis

CHAPTER 1: INTRODUCTION

1.1 Background

Water, which constitutes more than 70% of the Earth's surface, is undeniably the most valuable natural resource present on our planet (Anane 2023; Kilag *et al.* 2023). However, freshwater accounts for only 2.5% of the Earth's water (Mohd-Salleh *et al.* 2019). The phenomenon under consideration establishes the foundation for the development of life on Earth and constitutes a fundamental component of all present-day living organisms (Narain 2009). Access to clean water is an essential natural resource for the sustenance of all living organisms, including the human population, who rely on it for drinking, bathing, sanitation, and other domestic purposes. In addition, water plays a critical role in several sectors, such as agriculture, cattle ranching, horticulture, fishery, energy generation, industrial operations, and other forms of innovation (Narain 2009; Tyagi *et al.* 2013; Precious Sibiya *et al.* 2021). The growing demand has resulted in the world being confronted with the need to address the issue of securing sufficient water supplies to meet the needs of growing people and economies.

Over the past few years, the lack of access to clean and safe drinking water has increased waterborne diseases that are caused by harmful microorganisms such as bacteria, protozoa, and viruses that are spread by water (Akpor *et al.* 2014a; Landrigan *et al.* 2020). These viruses may cause disability, disease, or death if precautions are not taken promptly (Olaolu *et al.* 2014). Chemicals and compounds have resulted in an increasing detection of substances that exhibit potential environmental hazards to living organisms (Bolong *et al.* 2009). In recent decades, implementation of stringent regulatory measures aimed at limiting the concentrations of contaminants found in water or wastewater have been implemented on the discharge of wastewater (Simate *et al.* 2015; Mohd-Salleh *et al.* 2019). Wastewater treatment plants (WWTPs) are a substantial contributor of contaminants released into aquatic ecosystems (Chollom *et al.* 2020; Kweinor Tetteh *et al.* 2020). Wastewater tends to include diverse pollutants, such as lactose, oils and greases, proteins, nitrogen (nitrates) and phosphorus-rich substances (phosphates), sediments (turbidity and colour), various organic substances (chemical oxygen demand), and detergents (Sibiya *et al.* 2022; Salah-Tazdaït *et al.* 2023; Sibiya 2023).

Due to the abovementioned drawbacks, several methods have been investigated for treating wastewater before discharge. Wastewater contains organic compounds that are dissolved or suspended and may be decomposed biologically. These solids are known as "putrescible."

The conventional treatment of wastewater involves using a variety of physical, chemical, and biological processes (Balajii *et al.* 2020; Bahrodin *et al.* 2021) and activities to effectively eliminate particles, organic substances, and, sometimes, nutrients from wastewater (Saravanan *et al.* 2021; Al-Hazmi *et al.* 2023). In wastewater treatment, various degrees of treatment are categorised by preliminary, primary, secondary, tertiary, and/or advanced wastewater treatment (Mousazadeh *et al.* 2022). In some nations, pathogen removal by disinfection is occasionally implemented after the final treatment stage (Mousazadeh *et al.* 2022; Al-Hazmi *et al.* 2023). The first stage of the treatment procedure involves the reception of wastewater from its origin, followed by the process of sedimentation to eliminate solid particles and fine sand. The first stage of the treatment unit involves the implementation of a screening process, which segregates buoyant substances from those suspended in the medium. Aerators are used to eliminate gases from water, wherein the untreated water is exposed to air. Following that, chemical coagulation, flocculation, and clarifying procedures are carried out. Subsequently, a coagulant tank is used to introduce coagulants into the water. The coagulants are thoroughly blended using a flash mixer.

Coagulation is a physiochemical treatment process that is widely used in water and wastewater treatment because of its high efficiency in eliminating organic matter, suspended particles, turbidity, and colour (Abidin *et al.* 2013; Bahrodin *et al.* 2021). The coagulation process is widely used in wastewater treatment because of its simplicity and cost-effectiveness. This process is applied either as a pre or post-treatment step, which positively affects the efficiency of the overall treatment performance (Tzoupanos *et al.* 2008). The coagulation process has been closely connected to the flocculation process (Bahrodin *et al.* 2021). Flocculation is the acceleration of agglomeration and floc formation by the addition of a flocculant agent which is called a flocculant (Kurniawan *et al.* 2022). The treatment process of coagulation-flocculation can be subsequently divided into two steps. Coagulation is subsequently the destabilisation of colloidal materials, which are particles smaller than approximately 10^{-5} mm in wastewater; this is accomplished by a combination of two or more of the following mechanisms: compression of the electrical double layer, adsorption and charge neutralisation, adsorption and interparticle bridging and sweep flocculation. Due to its ability to efficiently decrease contaminants such as chemical oxygen demand (COD), turbidity, colour, suspended solids (SS), heavy metals, oil, and organic materials, coagulation has been widely used as a water treatment method (Bahrodin *et al.* 2021). The aim of a coagulant agent is to remove both

chemical and physical contaminants. Coagulants can be divided into two types, which are chemical and natural coagulants.

Chemical-based coagulants have been widely used in the treatment of wastewater. They can be divided into organic (aluminium sulfate, ferric chloride, alum) and inorganic coagulants (poly-aluminium chloride) (Diver *et al.* 2023; Nyambura 2023). Chemical coagulants have advantages, such as high efficiency at lower dosages, easy accessibility and dissolving in water. However, chemical coagulants have major drawbacks, such as a large production of non-biodegradable sludge, highly toxic to human and marine life over time and high operational costs (Bahrodin *et al.* 2021). The disadvantages of these conventional chemical coagulants have resulted in the investigation of an alternative that is sustainable and environmentally friendly. Natural coagulants or bio-coagulants have gained attention in the treatment of water and wastewater due to the advantages they have over conventional coagulants (Shukri *et al.* 2023). Natural coagulants are generally plant-based, animal-based and microorganisms (Nimesha *et al.* 2022). Banana peels, orange peels, moringa plant, eggshells, seashells, chicken bones are some of the bio-waste materials that can be used to produce bio-coagulants (Mogbo *et al.* 2020; Kumar *et al.* 2024). They are found to be cost-effective, easily accessible, and produces a biodegradable sludge (Bahrodin *et al.* 2021).

1.2 Problem statement

Water is an essential but scarce resource in the world. Not only do we need water for the survival of humanity, but it is also crucial to the growth of the country's economy (Hsiang *et al.* 2013). One of the significant enablers of poverty in South Africa has been the lack of access to clean, safe water. This affects agriculture, livestock production, forestry, fisheries, hydropower generation, and other innovation activities (Precious Sibiya *et al.* 2021). Statistically it is known that approximately 2.3 billion people don't have access to clean water in their households, and over four billion people face severe water outages at least once annually (Chartres *et al.* 2010; Makarigakis *et al.* 2019). With the exponential growth of the population and industries in South Africa, the need for additional water resources also increases (Ajala *et al.* 2018).

The United Nations has formulated Seventeen "Sustainable Development Goals (SDGs)" to tackle global concerns such as poverty, hunger, inequality, and the adverse impacts of climate change. This research speaks directly to SDGs 6, 9 and 12. SDG 6 specifically pertains to the provision of clean water and sanitation, SDG 9 pertains to industry, innovation

and infrastructure, which promotes inclusive and sustainable industrialization and fosters innovation and SDG 12, addresses responsible consumption and production, addresses the issue of ensuring sustainable consumption and production patterns (United Nations 2015; Albu 2021; Halkos *et al.* 2021).

A sustainable and cost-effective process is required to assist with the water crisis South Africa is currently facing. Over the past couple of years, a lot of attention and focus has been put on the study of natural coagulants in water treatment. This study will employ coagulation, a pre-treatment technique used in wastewater industries to lower organic pollutants before subsequent treatment operations. The coagulation process employs synthetic chemicals, which have proven to be unable to dissolve, dangerous to humans, and expensive. The interest in natural coagulants has not only been brought by the potential it has to act as an alternative to chemical coagulants but has also been found to be eco-friendly and generally classified as non-toxic (Abdullah I *et al.* 2020). One of the major advantages of bio-waste materials is that they are renewable, biodegradable, non-toxic, and cost-effective (Balajii *et al.* 2020). The increased water cuts cause a strain on the people of South Africa, industries and many businesses. This study focuses on establishing a new sustainable and cost-effective treatment that employs viable biowaste materials as coagulants for the treatment of water.

1.3 Aims and Objectives

The aim of this study is to identify an effective natural coagulant for the treatment of phosphates, ammonia, nitrate and phenols in wastewater, with the specific objectives:

1. To synthesize and characterize the natural coagulants (eggshells, seashells, and banana peels) and conduct a feasibility study.
2. To develop a predictive model for evaluating the coagulation treatment process with various operating conditions (mixing time, coagulant dosage, speed and settling time).
3. To apply and evaluate the coagulation treatment efficiency of using the synthesized and natural coagulants in comparison to that of poly-aluminium chloride (PAC) at optimized conditions.
4. To evaluate the removal of phosphates, phenols, ammonia and nitrates in industrial wastewater at the optimized conditions using the best coagulant.

1.4 Approach

This study was carried out in accordance with the following phases:

Synthesis and characterisation: The first step was to collect banana peels, eggshells and seashells as bio-waste materials. The three collected biowaste materials were prepared and synthesised using calcination to obtain the various bio-coagulants. The bio-coagulants were thereafter characterised to determine surface area, surface functionality and surface morphology (Section 3.2).

Optimisation: The wastewater was collected from a local wastewater treatment plant and characterised for pollutants, which included colour, turbidity, chemical oxygen demand (COD), phosphate, phenols, ammonia, and nitrates. The response surface methodology was used for the experiment design and optimisation, where the operation conditions were mixing time, mixing speed, dosage and settling time. The responses were colour, COD and turbidity. The optimisation was done on the various bio-coagulants in comparison to poly-aluminium chloride.

Evaluation: The optimum conditions from the various bio-coagulants and PAC were used to remove ammonia, nitrate, phosphate, and phenol. The bio-coagulants were mixed at different ratios with the PAC to remove the contaminants at various conditions.

Having clean and safe running water has become a luxury in South Africa. Water surges not only affect the communities but also affect agricultural production, livestock production, fisheries, hydropower generation and many other innovative industries (Adelagun *et al.* 2016). The pre-treatment of industrial wastewater using coagulation and flocculation processes has become crucial in the removal efficiency of organic matter. This significantly reduces the organic load before subsequent treatment processes (Saifuddin *et al.* 2011a; Nnaji *et al.* 2014). The coagulation and flocculation processes aim to remove inorganic and organic matter dissolved in natural water. This process improves the aesthetics and health aspects of water (Buenaño *et al.* 2019).

1.5 Structure of dissertation

Chapter one

This chapter presents a general introduction to the study's research background, problem statement, research aims and objectives, research approach, and thesis outline.

Chapter two

Chapter two is the literature review of the overall study, where wastewater is examined, focusing on the existing and conventional wastewater treatment methods. The extensive

literature on coagulation and the mechanism of coagulation, conventional and emerging coagulants, are reported. An in-depth review of the experiment design used to optimise the process is done. The background of coagulant kinetics is also reviewed.

Chapter three

Chapter three is the research methodology, where the synthesis of the bio-coagulants, materials used, procedures, and equipment descriptions are reported. The characterisation of the industrial water and bio-coagulants is also reported.

Chapter four

The chapter reports results and discussions, including the characterisation of the bio-coagulant and the application of these bio-coagulants with the aid of the response surface methodology software.

Chapter five

Chapter five presents a concise overview of the primary results derived from this study. This chapter presents conclusions obtained in this study, along with recommendations for further work.

CHAPTER 2: LITERATURE REVIEW

This chapter is an intensive look at previous work from other researchers on wastewater treatment, the contaminants found in wastewater, various treatment methods, and the advancements made in the coagulation process. The coagulation process's variables will also be investigated, focusing on the progress made in using natural coagulants instead of conventional chemical coagulants. This chapter also looks at the design of experiment software to optimise the process.

2.1 Wastewater treatment challenges

The discharge of untreated and/or partly treated industrial effluent into water-receiving bodies has given rise to significant economic and environmental concerns in both industrialised and developing nations (Keraita 2010). Water pollution may arise from several sources, including homes, industry, mining, and infiltration. However, one of the primary contributors to water contamination is the extensive water utilisation by the industrial sector (Anjaneyulu *et al.* 2005; Hai *et al.* 2007; Akhtar *et al.* 2021). There are typically four forms of water which include rainwater (which comes from impermeable surfaces), household wastewater, agricultural water, and industrial wastewater (Crini *et al.* 2019). The high concentration of organic and inorganic contaminants found in industrial effluent, some bio-accumulative, pose major health risks to aquatic and human beings. As a result, national and international environmental organisations have set strict dewatering restrictions to lower the amount of contaminants in industrial effluents (Simate *et al.* 2011).

The United Nations has proposed the Sustainable Development Goals (SDGs) with the aim of promoting a sustainable way of living that minimises ecological damage and fosters economic and social advantages. Water plays a pivotal role in the context of sustainable development, hence establishing a strong interconnectedness between all Sustainable Development Goals (SDGs) and the sustainable utilisation of water resources (United Nations 2015; Weerasooriya *et al.* 2021). To achieve water quality and equitable access to water and sanitation by 2030 and beyond, South Africa will need to do more than reduce water losses and water demand by adopting innovative solutions.

South Africa is a semi-arid country, and with the limited supply of water it is estimated that by 2025 the demand of water will surpass the available resources (Edokpayi *et al.* 2020). To

prevent crucial environmental and public health related issue it is imperative that constant monitoring of treatment facilities is done (Edokpayi *et al.* 2020).

Agricultural wastes often contain certain functional groups, such hydroxyl (-OH) or carboxylic acid(-COOH), that may provide adsorption affinity for heavy metal ions in bio-sorbents. These functional groups are often present in bio-sorbents, easily generated from agricultural wastes by a straightforward pre-treatment process. Consequently, the surface functional groups on the bio-sorbent and its propensity to bind metal ions have a considerable impact on the adsorption of metal pollutants (Chao *et al.* 2012).

2.2 South African legislation on water treatment and governance

2.2.1 The National Water Act (36 of 1998)

This act enables a legal basis of national framework for effective and sustainable management of water resources. It is to ensure that the national water resources are used in a way that will (Govenment 1998; Maphela *et al.* 2020):

- Meet the basic needs of humans,
- Increase access to water,
- Insure efficient, and sustainable use of water,
- Improve social and economic development,
- Promote dam safety,
- Manage floods and droughts,
- Meet international obligations,
- Reduce and prevent pollution and degradation of water resources,
- Protect aquatic and associated ecosystems and their biological diversity.

2.2.2 Water Act (Act 54 of 1956) / Act 36 of 1998

The main purpose of this act was to improve water infrastructure for industrial expansion, meet rising urban water demand, and combat water pollution. The long-term goal of this act was to amend laws on water control, conservation, and use for domestic, agricultural, and industrial purposes. It also promoted the state of South Africa to build and control government water works such as dams, irrigation schemes, and electricity generation (Govenment 1956; Tempelhoff 2017).

2.2.3 National Environment Management Act (NEMA, 107 of 1998)

This legislation aims to manage the environment and its ecological concerns. This comprises standard rules that ban the discharge of contaminants into the environment under specific

conditions. The National Waste Management Strategy aims to eliminate organic waste in landfills (Khumalo 2011).

2.3 Wastewater treatment

Wastewater may be described as a composite of liquid or waterborne waste that is extracted from various sources such as residential areas, institutions, and commercial and industrial facilities (Crini *et al.* 2019; Barchiesi *et al.* 2021; Dehghani *et al.* 2021; Saravanan *et al.* 2021; Kurwadkar *et al.* 2022). This composite also includes groundwater, surface water, and stormwater. Typically, it encompasses a substantial quantity of oxygen-demanding waste, pathogenic microorganisms, organic matter, plant growth-promoting nutrients, inorganic compounds, minerals, and sediment (Roets 2020; Mphuthi 2021). There are two broad classifications of wastewater which are not completely distinct from one another: domestic wastewater and industrial wastewater (Rodríguez-Vidal *et al.* 2020; Mustafa *et al.* 2021; Nath *et al.* 2021; Abdelfattah *et al.* 2023). Water treatment refers to the process of eliminating impurities and pollutants from contaminated water sources (Yaqoob *et al.* 2020; Saravanan *et al.* 2021; Koul *et al.* 2022; Kordbacheh *et al.* 2023). The treatment method used in wastewater treatment processes is dependent on the source and nature of the wastewater (Nath *et al.* 2021). The treatment of wastewater can be divided into three main stages: primary treatment, secondary treatment, and tertiary treatment as shown in Figure 2-1.

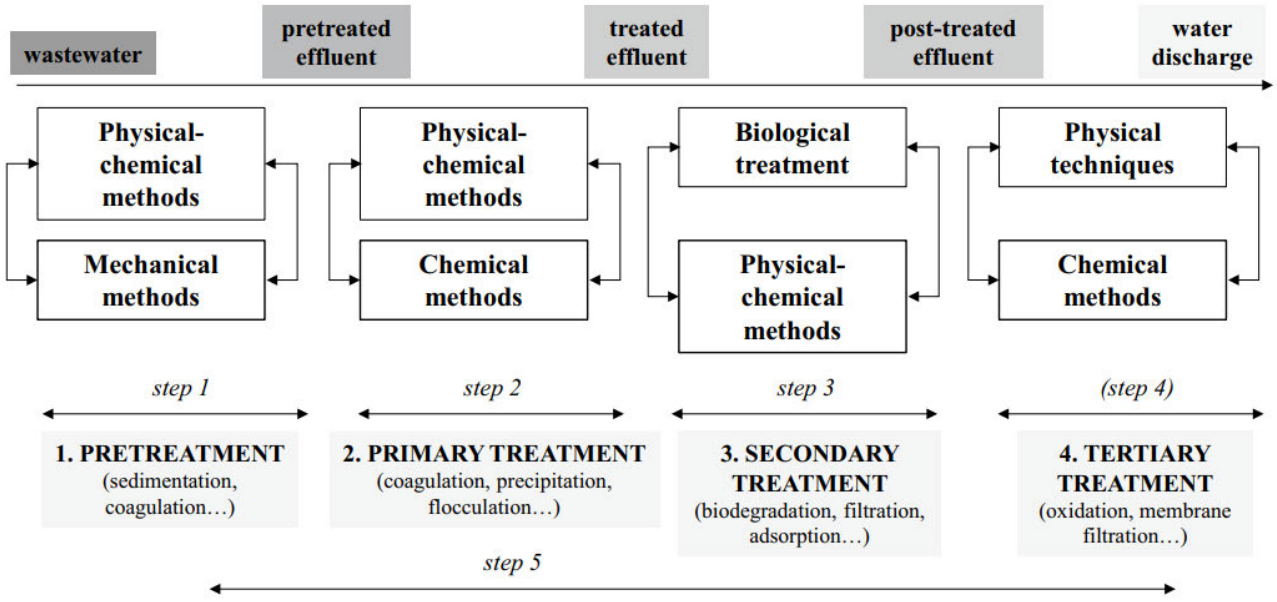

Figure 2-1: Conventional treatment processes (Crini *et al.* 2019)

2.3.1 Primary treatment

Primary treatment involves the removal of grit, screening, grinding, and sedimentation (Hanlon 1954; Saleh 2021). Primary treatment in domestic water removes roughly 25% of the organic content and all non-organic impurities with or without chemicals. Primary treatment eliminates around 35% of biological oxygen demand (BOD) and 60% of solids. Some of the processes used to accomplish this treatment process include sedimentation, settling, clarity, and thickening (Liu *et al.* 2020; Nath *et al.* 2021; Saleh 2021). The first stage of the treatment procedure involves the reception of wastewater from its source, followed by a settling process aimed at eliminating solid particles and fine sand. The first stage of the treatment unit involves the implementation of a screening process, which separates floating substances from those suspended inside the system. Aerators eliminate gases from water by subjecting the raw water to air exposure. Following this, the chemical operations of coagulation, flocculation, and sedimentation are carried out (Crini *et al.* 2019; Saleh 2021). Subsequently, a coagulant tank is used to introduce coagulants into the water. The coagulants are effectively blended using a flash mixer (Lin *et al.* 2013; Tisti *et al.* 2020).

2.3.1.1 Screening

Screening often serves as the first phase of a wastewater treatment procedure. The major objective of this process is to remove solid waste from the effluent, including fabric scraps, paper, wood, cork, hair, fibre, culinary waste, faecal solids, and other substances present in wastewater (Cripps *et al.* 2000; Hamed *et al.* 2004; Van Haandel *et al.* 2007). The efficient removal of these components is crucial to protect downstream systems from possible damage, unnecessary degradation, pipe blockages, and the build-up of unwanted substances that might disrupt the vital wastewater treatment processes (Cripps *et al.* 2000; Akpor *et al.* 2014b; Asthana *et al.* 2017).

Screening may be categorised into two distinct classifications: coarse screening and fine screening (Ghaly *et al.* 2014). The coarse screening process involves removing large particles, rags, and debris from wastewater (Rezai *et al.* 2021). Typically, the apertures of coarse screens measure around 6 mm (0.25 in.). On the other hand, small screens are designed with openings which can vary from the lowest size of 1.5 mm (0.06 in.) to the highest of 6 mm (0.25 in.), while very fine screens, with openings ranging from 0.2 mm (0.01 in.) – 1.5 mm (0.06 in.), are utilised to eliminate suspended particles to standards comparable to those achieved by primary clarity (Asthana *et al.* 2017). Filtration can be defined as a physical procedure used to eliminate suspended particles and turbidity contained in the wastewater (Shanmuganathan *et al.* 2017).

The filtering procedure entails the use of a filtration medium with apertures ranging from 0.1 mm to 0.5 mm for the elimination of particles that have particle size below 100 mg/L (Gupta *et al.* 2012; Ince *et al.* 2019). In a representative filtering procedure, the wastewater descends through the filter bed, accumulating a stratum composed of algae, plankton, and other microscopic flora on the surface (Gumbi 2020).

2.3.1.2 Coagulation

The coagulation process consists of three main steps: flash mixing, which is employed to introduce appropriate chemicals such as coagulants, flocculants, and pH adjusters into the water. This is done with the aid of stirring and mixing at high speeds. Secondly, slow-mixing coagulation and flocculation occur, where the water is continuously stirred to encourage the formation of large flocs. These flocs are then allowed to settle out. Lastly, sedimentation occurs, during which the floc formed during flocculation is permitted to settle and subsequently separated (Crini *et al.* 2019; Bahrodin *et al.* 2021).

2.3.1.3 Sedimentation

A sedimentation tank aids in the removal of particles. The second approach entails sand filtration after secondary sedimentation, which effectively eliminates any remaining particles present in the supernatant (Khiadani *et al.* 2014). As a result, secondary solids undergo sedimentation and accumulate towards the lower part of the tank, leading to an increase in viscosity. If water contains phosphate, it is possible to eliminate this compound using a process known as chemical precipitation. This involves the addition of certain substances such as ferric chloride ($FeCl_3$), alum ($Al_2(SO_4)_3 14H_2O$), or lime (CaO or $Ca(OH)_2$) in the form of salts. There are two primary methods for removing nitrogen from wastewater. The first method involves chemical treatment, specifically ammonia stripping. This process involves raising the pH of the wastewater to convert ammonium ions into ammonia, which can then be purged from the wastewater through a process like aeration. The second method is biological treatment, specifically nitrification/de-nitrification. This process occurs through an activated sludge process, where the detention time in the activated sludge basin is increased in a separate reactor (Lawler 1986; Teh *et al.* 2016; Saleh *et al.* 2021).

The inclusion of phosphate and nitrogen removal processes might be regarded as an integral component of modern treatment methods (Saleh *et al.* 2021; Tom 2021).

2.3.1.4 Filtration

The removal of suspended particles is achieved by passing them via the sieve pores of the filter medium (Zahrim *et al.* 2013). The efficiency of sand filters is in the retention of various suspended pollutants, including organic debris, fine sand, silt, micro-plastics, algae, pesticides, and nitrates (Hoslett *et al.* 2018; Gumbi 2020; Wolff *et al.* 2020).

It is recommended that filter beds undergo a backwashing or cleaning operation after about one to two months. Alternatively, another approach is to refill the top of the sand filters by 2 cm with fresh sand media (Zanacic *et al.* 2016).

Sand filtration media may be categorised into two types of filtering processes, namely slow and fast, depending on the driving power involved. Rapid gravity sand filters have been preferred over slow sand filters for treating coagulant-treated water (Deshmukh *et al.* 2016; Gumbi 2020).

2.3.2 Secondary treatment

Secondary treatment focuses on the oxidation of dissolved organic matter using biologically active sludge where suspended and residual organic matter and compounds are broken down, which is subsequently filtered out (Saleh 2021). Aerobic digestion, anaerobic digestion, bio-filtration and bio-trickling are the most often employed biological treatment methods in wastewater treatment plants (Tetteh *et al.* 2019c)

2.3.3 Tertiary treatment

The resistant organic molecules not removed during the secondary treatment are subjected to further treatment using improved technologies during the tertiary treatment. Advanced treatment refers to any method that generates effluent of superior quality compared to primary and secondary treatments. Tertiary treatment employs advanced biological methods for nitrogen removal, as well as chemical and physical techniques such as granular filtration and activated carbon absorption (Crini *et al.* 2019).

2.4. Water and wastewater treatment technologies

Various treatment technologies have been used for the remediation of wastewater loosely classified as conventional methods, established recovery processes and emerging technologies (Crini et al. 2019). These technologies include adsorption, coagulation/flocculation, advanced oxidation, chemical precipitation and ion exchange as shown in Figure 2-2 (Oller *et al.* 2011), (Hamdi 1996), (Kestioğlu *et al.* 2005), (Oller *et al.* 2011; Boczkaj *et al.* 2017). Furthermore,

there are various advantages and disadvantages that come with using wastewater treatment technologies, which are listed below in Table 2-1.

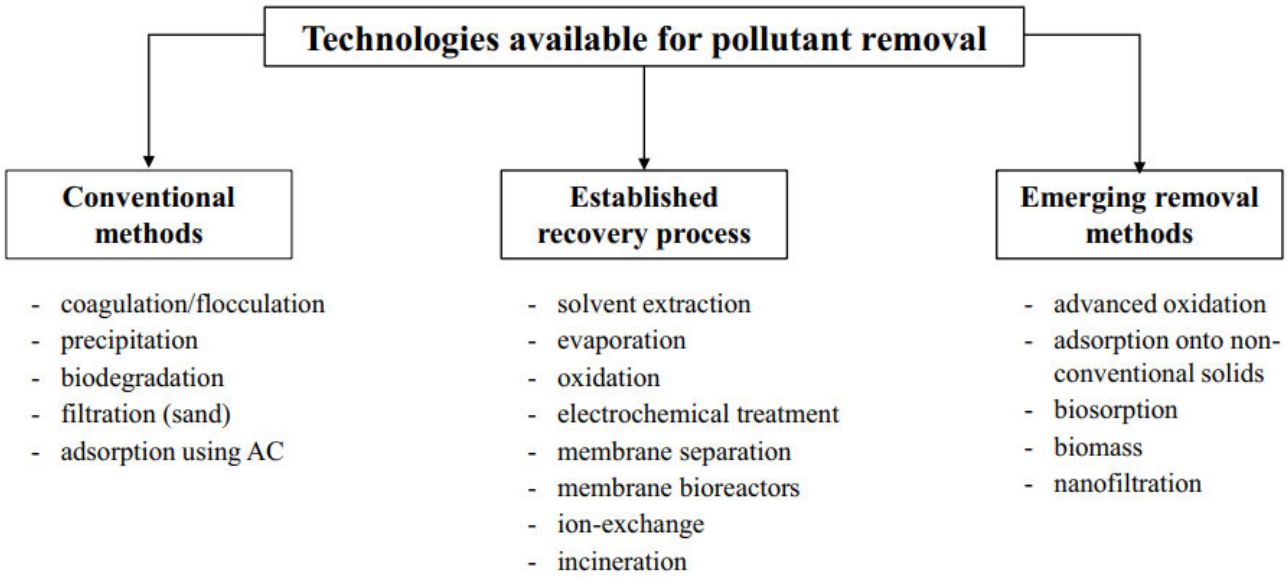

Figure 2-2: Treatment technologies available for pollutant removal (Crini *et al.* 2019)

Table 2-1: Wastewater treatment technologies

Treatment technology	Advantage	Disadvantage	References
Coagulation /Flocculation	• Process simplicity • Combined physical-chemical reactions. • A wide range of chemicals can be purchased commercially. • Low initial investment cost • Effective for colloidal particles and suspended solid removal • Good dewatering and sludge settling qualities • Both the chemical and biological oxygen demands have significantly decreased. • decrease in adsorbable organic halogen and total organic carbon. • The ability to inactivate bacteria • Quick and effective removal of insoluble pollutants	• Requires the use of non-reusable chemicals (coagulants, flocculants, aid chemicals) • Effluent physicochemical monitoring (pH) • Increased sludge production (management, treatment, cost) • Low arsenic removal	(Zinicovscaia 2016; El-taweel *et al.* 2023; Gan *et al.* 2023)

Adsorption	• Capable of very specific removal of the emerging contaminants • Accurate and efficient removal Can assist other treatment processes • Less complex and less expensive	• Difficult to remove the unknown type of contaminants, since adsorbents are highly specific	(Zinicovscaia 2016; El-taweel *et al.* 2023; Gan *et al.* 2023)
Advanced Oxidation Process	• Degradation of various trace organics by generation of a large number of highly reactive free radicals, surpassing the conventional oxidants by far in efficiency	• Pretreatment almost always necessary to remove suspended solids, radical scavengers and competing ions; formation of toxic by products; expensive, and very few full scale plants	(Zinicovscaia 2016)
Ion exchange	• Availability of commercial products • Technology simplicity • Adapted to high pollutant load	• Economic constraints • Large volumes requires large columns	(Zinicovscaia 2016; Crini *et al.* 2019; El-taweel *et al.* 2023; Gan *et al.* 2023)
Chemical precipitation	• Technology simplicity • Adapted to high pollutant loads • Economically efficient	• Chemical consumption • Sludge generation • High cost • Ineffective removal of metal ions	(Zinicovscaia 2016; Crini *et al.* 2019; El-taweel *et al.* 2023)

2.4 Coagulation

Coagulation is one of the most common treatment methods used in wastewater treatment plants. With the aid of a coagulant or a chemical, it merges microscopic particles to form bigger aggregates, known as flocs and binds dissolved organic materials to these aggregates (Tzoupanos *et al.* 2008; Verma *et al.* 2012; Iwuozor 2019; Bahrodin *et al.* 2021; Precious Sibiya *et al.* 2021). Flocculation occurs when destabilised suspended particles aggregate and form agglomerates (Hogg 2005; Precious Sibiya *et al.* 2021). This allows for the removal of contaminants in water and wastewater as shown in Figure 2-3. In the past decades, pre-treatment of industrial wastewater using coagulation and flocculation processes has become crucial to efficiently reduce the organic load before subsequent treatment processes (Saifuddin *et al.* 2011b; Nnaji *et al.* 2014). Eliminating organic substances by coagulation involves three primary components: neutralisation, destabilisation, and aggregation of positively charged metal ions and negatively charged organic colloids. Additionally, the combination of metal ions and soluble organic matter molecules forms insoluble complexes and precipitates. Furthermore, the surface of conventional coagulants experiences physical and chemical adsorption of organic substances. The agglomerated flocs may be removed using sedimentation, direct filtering, or flotation processes (Ugya ; Gumbi 2020; Kweinor Tetteh *et al.* 2020). Due to its negatively charged suspended particles, water exhibits repulsion and hinders aggregation and settling (Gumbi 2020). With the increasing severity of environmental pollution issues and the implementation of stricter water quality regulations, it is evident that traditional coagulation technology is inadequate in meeting the public's demand for water safety. It is crucial to address the removal of turbidity, colour, COD, and TSS in wastewater decontamination (Zheng *et al.* 2009; Gumbi 2020; Kordbacheh *et al.* 2023).

An effective coagulation process leads to the removal of about 90% of the suspended substances (Ahmad *et al.* 2006; Amuda *et al.* 2007; Bukhari 2008; Tetteh *et al.* 2019a).

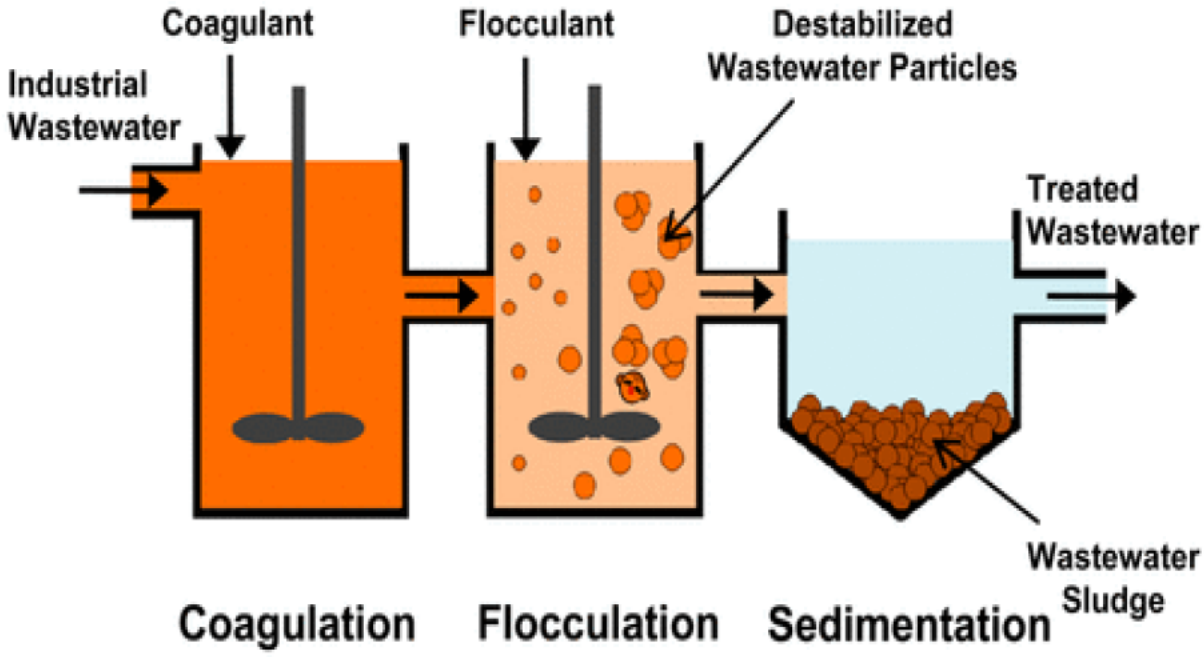

Figure 2-3: Mechanism of coagulation/flocculation process (Teh *et al.* 2016)

Coagulation is an essential mechanism involving the addition of coagulants responsible for the destabilisation and neutralization of suspended particles (Sahu *et al.* 2013; Balls 2014). Which form large flocs or aggregates. Typically, negatively charged suspended particles agglomerate with positively charged coagulants due to the adsorption of ions and ionisation of surface groups (Hossain *et al.* 2019b). These aggregates are removed by sedimentation, filtration, or flotation mechanisms (Tetteh *et al.* 2019b; Tetteh *et al.* 2021).

2.4.1 Colloidal suspensions

The constituents included in wastewater originate from the discharge of industrial and domestic waste, the dissolving of minerals, the decomposition of vegetation, and the erosion of land. In the context of wastewater, this material might consist of suspended and/or dissolved organic and/or inorganic substances, and also various living entities such as algae, bacteria, and viruses (Tatsi *et al.* 2003; Renou *et al.* 2008). Table 2.2 demonstrates that a significant portion of the suspended debris in wastewater is in the microscopic to sub-microscopic size range.

Particles of a size lower than about 10^{-5} mm are classified as colloids. They are surrounded by various things such as mineral compounds, biopolymers, minute aggregates of precipitated and flocculated matter, macromolecules, silt, viruses, bacteria, and plankton. Particles smaller than roughly 10mm to 6 mm are commonly referred known as solutions. The materials included in this category consist of inorganic substances such as simple and complex ions, polyelectrolytes,

molecules, and polymeric species, as well as undissociated solutes, organic molecules, and tiny aggregates (Shammas, 2005; Bratby, 2006).

Table 2-2: Classification and examples of particle sizes (Bratby 2016)

Particle size (mm)	Classification	Examples	Total surface area (m^2/cm^3)	Time required to settle 100 mm if specific gravity = 2.65
10	Coarse dispersion (visible to naked eye)	Gravel, coarse sand, mineral substances, precipitated and flocculated particles, silt, macroplankton.	6×10^{-4}	0.1 s
1			6×10^{-3}	1 s
10^{-1}			6×10^{-2}	13 s
10^{-2}	Fine particulate dispersion (visible under microscope)	Mineral substances, precipitated and flocculated particles, silt, bacteria, plankton, and other organisms.	0.6	11 min
10^{-3}			6	20 h
10^{-4}			60	80 days
10^{-5}	Colloidal dispersion (submicroscopic)	Mineral substances, hydrolysis and precipitated products, macromolecules, biopolymers, viruses.	600	2 years
10^{-6}			6000	20 years
$<10^{-6}$	solution	Inorganic simple and complex ions, molecules and polymeric species, polyelectrolytes, organic molecules, undissociated solutes.		

2.4.2 Coagulation mechanism

Coagulation may be divided into four basic mechanisms: the electric double layer, charge neutralisation, inter-particle bridging, and sweep floc as shown in Figure 2-4. Adsorption of ions or polymers with opposite charges may destabilise particles. Positively charged hydrolyzed metal salts, prehydrolyzed metal salts, and cationic organic polymers may disrupt particles by balancing the charge on their surfaces. The electric double layer will disappear if the charge on the particle's surface is neutralised, enabling van der Waals force to cause the particles to attach to one other effectively. Polymer chains cling to particle surfaces at certain points along their length, leading to coulombic (charge-charge) interactions, dipole interactions, hydrogen bonding, and van der Waals forces of attraction. Insoluble sedimentation will occur if enough aluminium or iron is added, and particles will be trapped within the amorphous precipitates.

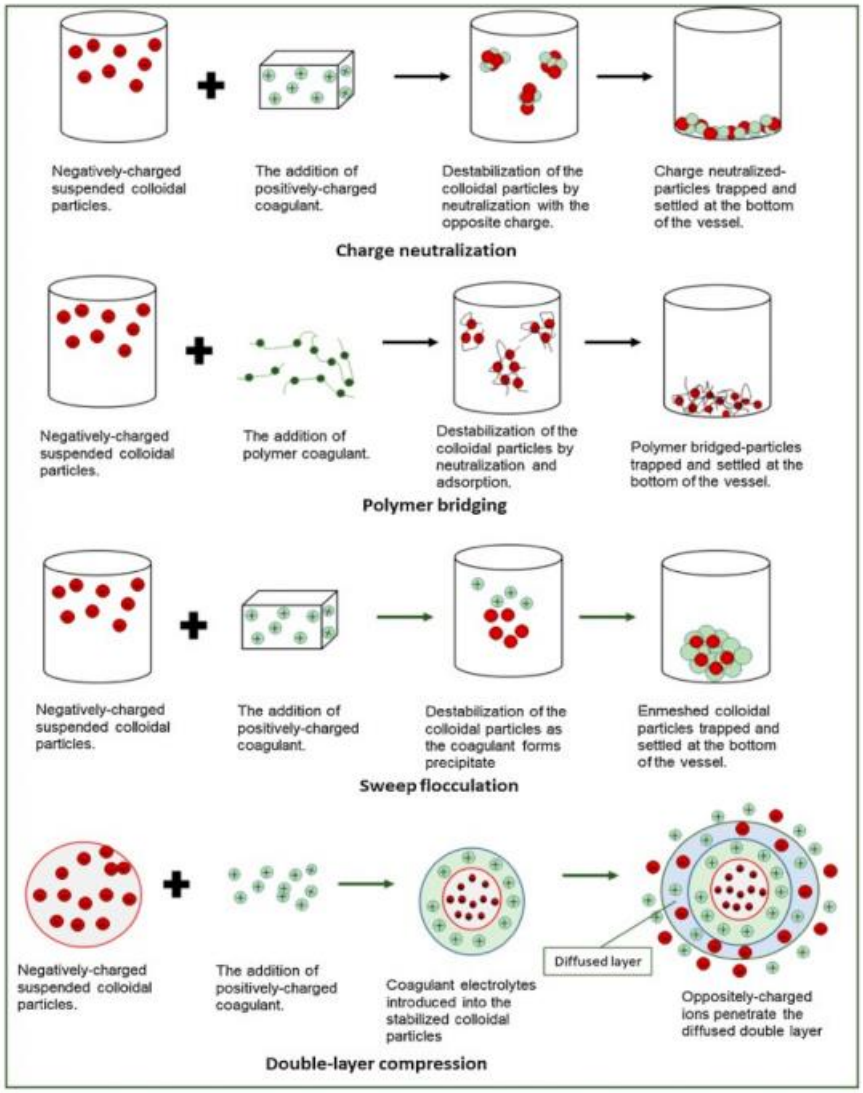

Figure 2-4: Schematic representation of the mechanisms involved in natural coagulation process (Koul *et al. 2022)*.

2.4.2.1 Double layer compression

Figure 2-5 represents a visual representation of a double-layer compression, it can be defined as the process that breaks through the double layer surrounding colloids by using ions that have the opposite charge to the colloids. The counter ions will alter the properties of the double layer thinner and smaller in volume. This procedure may result in colloid instability when it causes a shift in ionic strength brought about by the addition of more coagulants, which reduces the double layer around the colloidal particle (McBride 1997; Xia *et al.* 2020a; Sonal *et al.* 2021; Chu *et al.* 2023). Counter-ions are drawn to the solution's negatively charged suspended particles (Teh *et al.* 2016; Vepsäläinen *et al.* 2020). Ions with the same charge travel away from the interface of an electrolytic solution, causing repulsion, whereas ions with opposite charges move in the other direction. The Stern layer combines Van der Waals and electrostatic forces.

This phenomenon is separated into the Stern/Helmholtz layer, the inner plane, and the Gouy-Chapman layer, the outer plane (Brown *et al.* 2015; Tofail *et al.* 2016). A diffuse layer surrounds the Stern Layer because the main colloid's co-ions are drawn onto the counter-ions size (Tripathy *et al.* 2006; Bhamidipati *et al.* 2021). Charge separation is observed at the top of the colloidal particle when an electrical double layer causes it. As the ionic strength rises, the thickness of the double layer decreases, and peak destabilisation occurs when the colloidal surface's zeta potential approaches 0 mV (Schneider *et al.* 2011; Cruz *et al.* 2017; Bhamidipati *et al.* 2021).

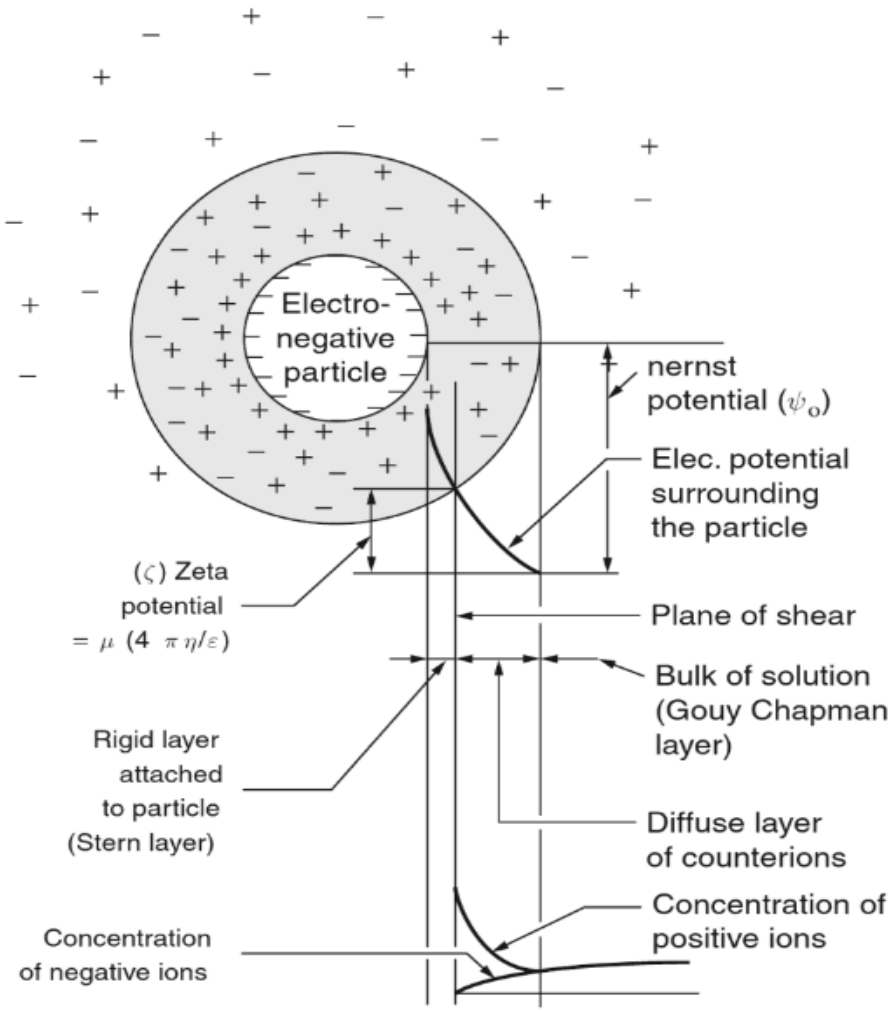

Figure 2-5: Graphical depiction of the electrical double layer (Bratby 2016).

2.4.2.2 Sweep

Sweep flocculation is the addition of inorganic salts into water for the precipitation of metal hydroxide, impurity particles, at a higher dosage can result in the interconnection of these precipitates, as they are produced and later collide, hence resulting in them being removed from water by settling (Duan *et al.* 2003; Kurniawan *et al.* 2020; Wang *et al.* 2021b). The

destabilisation of colloidal particles by charge neutralisation generally significantly improves particle removal through sweep flocculation. Thus, the aggregation rate significantly improves because of the increased solids concentration. (Ghernaout *et al.* 2012; Wang *et al.* 2021b; Khazaie *et al.* 2022). The open structure of the hydroxide precipitates substantially affects the volume concentration, even at a lower mass, which predominantly increases the possibility of capturing other particles. In addition, bridging particles by precipitated hydroxide can lead to more substantial aggregates. Increasing the coagulant dose in the sweep region allows for more significant quantities of sediment. Nevertheless, beyond the experimentally determined optimal dose, there is minimal additional enhancement in particle removal (Ghernaout *et al.* 2012; Nan *et al.* 2016; Wei *et al.* 2018). There are four coagulant dosage zones that are defined based on the mechanisms, influencing the negatively charged particles as follows:

- Minimal coagulant dosage; particles remain negatively charged and hence stable,
- Sufficient dosage for charge neutralization and subsequent coagulation,
- Increased dosage resulting in charge neutralization and restabilization,
- Elevated dosage leading to hydroxide precipitate and sweep flocculation.

2.4.2.3 Charge neutralisation

In the coagulation process, the specific adsorption of cationic species from solution is used to neutralise negatively charged particles. Charge destabilisation could be responsible for various materials such as iron, magnesium, aluminium, calcium, and silicon salts to produce cationic hydrolysis species and for their function as coagulants (Duan *et al.* 2003; Saxena *et al.* 2018). Electrostatic forces or a type of surface complex formation can cause the adsorption of cations on negatively charged surfaces, which subsequently decreases the repulsive energy barriers, thus causing increased coagulation (Wang *et al.* 2005; Ghernaout *et al.* 2012). Typically, minimal quantities of hydrolysing coagulant can cause the destabilisation of particles, with optimal destabilisation occurring when the particle charge is neutralised. Consequently, resulting in the colloidal particles gaining a positive charge and being restabilised. When the particle concentration is low, micromolar concentrations of coagulant causes the destabilisation and the restabilisation of particles (Stumm, 1992; Stumm and Morgan, 1962; Stechemesser and Dobiáš, 2005). Even if the species responsible for charge neutralisation include dissolved cationic hydrolysis products, there is evidence indicating that neutralisation could also occur through charged precipitates. This can occur through surface precipitation, or the adsorption of colloidal hydroxide precipitated in bulk solution and transmitted to the particles (Bratby 2016).

2.5 Chemical based coagulants

Conventional coagulants are used commercially in the industrial sector or laboratory, they are commonly used in the coagulation/flocculation process of wastewater. These conventional coagulants are separated into two categories, aluminium based which includes Poly-aluminium chloride, aluminium sulfate, aluminium chloride, sodium aluminate, poly-aluminium silicate amongst others and iron based which includes ferric chloride, ferric sulfate, ferrous sulfate, poly-ferric sulfate, ferric salts amongst others. Conventional coagulants are commonly used not only because they are effective but also because they are readily available and relatively low in cost, and they can operate over a broad pH spectrum. Conventional coagulants are effective in small concentrations and are capable of removing heavy metals, turbidity, organic and inorganic pollutants (Tolkou *et al.* 2021). A major disadvantage that comes with using chemical coagulants is the production of dangerous, toxic sludge, which requires an expensive method of disposal (Hossain *et al.* 2019b; Mat Yasin *et al.* 2020; Ngteni *et al.* 2020). Chemical coagulants are not biodegradable, which means that the treated water contains traces of these chemicals which may cause disease in humans. These coagulants can form multi-charged polynuclear complexes in solutions with enhanced adsorption characteristics.

2.5.1 Poly-aluminium chloride

There are numerous formulations of poly-aluminium chloride (PAC) preparations apart from aluminium choro hydrate. Most are in liquid form, but some are granular ground powder. When compared to other chemical coagulants such as alum at the same dosage, PAC causes faster flocculation and forms larger flocs (Abujazar *et al.* 2022). This is because these coagulants are pre-neutralized, have less of an effect on the pH of water, and so need less pH correction. The results obtained with this coagulant are equivalent to using aluminium sulphate in conjunction with a polyelectrolyte. However, neither the precise chemical nature of the product nor the reason for its enhanced performance is perfectly understood. Approximately half the dosage is required for turbidity removal, but the same dosage as aluminium sulphate is required for predominantly coloured waters. In cases where waters are predominantly turbid, the use of this coagulant may significantly reduce sludge disposal problems (Iwuozor 2019)Relative basicities range from 30 to 80%, and aluminium contents range from 5 to 12%, which is A1 in liquid products. The specific gravities of the liquid products range from 1.2 to 1.4 at 20^{o}C.

2.6 Emerging bio-coagulants (Natural coagulants)

Recently, advancements have been made in finding substitutes for chemical coagulants and flocculants in wastewater treatment (Kurniawan *et al.* 2022). These alternatives are called bio-

coagulants and bio-flocculants and can be produced from animals, microorganisms and plants (Kurniawan *et al.* 2022). Bio-coagulants are environmentally friendly green products, are low in cost, and can be used directly. The benefits of natural coagulants are presented in Figure 2-6 and Figure 2-7. Frequently used biosorbents for the remediation of heavy metal toxicants in the solution are agricultural wastes, including fruit peels, straw, coconut coir, and so on (Rocha *et al.* 2009; Zheng *et al.* 2009; Reddy *et al.* 2011).

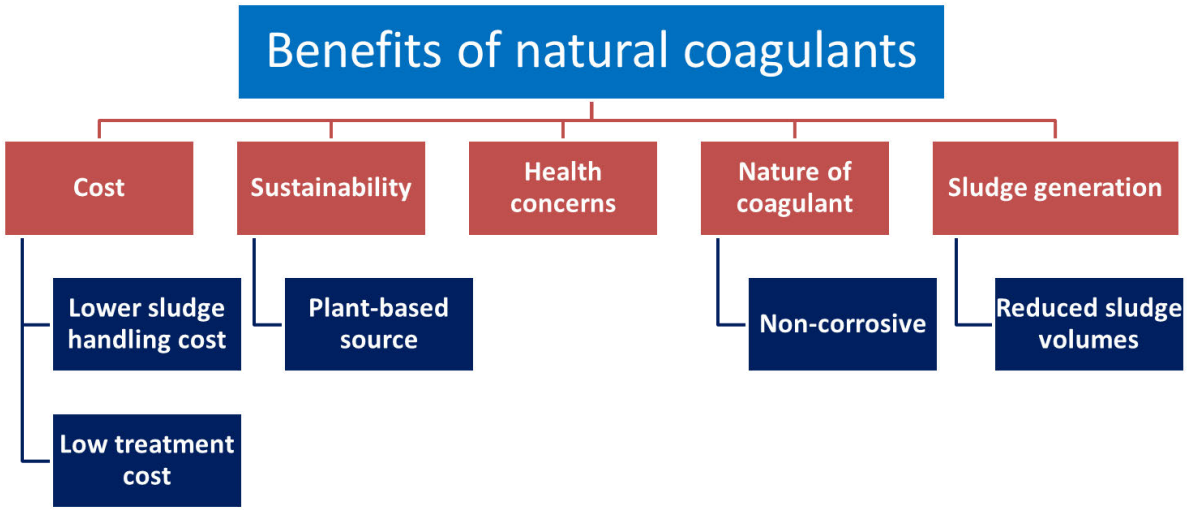

Figure 2-6: Advantages of natural coagulants over chemical coagulants (Koul *et al.* 2022).

Additionally, functional groups, such as carboxyl (–COOH), amino ($–NH_2$), and hydroxyl (–OH) may be present at the surface of the biosorbents, which can provide the site for complexation with the metal cations (Zheng *et al.* 2009). The oxygen or nitrogen atoms at the surface functional groups can form a coordinate bond with the divalent metal cations using non-bonding electrons. In other words, the presence of coordination sites or functional groups on the surfaces of biosorbents acts as a dominant factor in determining the adsorption capacities of these materials.

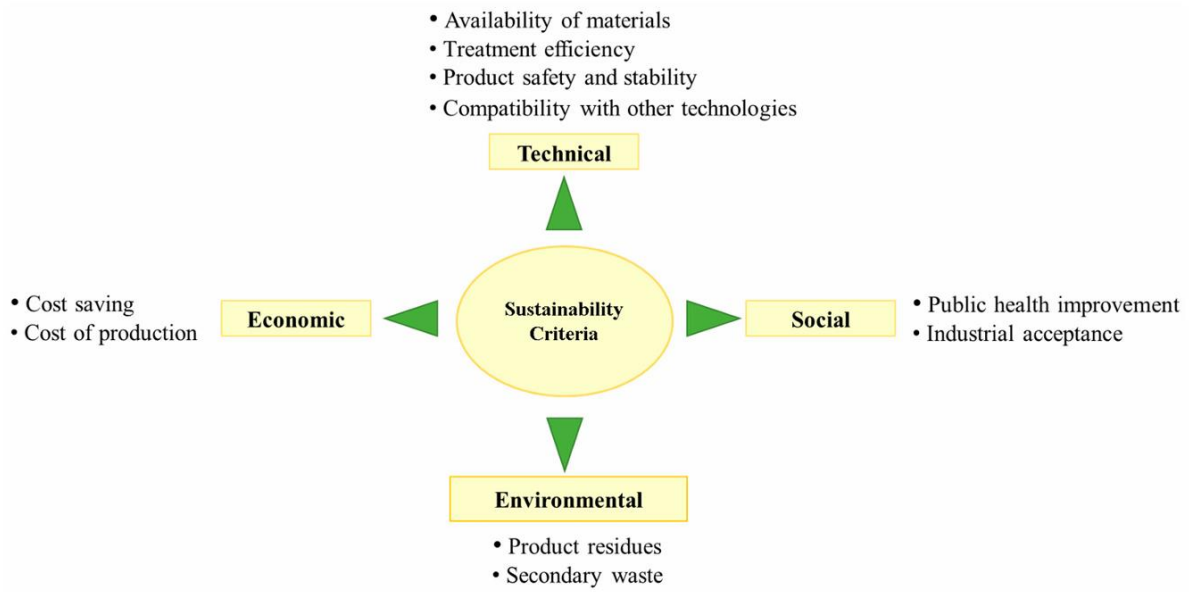

Figure 2-7: Criteria of natural coagulants (Koul *et al.* 2022).

2.6.1 Banana peels

As one of the most consumed fruits globally, the banana is a prevalent fruit. The primary banana residue is the fruit peel, which accounts for 30-40% of the total fruit weight (Mohammed *et al.* 2014). Various chemical groups exist on the banana peel surface, including carboxyl, hydroxyl and amide groups, which have been extensively proven to play a critical role in the biosorption processes (e.g. enhancing biosorption capacity and shortening the stable time) (Liu *et al.* 2012)

2.6.2 Eggshells

Eggs have been a staple of human diets for ages because they are packed with numerous critical elements, including high-quality protein. Besides milk, eggs are an excellent source of protein for people. Additionally, it is abundant in minerals, critical minerals, easily digestible lipids, carbohydrates, and amino acids (Bashir *et al.* 2015; Ajala *et al.* 2018). Recent years have shown a rise in the disposal of waste in landfills, which is directly attributable to the increase in the world population. The chicken eggshell is composed of a cuticle, crystal layer, spongy calcareous layer, pores, cores, and mammillary layer, as shown in Figure 2-8 and Figure 2-9. Eggshells are mainly composed of protein fibres, crystals of calcium carbonate ($CaCO_3$), magnesium carbonate ($MgCO_3$), and calcium phosphate ($Ca_3(PO_4)_2$). Eggshells are also composed of organic substances such as water, and calcite ($CaCO_3$), which is 90 – 98% of the eggshell (Mittal *et al.* 2016; Chou *et al.* 2023). The hard protective cover of the eggshell is derived by the outermost layer (cuticle), the calcium carbonate layer (testa) and the innermost

layer (Mammillary layer). The membrane in the eggshell consists of two different layers, which are the inner layer (surrounding the albumen) and the outer layer (attached to the tip of the calcified material of the shell) (Ajala *et al.* 2018).

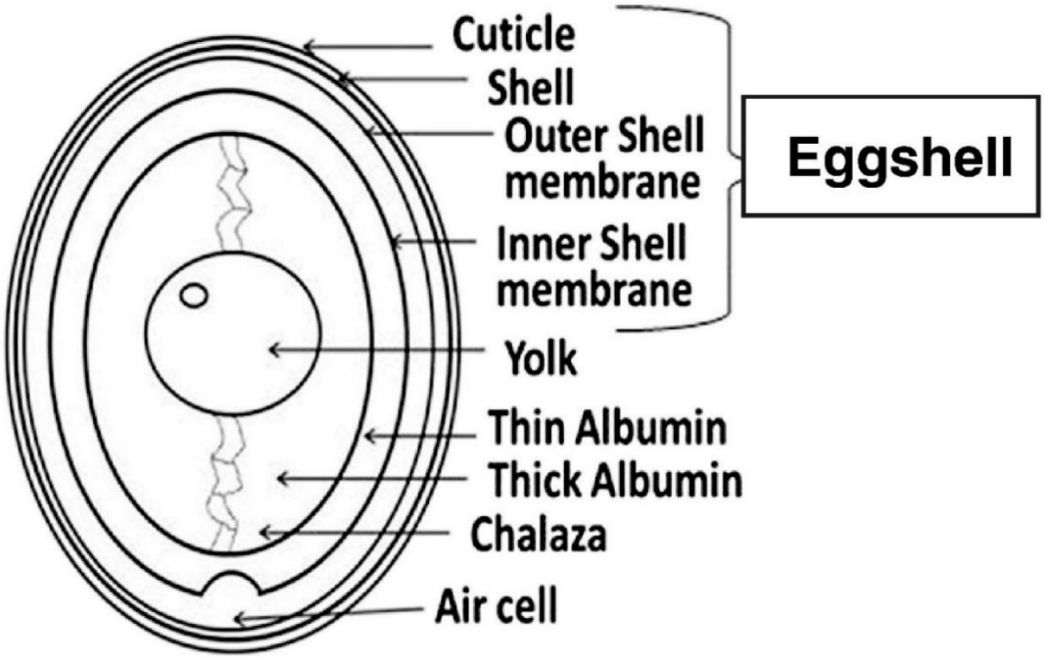

Figure 2-8: Egg and eggshell structure (Mittal *et al.* 2016; Ajala *et al.* 2018)

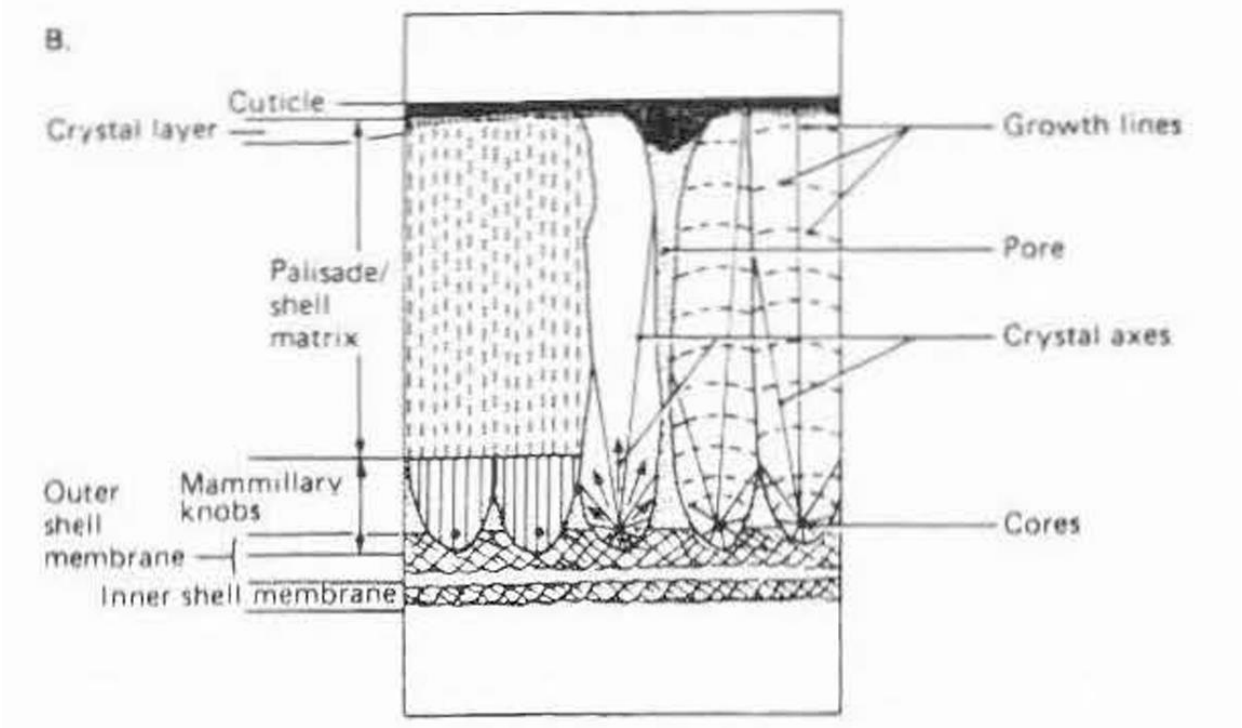

Figure 2-9: Schemetic diagram of the principal components of an eggshell (Hamilton 1986; Ajala *et al.* 2018)

With an annual production of 110 billion tons, attempts are being made to try and create commercial interest for eggshells adding value to the waste (Marques Correia *et al.* 2017; Chou *et al.* 2023). The eggshell can be utilised in various ways, which includes wastewater treatment. This is due to the many advantages the eggshell has, such as easy availability, its porous nature, cost-effectiveness, readily availability for use and no pre-treatment required before use.

2.6.3 Seashells

Seashells are exoskeletons of invertebrates generally found as waste along the shores of oceans. Seashells are also found in high amounts in landfills since due to the disposing of these materials from the seafood industry. Seafood is seen as a delicacy for many, but during preparation only the flesh is used, and the rest is disposed (Hassan *et al.* 2022). Seashells are renewable resources which can be recycled and used as secondary raw materials in various applications (Janković *et al.* 2022).

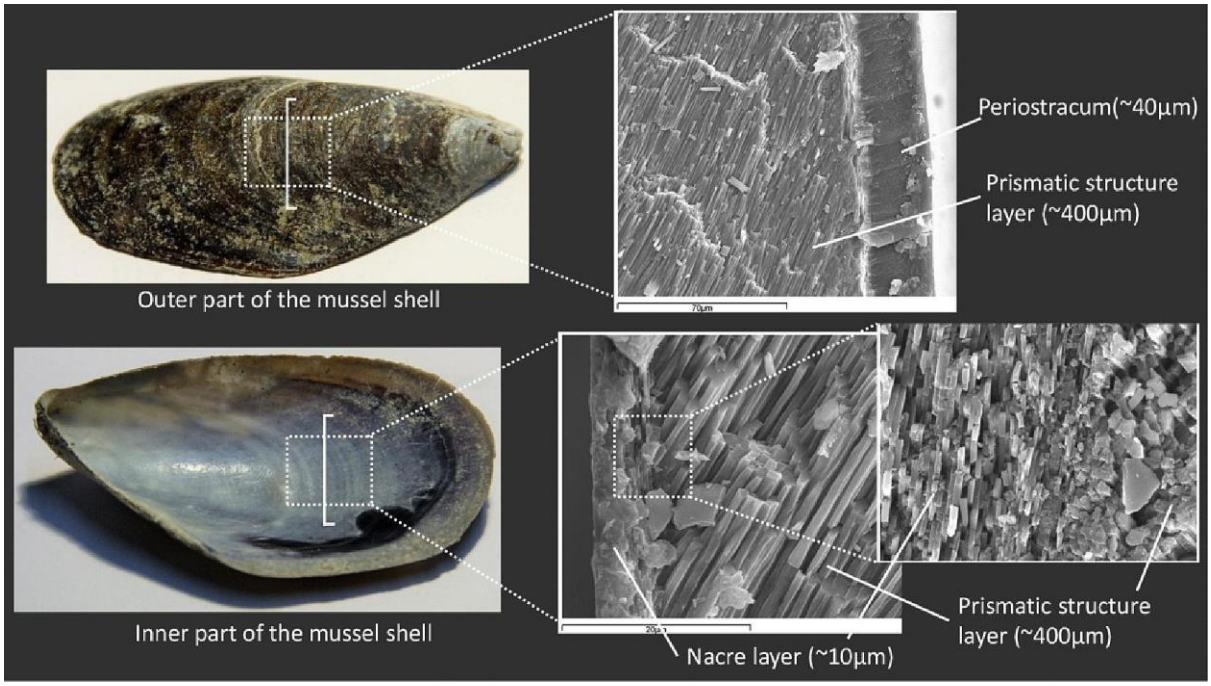

Figure 2-10: Structure of a seashell (Hamada *et al.* 2023)

Seashells are natural materials which are composed of an outer layer of protein, an intermediate layer of calcite and a smooth inner layer of calcium carbonate (Bulut *et al.* 2018; Tamjidi *et al.* 2020). Seashells are composed of 95% of calcium carbonate which makes it easier to absorb contaminants onto their active surfaces (Abraham *et al.* 2015; Tamjidi *et al.* 2020).

2.7 **Factors affecting coagulation**.

Various parameters need to be considered in optimising the coagulation process in water and wastewater treatment. To achieve the highest efficiency, various optimal conditions can be achieved for different coagulants with different operating conditions. Coagulant dosage, mixing speed, pH, mixing time, temperature and coagulant type are the main factors affecting the coagulation process's effectiveness and efficiency in water and wastewater treatment as seen in Figure 2-11.

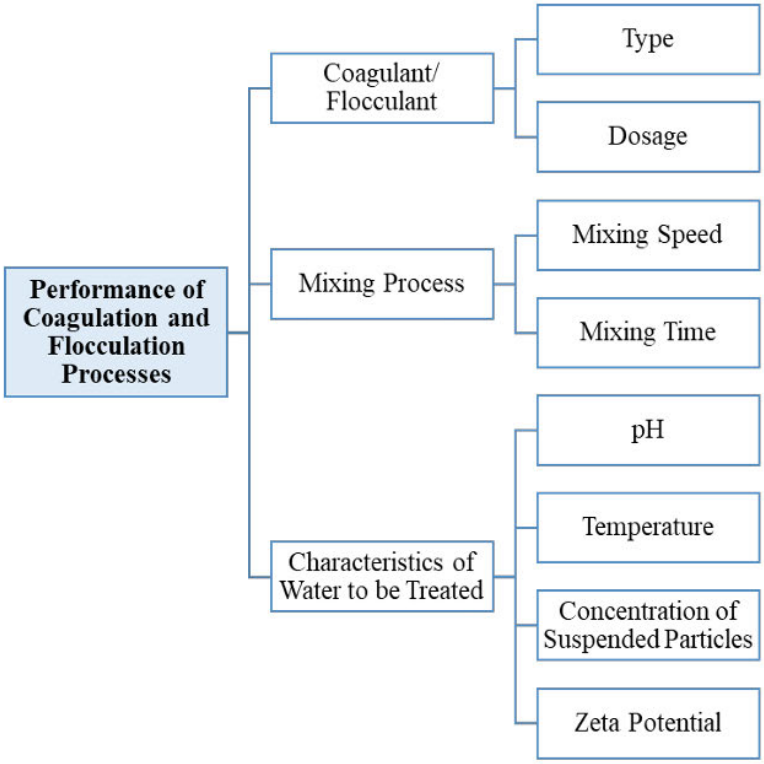

Figure 2-11: Factors affecting the coagulation process (Kurniawan *et al.* 2020).

2.7.1 Coagulant dosage

The optimum coagulant dosage is a vital parameter that entirely controls coagulation reactions. The impact of the coagulant dosage can be analysed and discussed in three different levels namely, underdosage, optimum dosage and overdosage (Yang *et al.* 2016). The optimum coagulant dosage causes aggregation of colloidal particles in both water and wastewater. If the dosage is under the optimum conditions disrupts the correct arrangement of colloidal particles, whereas excessive dosage contaminates the wastewater and increases the organic load, turbidity and sludge volume (Bahrodin *et al.* 2021). The optimum dosage becomes vital for charge neutralisation since excess dosage can result in destabilisation. The addition of the correct dosage will further neutralise the electrical load until it reaches zero zeta potential,

enhancing efficient attraction and adsorption of pollutants to coagulants (Yang *et al.* 2016; Zhao *et al.* 2021).

2.7.2 Mixing conditions

Mixing is an essential step in the coagulation process, these can be divided into two steps, fast (75-700 rpm) and slow mixing (30-150) (Abujazar *et al.* 2022). Fast or rapid mixing occurs after the addition of a coagulant and enables even distribution of the coagulant in wastewater for efficient treatment. Rapid mixing enhances the rate of formation of flocs and the adsorption, and it is also crucial for charge neutralisation because insufficient mixing can lead to local overdose or re-stabilisation of particles (Abujazar *et al.* 2022). Slow mixing occurs straight after fast mixing and it is essential for forming flocs via primary particle cohesiveness during flocculation (Lin *et al.* 2013). The intensity of slow mixing affects the size and structure of flocs during floc growth (He *et al.* 2012; Lin *et al.* 2013). Both slow and fast mixing influences the strength and size of the flocs formed.

Mixing time has an important role in ensuring successful collision efficiency by allowing ample time for aggregates to restructure into a more compact shear resistant floc when compared to mixing speed. Relatively shorter fast mixing time allowed for larger floc growth except the flocs were less shear resistant (less compact), whereas stronger but smaller flocs were formed in treatments with extended fast mixing time. This phenomenon could be explained by the presence of lower collision efficiency of small flocs due to extended high shear rate and floc breakage to a limiting size when fast mixing time is extended.

2.7.3 Temperature

The performance of the coagulation process is highly influenced by the temperature of the wastewater, as it affects the particle transport and collision rate by changing the density and viscosity of the suspension at various temperatures (Tetteh *et al.* 2019a; Dayarathne *et al.* 2022). The effectiveness of a coagulant is greatly affected by the temperature of the wastewater. The coagulation process is generally more effective when performed under warm temperatures. The aggregation of coagulants and contaminants occur in the coagulation process, and warmer conditions enable particles to travel quicker, and frequent collisions between pollutants occur, forming larger flocs (Bahrodin *et al.* 2021). Cold water, on the other hand, decreases the performance of the coagulation process since it will diminish the coagulant solubility and kinetic energy for particle flocculation and increase water viscosity (Sahu *et al.* 2013). Low water temperatures decrease the dissolution and floc formation of the coagulation process (Xiao *et al.* 2008; Dayarathne *et al.* 2022)

2.8 Contaminants in wastewater

Contaminants in wastewater has not only become a global environmental threat, it has also threatened the survival of the human society. Globally approximately 14000 people die daily, due to the consumption of contaminated water (Chaudhry *et al.* 2017). The contentment's in water can be divided into organic pollutants (pesticides, detergents, biomaterials, and pharmaceuticals), inorganic pollutants (heavy metals), and bio-organisms (Abdullah *et al.* 2022).

2.9 Emerging contaminants in wastewater

Emerging contaminants (ECs) refer to compounds, whether man-made or naturally occurring, with various properties that may remain in the environment and accumulate in animal and human tissues, with the potential to generate hazardous consequences even at low dosages. These compounds can disturb the normal functioning of endocrine systems by acting as endocrine disruptors. They are becoming a significant source of concern as pollutants. These are primarily organic compounds recently discovered in natural wastewater streams. Industrial and domestic activities produce them, including pesticides, medications, hormones, plasticizers, food additives, wood preservatives, laundry detergents, surfactants, disinfectants, flame retardants, and other organic compounds. These contaminants are released into aquatic ecosystems and different bodies of water, presenting health and environmental hazards. In this study, the removal of phenols, phosphates, nitrates, and ammonia were the contaminants of interest The discharge limits are presented per the South African National Standards and World Health Organisation in Table 2-3.

Table 2-3: The discharge limit of contaminants in wastewater.

Contaminant	**Source**	**Discharge limit from SANS 241 guidelines** (SANS-241 2015)	**Discharge limit from WHO guidelines** (WHO 2004)
Phenol	Gas and coke manufacturing, chemical plants	0.1 mg/L	-
Phosphate	Soap and detergent		3 mg/L
Ammonia	Coke/gas and chemical Manufacturing	≤1.5 mg/L	-
Nitrate	Inorganic fertilisers	11 mg/L	50 mg/L

The presence of nitrogen and phosphorous are essential for the growth and development of the structure and functioning of living organisms, and the presence of these elements in surface water and wastewater are significant indicators (Zhang *et al.* 2020; Shao *et al.* 2022; Zhao *et*

al. 2022). However, an excess of phosphorus and nitrogen can result in the occurrence of eutrophication in various water bodies (Xia *et al.* 2020b; Zhang *et al.* 2020). Phenol is an essential raw material in industry, however, the discharge of phenols into water bodies is toxic to humans and the environment (Said *et al.* 2021). The increase in agricultural activities has resulted in an increased ammonia discharge in wastewater and sludge digestion fluid. Ammonia has negatively impacted human health and has been extremely harmful to the aquatic environment, due to the excessive growth of harmful algae (Weralupitiya *et al.* 2021; Gao *et al.* 2023).

2.9.1 Phosphate

Phosphorus is a vital mineral nutrient essential for living organisms, however, an excess of this nutrient in water sources generates untreated waste from agricultural, household, and industrial sources as shown in Figure 2-12, which creates eutrophication issues (Farmer 2018; Vikrant *et al.* 2018; Capa-Cobos *et al.* 2021). Due to the increase in human population, the amount of phosphates released into the aqueous ecosystems has increased (Vikrant *et al.* 2018). As a result of the high concentration of phosphates in water streams, stringent laws have been placed to try to prevent eutrophication (Wu *et al.* 2020).

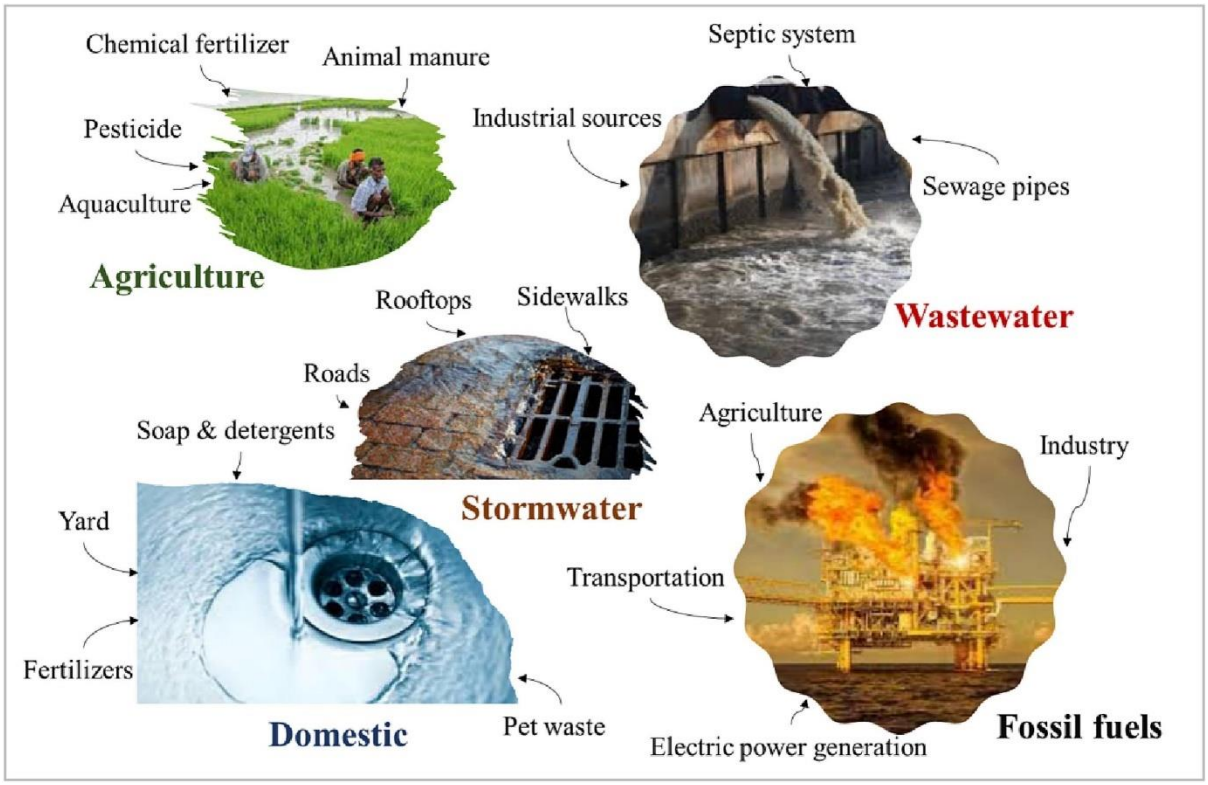

Figure 2-12: Sources of phosphorus (Owodunni *et al.* 2023).

2.9.2 Phenol

Phenol pollution has attracted significant attention due to the presence of organic compounds, such as phenol, in many types of industrial effluent. Phenol is recognized for its detrimental effects on ecological systems. Phenol in wastewater discharge is mostly derived from industries such as oil refining, pesticide manufacture, petrochemicals, and coke production. The increase in the use of phenolic compounds and their byproducts has led to the buildup of large amounts of aqueous effluent with high levels of phenolic pollutants (Mohammed *et al.* 2023). Phenol poses a significant environmental hazard due to its toxicity towards living organisms, even at minimal concentrations, resulting in detrimental effects on many bodily systems such as the skin, eyes, lungs, liver, kidneys, and central nervous system. Consequently, the presence of phenol in surface water is subject to stringent regulations set out by international regulatory bodies.

2.9.3 Ammonia

In wastewater, ammonia is a soluble nitrogenous chemical which consists of hydrogen and nitrogen atoms, as shown in Figure 2-13. Ammonia is the most common contaminant discharged into water streams, this is generally from industrial, agricultural and domestic wastewater (Karri *et al.* 2018). High concentration of ammonia in wastewater has a negative impact in the survival and well-being of the aquatic organisms (Mokgawa 2020; Bhat *et al.* 2021; Medhi 2021). It has the potential to negatively impact metabolism and reduce oxygen levels in water, resulting in the proliferation of algal blooms and the death of fish. Therefore, it is imperative to eliminate it to save the ecosystem (Medhi 2021).

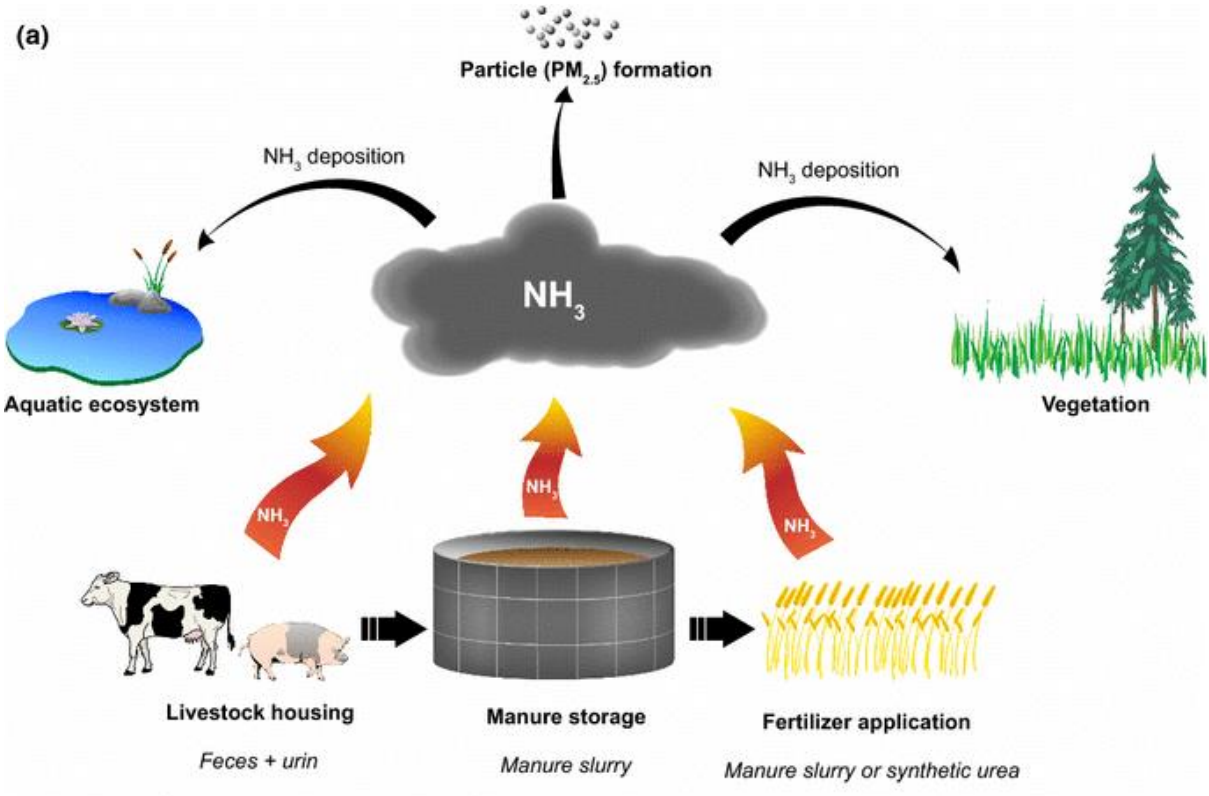

Figure 2-13: Ammonia emission from agriculture (Sigurdarson *et al.* 2018).

2.9.4 Nitrate

Nitrogen is an essential element for organic growth; however, in high concentration, nitrogen will produce excessive algae and eutrophication (which exist in the form of nitrates) in rivers, lakes and reservoirs (Zhang *et al.* 2020; Zhao *et al.* 2022). Nitrate pollution in groundwater is caused by nitrogen manure, sewage irrigation, organic manure, and livestock farming as shown in Figure 2-14 (Lin *et al.* 2020). High nitrate concentrations in wastewater have led to eutrophication in natural water bodies in recent years. Nitrate may be hazardous to people since it reduces to nitrite, which can change into carcinogenic nitrous amine (Xu *et al.* 2018). Due to the rise in population and development, there has been a rise is nitrate production worldwide and because of those reasons restrictions have been placed by governments before disposal of nitrates and other contaminants (Lin *et al.* 2020; Zhang *et al.* 2020).

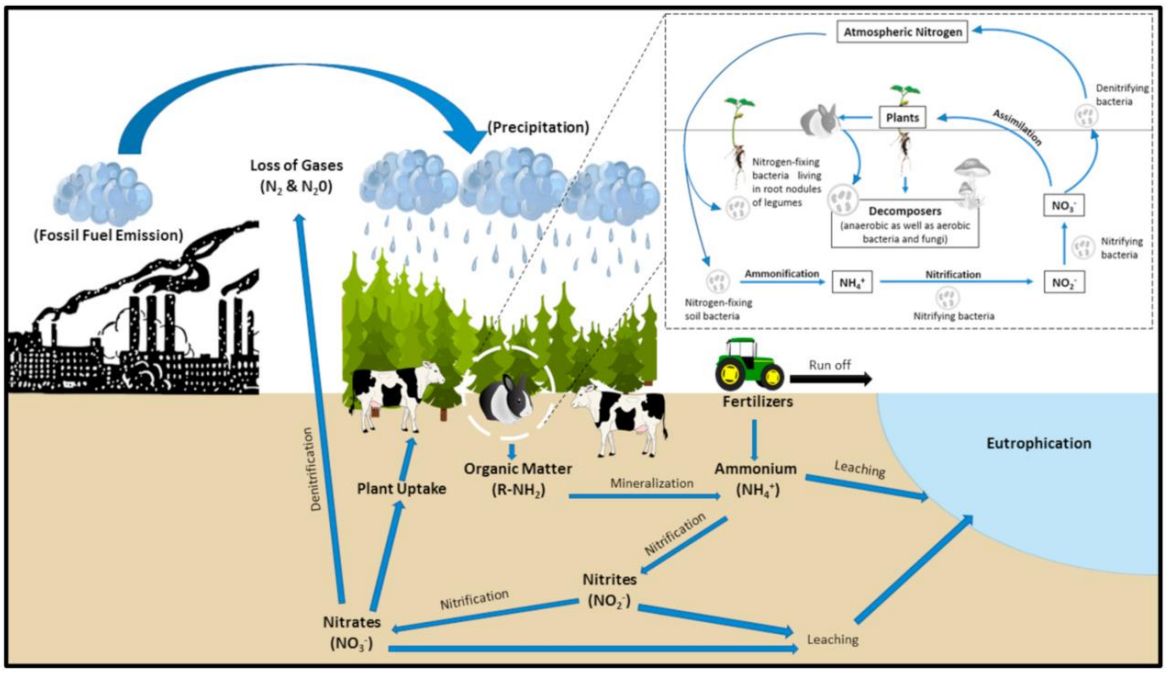

Figure 2-14: Sources of nitrates and their distribution and contamination of the environment (Singh *et al.* 2022).

2.9.5 Water quality parameters

The coagulation process enhances the degree of removal of contaminants and colloidal matter in water and wastewater treatment. These can include Turbidity, chemical oxygen demand (COD), biochemical oxygen demand (BOD), total suspended solids (TSS), colour, and total dissolved solids (TDS).

2.9.5.1 Turbidity

Turbidity is a quantitative assessment of the clarity of water. The colloidal particles and the presence of suspended solids in water greatly influence it. The primary cause of turbidity in surface water is the erosion of colloidal particles such as clay, silt, rock pieces, and microorganisms. The units of measurement used for turbidity include the Jackson Turbidity Unit (JTU), the Formazine Turbidity Unit (FTU), and the Nephelometry Turbidity Unit (NTU). A suspended solid refers to any material that is suspended in water and meets the criteria for being classified as a suspended solid. The determination is achieved by the process of filtering, followed by the measurement of the weight of the filter paper after it has been dried and then deducting the weight of the filter paper. The unit of measurement is milligram per Liter (mg/L). These suspended particles are present in both surface water and wastewater, originating from domestic and industrial areas.

2.9.5.2 Chemical oxygen demand

Chemical Oxygen Demand (COD) quantifies the oxygen required to completely oxidise organic substances in a water sample. COD is used to evaluate the water quality and the environmental implications of wastewater discharge. Higher COD levels indicate increased organic pollution, decreasing dissolved oxygen (DO) levels and posing a threat to aquatic organisms. COD emissions can minimised by treating wastewater before release. Water with elevated chemical oxygen demand (COD) often indicates the presence of significant amounts of decomposing plant matter, human excrement, or industrial discharge.

2.9.5.3 Colour

The colour of the wastewater discharged into various receiving water bodies has become an environmental hazard, especially to aquatic life. The discolouration of wastewater released into aquatic life reduces the penetration of solar radiation into the water, affecting the photosynthetic activity and hence affecting the growth of aquatic plants (Khattri *et al.* 2000; Collivignarelli *et al.* 2019).

2.10 Design of experiment

Traditionally, the ‘one-factor-at-a-time ‘technique was used for the optimisation of the treatment process, in which one parameter would be varied while the others were kept at a constant level. However, this technique not only fails to identify possible interactions between variables but is also time-consuming and expensive because a large number of experiments must be carried out (Teh *et al.* 2014). Statistically designed experiments allow efficiency and are quite economical in that they require a relatively small number of experiments but are still able to be analysed by statistical methods and result in valid and objective conclusions. The statistical approach to experimental design is crucial if meaningful conclusions are to be drawn from the data. When the problem involves data that are subjected to experimental errors, a statistical method is the only systematic approach to analyse the data (Zainal-Abideen *et al.* 2012).

2.10.1 Predictive mathematical modelling

Response surface methodology is a collection of statistical and mathematical methods that are useful for modelling and analysing engineering problems. In this technique, the main objective is to optimize the response surface that is influenced by various process parameters (Khuri *et al.* 2010; Eyjolfsson 2015; Myers *et al.* 2016). Response surface methodology also quantifies the relationship between the controllable input parameters and the obtained response surfaces.

Response surface methodology (RSM) was developed by Box and Wilson (1951) to improve production processes in the chemical industries (Myers *et al.* 2016; Mahallati 2020). Certain procedures need to be followed when using RSM, this includes, designing a series of experiments for adequate and reliable measurement of the response of interest, developing a mathematical model of the second-order response surface with the best fittings, finding the optimal set of experimental parameters that produce a maximum or minimum value of response and Representing the direct and interactive effects of process parameters through two and three-dimensional plots (Aslan *et al.* 2007).

2.11 Kinetic study

The kinetic model best describes the factors that affect the rate of adsorption such as mass transfer and reaction processes (Sukmana *et al.* 2021). The kinetic model can be classified as coagulation reaction models and adsorption diffusion models. The coagulation reaction model is crucial for understanding the physical and chemical behaviour of coagulants, including physisorption and chemisorption, and determining the rate of coagulant absorption (Mat Yasin *et al.* 2020). Whereas the adsorption diffusion model only constructed based on external diffusion, internal diffusion and mass transfer (Musah *et al.* 2022). Coagulation kinetics may be analyzed using linear or non-linear models. The accuracy of fit index determines the optimal model to explain the process (Wang *et al.* 2020b).The pseudo-first order and the pseudo-second order are one of the proposed models to describe data of coagulation and adsorption as shown in Table 2-4. The pseudo-first-order rate is a first-order rate equation that describes the rate of adsorption at a given time. This is directly proportional to the difference in concentration and rate of removal over time (Hu *et al.* 2022). The pseudo second-order models describe the reaction rate that relies on the square of the concentration of a single reactant (Shahwan 2014; Salvestrini 2018).

Table 2-4: Kinetic models used for coagulation/adsorption reactions (Sukmana *et al.* 2021; Hu *et al.* 2022)

Kinetic model	**Equations**		**Plot to be drawn**	**Nomenclature**
	Non-Linear form	**Linear form**		
Pseudo-first order kinetic model		$ln(qe - qt) = lnqe - k_1 t$	$ln(qe - qt)\ vs\ t$	k_1 (min-1) - pseudo first-order rate constant qt (mg/mg) - adsorption capacities at time t qe (mg/mg) – equilibrium adsorption at time t

				t (min) - coagulation time.
Pseudo-second order kinetic model	$\frac{dq_t}{dt} = k_2(qe - qt)^2$	$\frac{t}{qt} = \frac{1}{k_2 qe^2}\frac{1}{qe}t$	$\frac{t}{qt}\ vs\ t$	k_2 (L/mg min) - pseudo-second-order rate constant, qe (mg/mg) the adsorption capacity of impurity at equilibrium and qt (mg/mg) - adsorption capacity of impurity at time t t (min) - coagulation time.

2.12 Adsorption isotherm

Isotherm modelling is a mathematical method used to characterise the equilibrium of coagulation between a coagulant and an adsorbate (Hossain *et al.* 2019a; Mat Yasin *et al.* 2020). This provides data on the partitioning of adsorbable solutes across the liquid and solid phases at different equilibrium concentrations (Rangabhashiyam *et al.* 2014). Various isotherm equations have been used to depict the equilibrium curve for eliminating organic contaminants from different industrial effluents. These equations include both conventional and modified isotherm models (Ajiboye *et al.* 2021). The various adsorption isotherm models are represented in the Figure 2-15.

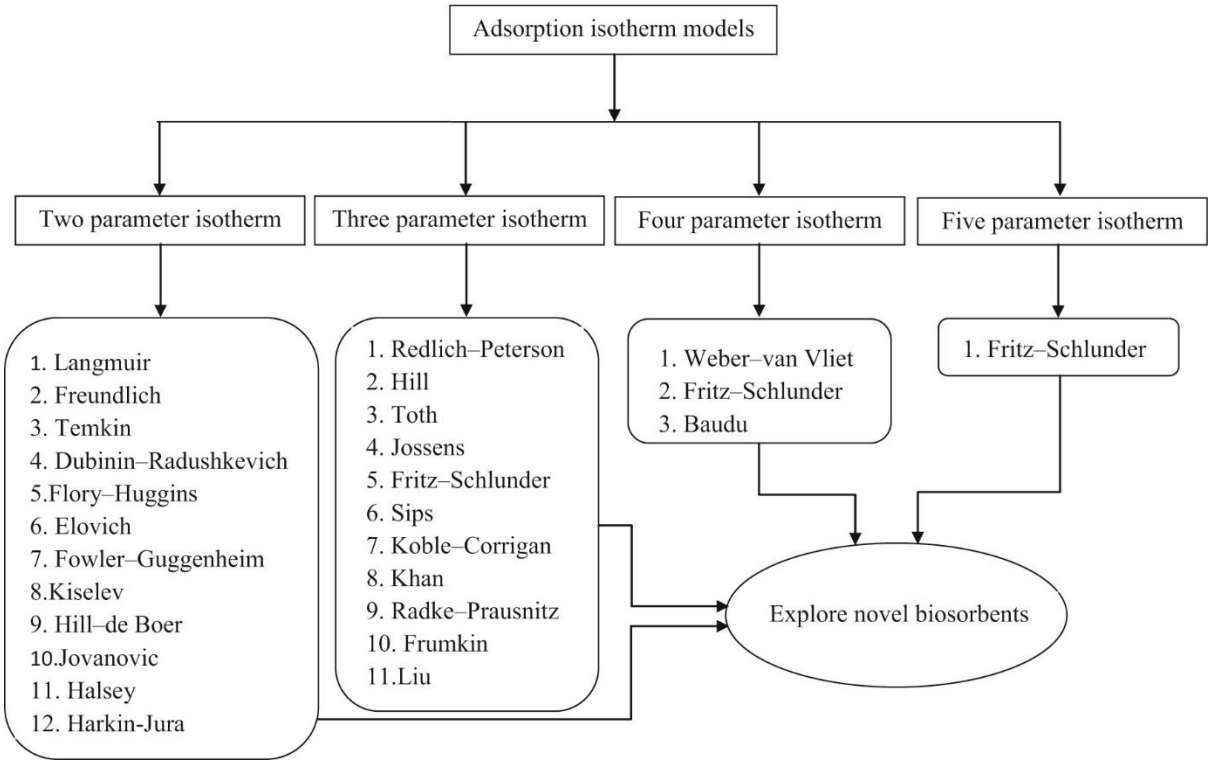

Figure 2-15: Adsorption isotherm models (Rangabhashiyam *et al.* 2014)

The Langmuir and Freundlich models are widely utilised for the removal of organic contaminants (Ajiboye *et al.* 2021). The Langmuir model quantitatively describes the formation of monolayer adsorbate on the outer surface of the adsorbent, where no absorption occurs after (Scheufele *et al.* 2016). Monolayer adsorption, homogeneous sites, constant adsorption energy, and no lateral interaction between the adsorbed modules are assumptions made to write the Langmuir isotherm, which is listed in the table below. The Freundlich isotherm is an empirical model that may be described as the process of multilayer adsorption on sites that are not uniform in nature. The statement presupposes that heat distribution during adsorption and the attraction towards the heterogeneous surface is not uniform. The equations for the Langmuir and the Freundlich isotherms are represented in Table 2-5.

Table 2-5: Adsorption isotherm models used for the coagulation/adsorption reaction (Girish 2017; Ajiboye *et al.* 2021).

Isotherm types	**Equations**		**Plot to be drawn**	**Nomenclature**
	Nonlinear form	**Linear form**		
Langmuir	$q_e = \frac{q_m b C_e}{1+bC_e}$	$\frac{C_e}{q_e} = \frac{1}{q_m b} + \frac{C_e}{q_m}$	$\frac{C_e}{q_e}\ VS\ C_e$	q_e – Equilibrium metal adsorption capacity. q_m and b – Langmuir constant associated to maximum adsorption capacity (monolayer

		$\frac{1}{q_e} = \frac{1}{bq_mC_e} + \frac{1}{q_m}$ $q_e = q_m - \frac{q_e}{bC_e}$ $\frac{q_e}{C_e} = bq_m - bq_e$	$\frac{1}{q_e}\ VS\ \frac{1}{C_e}$ $q_e\ VS\ \frac{q_e}{bC_e}$ $\frac{q_e}{C_e}\ VS\ q_e$	capacity) and bonding energy of adsorption, respectively. C_e – Equilibrium solute concentration in solution.
Freundlich	$q_e = kC_e^{\frac{1}{n}}$	$\log q_e = logk + \frac{1}{n}\ logC_e$	$logq_e\ VS \log C_e$	k - Adsorption equilibrium constant. n – intensity of absorption constant.

2.13 Summary

The literature review has shown that the discharge of untreated industrial effluent has been detrimental not only to the environment but also to human life. Coagulation has been frequently used for the treatment of effluent. However, the treatment of emerging contaminants using conventional/chemical coagulants has proven to be inefficient in the treatment of contaminants in wastewater and produces secondary pollutants. The various drawbacks that come with using chemical coagulants have resulted in an active search for a more sustainable and environmentally friendly solution for contaminant removal. As a result, researchers and various wastewater treatment institutions have investigated bio-coagulants as a substitute to chemical coagulants.

Bio-coagulants are environmentally friendly green products that are easily accessible and can be produced from animals, plants and microorganisms. In this research eggshells, seashells and banana peels were chosen as bio-coagulants for the treatment of wastewater. These bio-coagulants have many advantages over conventional coagulants. They are non-toxic, simple to handle, and produce biodegradable sludge that can be reused and economical.

Chapter 3: Materials and methods

The experimental techniques and various concepts of this study are thoroughly explained in this chapter. The instructions used for the application of this study are discussed. The step-by-step preparation of the bio-coagulants and characterisation of these bio-coagulants are also found in this chapter.

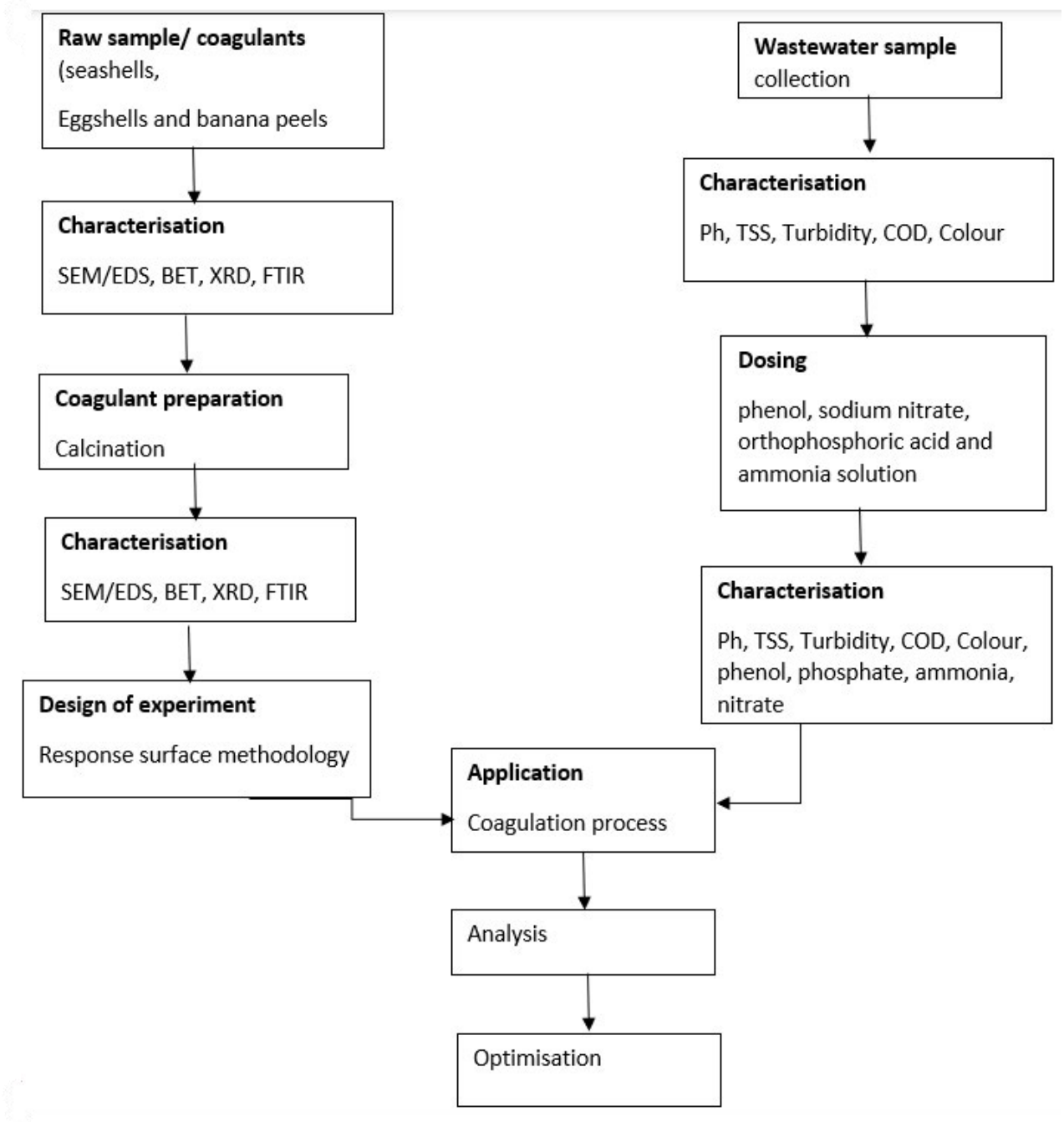

Figure 3-1: A visual summary of the research done.

3.1 Materials and equipment

3.1.1 Chemicals and reagents

All the chemicals and reagents used in this research were analytical grade and purchased from a local supplier in South Africa and used for the synthesis of the wastewater. Four chemicals were used for the synthesis of the wastewater:

- 90% liquified phenol (United Scientific, South Africa)
- Sodium nitrate ($NaNO_3$: 84.99, Associated chemical enterprises, South Africa)
- 85% Orthophosphoric acid (H_3PO_4 : 98, Associated chemical enterprises, South Africa)
- 25% Ammonia solution (H_5NO, Minema Chemicals, South Africa)

Poly-aluminium chloride was used as a coagulant in the coagulation process.

3.1.2 Analytical instruments

The analytical instrumentation used in this study are listed below. This includes instruments used to analyse wastewater contaminants before and after treatment.

Table 3-1: Analytical instruments used in the study

Water quality parameters	Instruments
COD (mg/L)	DR3900 HACH spectrophotometer
pH	Hanna pH meter (HI2002 edge)
Turbidity (NTU)	HACH 2100N turbidimeter
Colour (Pt. Co)	DR3900 HACH spectrophotometer
Phosphates	Handheld Colorimeter phosphate
Phenols	Handheld Colorimeter phenol
Ammonia	Handheld Colorimeter ammonia
Nitrate	Handheld Colorimeter nitrates

3.1.3 Wastewater sampling

Municipal wastewater was used for this study. The wastewater was collected from the Amanzimtoti wastewater treatment plant at the pretreatment section in the Kwa-Zulu Natal province in South Africa. The point of collection was effluent, and the sample collected was the feed to the clarifiers.

3.2 Synthesis and characterisation of wastewater

3.2.1 Synthesis of wastewater

After collection, the wastewater was characterised as per APHA (2012). The raw water was characterised by various parameters such as turbidity, pH, colour, COD, Phosphate, nitrate, ammonia and phenol as shown in Table 3-2.

Table 3-2: The characterisation of raw wastewater before treatment

Water parameters	Before treatment
Colour	1803,184 uS/cm
Turbidity	372 NTU
COD	1408 mg/L
Ph	6.97
Nitrate	50 mg/L
Phosphate	5 mg/L
Phenol	1 mg/L
Ammonia	5 mg/L

3.3 Preparation and characterisation of bio-coagulants

3.3.1 Calcination

Calcination is a thermal treatment process that uses extremely high temperatures in the absence of oxygen for the alteration of physical or chemical properties of solid materials. This process produces an adsorbent that is more porous and rougher and leaves voids behind that eventually become pores. This is a result of volatiles inside the particles' microstructure escaping due to high temperature, calcination Also, it was discovered that, although chemical modification reduces the adsorbent's overall surface area, it increases the adsorption capacity due to changes in functional groups (Ighalo *et al.* 2020).

3.3.2 Sample Preparation

3.3.2.1 Banana peels

Fresh waste banana peels were collected from a local Fruits and Vegetables Market in Durban, South Africa. Banana peels were thoroughly washed using deionised water (ELGA PURELAB Option-Q water deionizer, UK) to remove the dirt and associated impurities. The washed peels were placed on trays and oven dried at a temperature of ±105^{o}C for 24 hrs to remove any moisture content. Thereafter, dried banana peels were cut into small pieces and ground to powder using a blender and using laboratory sieve trays, was sieved to uniform particles of 300

– 425 µm. The ground powder was calcinated at 600^{o}C for 2 hours . The calcinated banana peel were stored in an airtight container prior to being characterised.

3.3.2.2 Seashells

Seashells were collected from a local public beach as beach sand leachate in Durban, South Africa. The seashells were thoroughly washed using tap water to remove dirt material, followed by rinsing using deionised water. The seashells were then oven dried at ±105^{o}C for 24 hours. The dried seashells were first crushed into small pieces and ground using a blender to a fine powder and sieved to uniform size particles ranging at 300 – 425 µm using laboratory sieve trays. Ground seashells were calcinated at 800^{o}C for 3 hours, thereafter, the calcinated seashells were stored in an airtight container.

3.3.2.3 Eggshells

Eggshells were collected from a local bakery as waste in Durban, South Africa. The eggshells were thoroughly washed using tap water to remove all adhering dirt followed by rinsing using deionised water. The eggshells were oven dried at ±105^{o}C for 24 hours. The dried eggshells were first crushed, and ground using a blender to fine powder and sieved to uniform particle sizes ranging at 300 – 425 µm thereafter calcinated at 800^{o}C for 3 hrs and stored in an airtight container.

3.3.2.4 Characterisation

The following analytical techniques were used for the characterization of the calcined and uncalcined bio-materials:

- X-ray diffraction spectroscopy (XRD),
- Fourier-transform infrared spectroscopy (FTIR),
- Scanning electron microscopy combined with energy dispersive x-ray spectrometry (SEM/EDS),
- Brunauer-Emmett-Teller (BET).

3.3.2.5 Scanning electron microscopy/ Energy dispersive x-ray spectrometry SEM/EDS

The SEM/EDS utilises electron beam to generate high-resolution and high-magnification images of the sample surface. This this approach provides comprehensive imaging data on the morphology and surface texture of individual particles (Ali *et al.* 2023). In this study, the (SEM/EDX) (JOEL JEM 2100 combined with a Thermo Fischer detector for EDS) were used to analyse the morphology of bio-coagulants at the Council for Scientific and Industrial Research in CSIR South Africa. A 200 kV acceleration voltage was used. The samples were

dissolved in Ethanol and sonicated for ±20 minutes and dispersed on a carbon coated copper grid for analysis.

3.3.2.6 Fourier-transform infrared spectroscopy (FTIR)

FTIR is an analytical technique wherein a beam of infrared light passes through the sample, inducing vibration of chemical bonds. This results in the samples absorption of infrared radiation. Light is transmitted and indicates that the quantity of energy that was absorbed at each wavelength. This technique is executed with a monochromatic beam that varies in wavelength over time, or by employing a Fourier transform apparatus that simultaneously measures infrared wavelengths. An absorbance or transmittance spectrum will be done, which will reveal at which infrared wavelengths the sample absorbs, this is followed by characterising the absorbed wavelength for the chemical groups (Griffiths and Haseth, 2007; Mackenzie, 1988; Smith, 2011). The functional groups and molecular decomposition of the model bio-coagulants were ascertained using the FTIR spectrometer (Agilent technologies microlab model) at room temperature over the wavenumber range of 400-4000 cm^{-1}. This was done to record the functional groups of the bio-coagulant and the organic, inorganic, and polymeric molecular structures.

3.3.2.7 X-ray diffraction spectroscopy (XRD)

The XRD technique is utilised to identify the mineralogical composition of the crystalline materials. It is used an analytical tool that is non-destructive used for phase identification of minerals and ores in mining and mineral processing. It is an essential analytical technique in engineering, as it is used for the characterisation of samples and quality control. Fundamental, the principle of the XRD technique is the interaction between x-rays and a crystalline materials which generates a diffraction pattern which is always the same for 88 material. Each individual material within a mixture exhibits a distinct diffraction pattern. This pattern is characterized by an incident beam that forms an angle theta (θ) with the crystal planes that remain stationary. Consequently, a diffracted beam is generated at an angle 2-θ relative to the incident beam (Tran *et al.* 2024). In this study (XRD), patterns were recorded using a diffractometer system (XPERT PRO) at the Council for Scientific and Industrial Research in CSIR South Africa to identify the composition and phase of the bio-coagulants. Using anode material Cu, radiation at 45 kV and 40 mA.

3.4 Coagulation equipment design

The coagulation process was done using a jar tester (JTL6) which had six paddles as shown in Figure 3-2. This process simulates the coagulation process in water treatment plant. All the experiments were conducted with 500mL of wastewater in a 1L beaker (Appendix A – Figure 6-6).

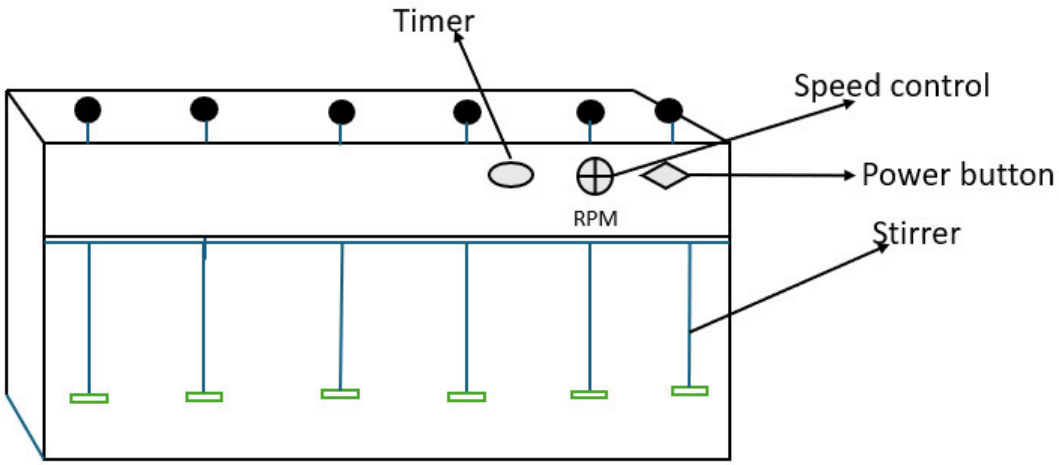

Figure 3-2: Schematic diagram of a jar tester

3.5 Coagulation experimental procedure

The optimum dosage of the calcined and uncalcined bio-coagulants was obtained at a range of 1-6 g/L. The mixing rate of 150 rpm fast mixing and slow mixing of 30-150 rpm was also investigated to obtain the optimum mixing speed. The effect of mixing time and settling time (20-120 min) was also investigated to obtain the optimum conditions. After settling approximately 10mL of the wastewater, was collected at the surface of the beaker using a syringe for analysis. The treated sample was furthermore characterized for turbidity, colour, and TSS, whereby the percentage removal was calculated using the Equation 3-1.

$$Percentage\ (\%) removal\ efficiency\ C^n = C^i - C^f C^i \times 100 \qquad \text{Equation 3-1}$$

3.6 Response surface methodology (RSM)

RSM was used to determine the optimum dosage (g/L), mixing time (Min), mixing time (min) and settling time (min) of the various bio-coagulants as shown in Table 3-3. The Design-Expert software version 13 was used to develop the matrix used for the experiments. The experiments were done in duplicates for verification, with the responses being colour (uS/Cm), turbidity (NTU) and COD (mg/L). A four-factor, three-level, Box-Behnken design with 26 experiments was used to obtain the best operating parameters and to optimise the percentage removal efficiency in the coagulation process. This is crucial for collecting data that can be utilised to

develop and refine modelling techniques for each response, to establish comprehensive knowledge and to show interactions and relationships between the input variable and the responses.

Table 3-3: Input variable with lower and upper limits

Input factor	Lower Limit	Upper Limit
Speed	30 rpm	150 rpm
Dosage (bio-coagulant)	1 g/L	6 g/L
Dosage (poly-aluminium chloride)	0.1 g/L	0.6 g/L
Mixing time	2 min	15 min
Settling time	20 min	120 min

3.7 Kinetic study and coagulation isotherms

A kinetic study was conducted to better understand the rate of coagulation. 1 L of the wastewater was poured into a 2 L beaker. The optimal bio-coagulant (based on removal efficiency) was added into the wastewater and placed into a jar tester. The optimum conditions were adopted from RSM and were used to conduct the experiment. Sampling took place at 10-min intervals from 0 to 100 min. Where the solution was removed from the beaker using a syringe and analysed using the HACH 2100N turbidimeter. The data obtained were used to fit the model of the adsorption kinetics using the Pseudo-first and Pseudo-second order models shown in Equation 3-2 and Equation 3-3, respectively (Sukmana *et al.* 2021; Hu *et al.* 2022).

$$\ln(\mathrm{qeq} - \mathrm{qt}) = \ln(\mathrm{q}eq) - k1t \qquad \text{Equation } 3-2$$

$$\left(\frac{t}{q_t}\right) = \frac{1}{k_2 q^2{}_{eq}} + \frac{1}{q_{eq} t} \qquad \text{Equation } 3-3$$

Where q_{eq} is the concentration of contaminant in the sample at equilibrium (mg/L), it is the concentration of contaminant in the sample at any time (t), k_1 is the pseudo-first-order rate constant of adsorption, and k_2 is the pseudo-second-order rate constant of adsorption.

The Langmuir and Freundlich isotherm models are frequently used in adsorption investigations to determine the equilibrium concentration and adsorption capacities of the bio-coagulant/adsorbent . The Langmuir isotherm model suggests monolayer adsorption with the same adsorption energy across every point. The model equation for Langmuir and Freundlich are provided in Equation 3-4 and Equation 3-5 (Wang *et al.* 2020a) .

$$q_e = \frac{q_m b C_e}{1 + b C_e} \quad \text{Equation } 3-4$$

$$q_e = k C_e^{\frac{1}{n}} \quad \text{Equation } 3-5$$

Chapter 4: Results and discussion

This section summarizes the findings from the experimental study done. The synthesis and characterization of bio-waste materials that may replace poly-aluminium chloride (PAC) for wastewater coagulation. In addition, the feasibility study for wastewater treatment using bio-coagulants is included. Furthermore, RSM was used to optimize both the bio-coagulant and the conventional coagulant, followed by a kinetic study.

4.1 The characterisation of the bio-coagulants

This section presents the results obtained in line with objective one, which focuses on the synthesis and characterisation of the biowaste materials.

4.1.1 Scanning electron microscope (SEM)

The morphology of the banana peels (BP), eggshells (ES), seashells (SS), calcined banana peels (CBP), calcined eggshells (CES) and calcined seashells (CSS) was analysed using the SEM. The SEM micrographs in Figure 4-1 show the morphological behaviour of the raw and calcinated model bio-coagulants before and after calcination. It was apparent that surface modification of the bio-coagulants resulted in variation in morphological structure for all samples.

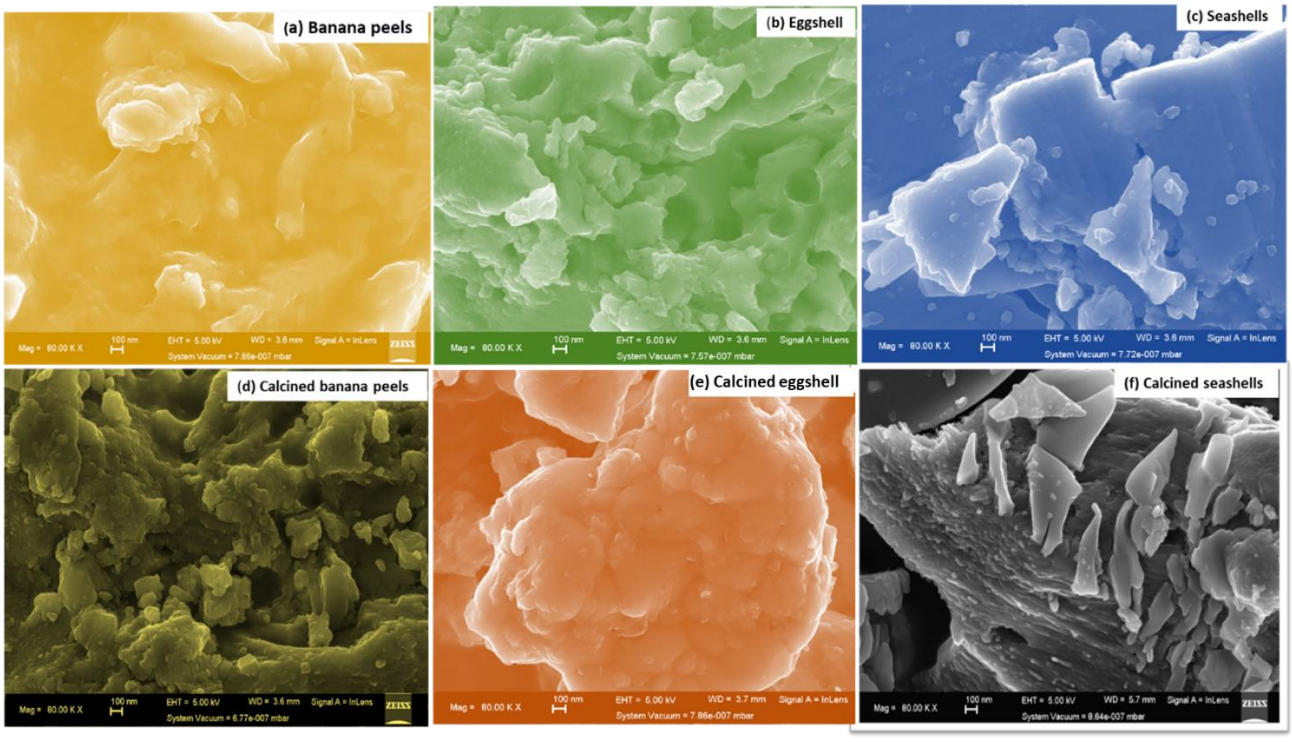

Figure 4-1: SEM magnified images (a-f) showing uncalcined and calcined bio-coagulants

The SEM results of BP, ES, SS and CBP are represented with a width distance of 3.6 mm whereas the CES have a width distance of 3.6 mm and 5.7 mm for CSS. The magnification of all the images were viewed at 80 KX with a microscale of 100 nm and an acceleration voltage of 5 kV. The difference in appearance of the uncalcined and calcined bio-coagulants was due to the calcination process, which occurred at a temperature of 600°C for BP and 800°C for ES and SS, this process is known to increase the liquid-solid adsorption capacity (Amo-Duodu *et al.* 2021; Precious Sibiya *et al.* 2021). BPs (Figure 4-1a) structure has an amorphous and irregular shape as compared to the CBPs' structure (Figure 4-1d) (Dmochowska *et al.* 2020). The ascertained SEM results are attributed to the BP particles being linked together, creating nanoscale spherical agglomerated structures, which result in dispersed nano-sized inter-particular spaces (Ezekannagha *et al.* 2023). The CBP (Figure 4-1d) appeared as aggregated particles. In comparison to the depiction of the BP, the surface of the CBP is rougher with high micropores. ES (Figure 4-1b) have an irregular, crystal-like structure with poorly defined voids, in contrast to the CES (Figure 4-1e), which has a smooth surface with rod-like fibrous structures, and it is more porous compared to the ES. The morphology of SSs (Figure 4-1c) is characterised by a flat, glass-like surface. From Figure 4-1c, it is apparent that the SS bio-coagulant has an angular pattern of fragmentation, whereas on the other hand, the CSS (Figure 4-1f) has a course, permeable, and agglomerated surface (Dampang *et al.* 2021).

4.1.2 Energy Disperse X-ray (EDX)

The elemental analysis was done using EDX to ascertain the composition of the model bio-coagulants, elemental analysis was done using energy dispersing X-ray (EDX) analysis for both raw and calcinated bio-coagulants. The EDX characterisation results are depicted in Figure 4-2.

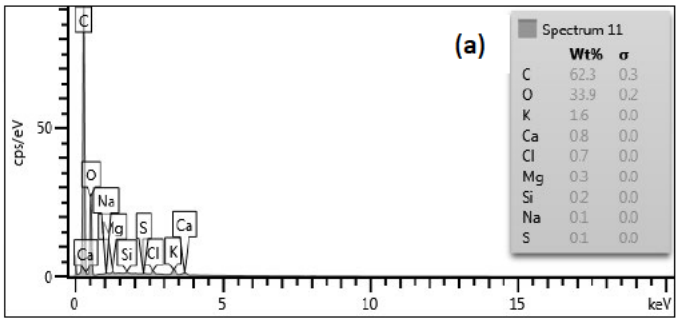

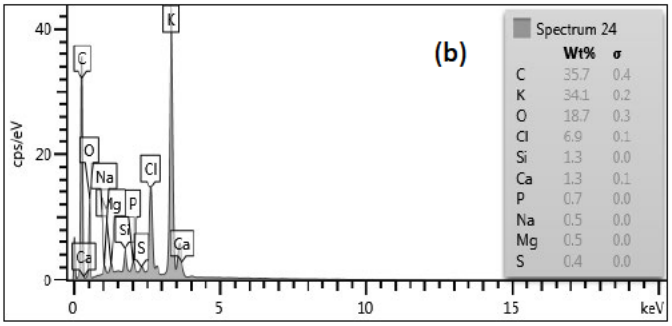

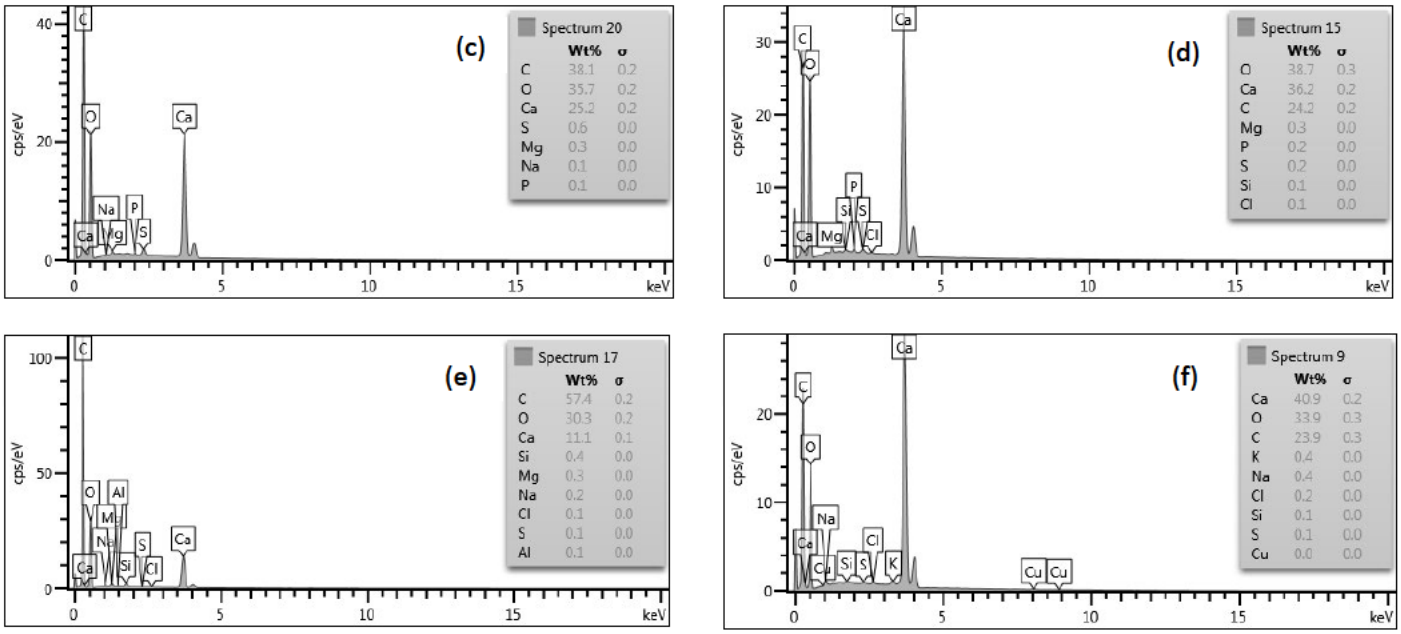

Figure 4-2: EDX results showing the elemental compositions of (a) raw banana peels; (b) calcined banana peels; (c)raw eggshells; (d) calcinated eggshell; (e) raw seashells; and (f) calcinated seashell

The elemental composition of BP was found to be in the order of carbon (C) > oxygen (O) > potassium (K) > calcium (Ca) (Figure 4-2a). The observed elemental composition can be attributed to the presence of proteins and polysaccharides in banana peels (Kamsonlian *et al.* 2011). A significant change in elemental composition was observed for the calcinated banana peels (Figure 4-2b). Such a change in the elemental composition of the CBP is attributed to the high affinity of potassium to negatively charged areas through a weak electrostatic attraction induced through calcination (Oladipo *et al.* 2019). The high composition of element C could be attributed to the doping of carbon gas during the analysis. Figure 4-2c depicts the characterisation results for raw ES. It is apparent that surface modification of raw eggshells by calcination resulted in an increase in terms of elemental composition. The increase in mass composition (Figure 4-2d) of Ca can be attributed to the presence of calcium carbonate, which enhances the adsorption process of targeted contaminants in aqueous environments (Warren et al. 2001). However, this is not explicitly accounted for in the present study. Moreover, the efficacy of the solid-liquid adsorption process increases with increasing C and decreasing O content in the adsorbent. A higher surface area for the adsorption of target pollutants is made possible by the ability of the shell to develop pores onto the surface of the carbon when there is C present. The results presented in Figure 4-2c and 4-2d suggest that comparison studies need to be conducted aimed at investigating the effect of C content and calcium carbonate in

the form of Ca on the adsorption process efficacy. The composition of SS and CSS are presented in Figures 4-2e and 4-2f, respectively. It was observed that SS have a high mass composition of elemental carbon. However, following calcination the elemental mass compositions changed as seen depicted in Figure 4-2f, where calcium mass composition increased and lowered the composition of carbon (Nordin *et al.* 2015). This proves that calcination also has an effect on the elemental compositions of a material.

4.1.3 Fourier transform infrared spectroscopy (FTIR)

The FT-IR spectra of raw and calcinated bio-coagulants were obtained to determine the functional groups present on the surface of each model bio-coagulant. The results are presented in Figure 4-3 and Table 4-1.

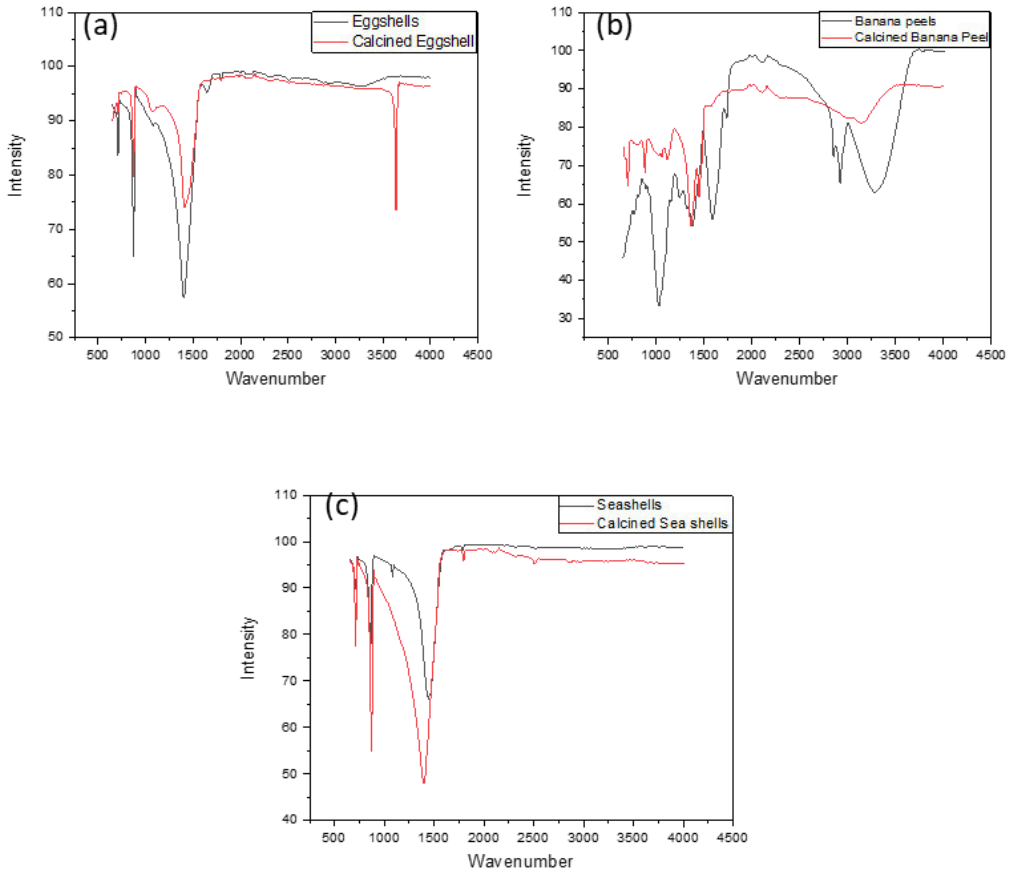

Figure 4-3: FTIR spectra images for (a) eggshell, (b) banana peel, and (c) seashells

As presented in Table 4-1, bands of the various bio-coagulants appearing at 3300 cm^{-1}, 3000 cm^{-1}, 1420 cm^{-1}, 1085 cm^{-1}, 1070 cm^{-1}, and 900 cm^{-1} are attributed to O-H stretching (carboxylic acid), C-H stretching (alkane), O-H bending (alcohol), C-O stretching (primary alcohol), S=O stretching (sulfoxide), and C-H bending (1,2,4-trisubstituted), respectively (Lin-

Vien *et al.* 1991). The carboxylic acid and hydroxyl functional groups facilitated the adsorption of heavy metal ions in aqueous environments (Memon *et al.* 2008; Muhamad *et al.* 2020).

Table 4-1: The functional groups and class compounds found in the FTIR spectra (Popa 2006; Ellerbrock *et al.* 2021)

Absorption (cm^{-1})	Functional group	Compound class
3300-2500	O-H stretching	carboxylic acid
3000-2840	C-H stretching	Alkane
1420-1330	O-H bending	Alcohol
1070-1030	S=O stretching	Sulfoxide
1085-1050	C-O stretching	primary alcohol
900-700	C-H bending	1,2,4-trisubstituted

The raw banana peels' spectra show strong, distinct bands which can be attributed to the alkyne group near the 3280.1 cm^{-1} peak. The banana peels strong band can also be attributed to the stretching of the C-H group, whereas the stretching of the strong S=O group was at 1029 cm^{-1}. The bands at 3153 cm^{-1} and 1364 cm^{-1} in the FT-IR spectra of the calcined banana peels indicate the presence of the carboxylic acid (COOH) group on the surface of the bio-coagulant. This can be attributed to the stretching vibrations on these O-H bands and the potential existence of the sulfonamide group, respectively (Popa 2006). In Figure 4-3, it is apparent that all the bio-coagulants reported for the current work exhibit bands between 1300 cm^{-1} and 1600 cm^{-1}, which suggest that all model bio-coagulants exhibit stretching on the O-H functional group and may belong to the class of alcohol compound. It should be noted that O-H functional groups acts as adsorption sites for contaminant remediation in aqueous environments (Yang *et al.* 2019). A shift in the peaks signifies that calcination does alter the functionality of the materials, which is another way to validate that calcination does bring about, not only structural changes, but also chemical changes.

4.1.4 Brunauer Emmett Teller (BET)

The surface area, pore volume and pore size of the model bio-coagulants were determined using the BET. The results are presented in Table 4-2.

Table 4-2: BET surface area, pore volume and pore size of the model bio-coagulants

Bio-coagulant	Surface Area (m^2/g)	Pore Volume (m3/g)	Pore Size, (Å)
Banana peels	2.7190	0.0054	0.569
Eggshells	0.8734	0.000127	5.515
Seashells	0.7921	0.0128	2.364
Calcined banana peels	4.3889	0.00569	3.167
Calcined eggshells	2.2272	0.00116	2.193
Calcined seashells	2.0920	0.00108	3.923

Calcined banana peels have the highest surface area and pore volume of 4.3889 m^2/g and 0.00569 m^3/g, respectively, when compared to the calcined eggshells and seashells. Despite the least surface area and pore volume demonstrated by calcined seashells, a pore size of 3.923 Å was recorded, which was bigger than that of calcined banana shells and eggshells. The large pore size of the calcined seashells suggests that in an aqueous environment, the pore-filling will be the dominant mechanism in contaminants remediation in a typical adsorption process, however, the pore-filling mechanism is not explicitly accounted for in the present study (Kleitz 2009).

4.1.5 X-ray diffraction (XRD)

The X-ray diffraction method was used to study the crystallographic behaviour of seashell powder, calcined seashell powder, eggshell powder, calcined eggshell, banana peel and calcined banana peel. Figure 4-4 shows stacks of XRD traces, the main peaks of seashells (SS) appeared at $2\theta = 26.2^o$, 27.2^o, 29.3^o, 33.1^o, 37.1^o, 36.8^o, 38.6^o, 41.1^o, 42.9^o, 45.8^o, 47.5^o, 48.3^o, 50.2^o, 52.4^o, 65.9^o and 68.93^o.

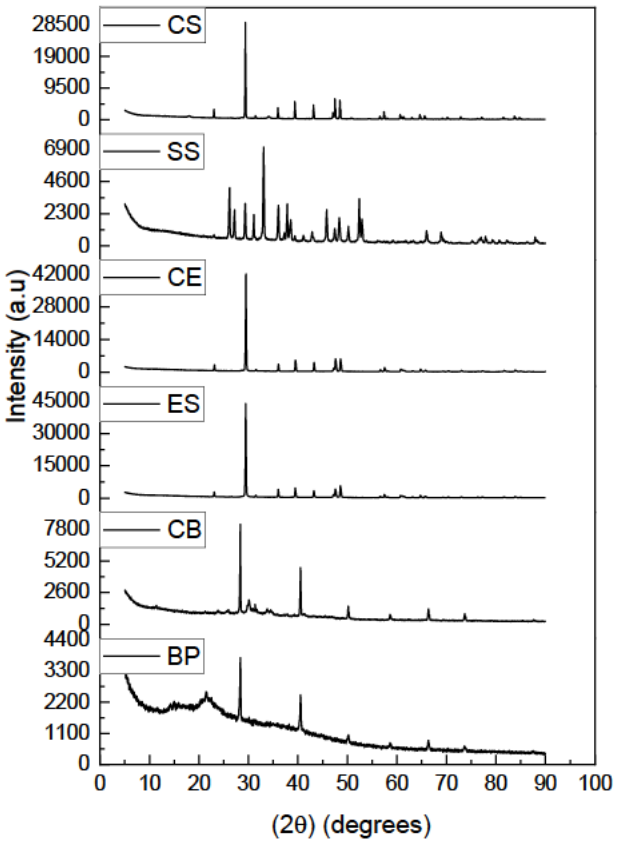

Figure 4-4: XRD diagram for banana peel (BP), calcined banana peel (CB), eggshell (ES), calcined eggshell (CE), seashell (SS), and calcined seashell (CSS).

The main reflection peaks appearing at 2θ = 26.2°, 27.2°, 33.1°, 36.1°, 38.5°, 48.4° and 52.4° shows that there is a presence of biogenic aragonite, which make up the nacreous layer (Yoshioka *et al.* 1985; Janković *et al.* 2022). When heat was applied to seashells there was a shift in 2θ depending on the temperature range, thus resulting in a structural change (Koga *et al.* 2013). The peak at 2θ = 29.4° is associated with the presence of limestone (Jung *et al.* 2000). The peaks at 2θ = 39.4°, 43.1° and 48.5°, also shows the presence of calcite (Janković *et al.* 2022) in the form of aragonite (Antao *et al.* 2010; Ferraz *et al.* 2019; Ouafi *et al.* 2021). Due to the exposure of heat in the process of calcination, aragonite is transformed to calcite in calcined seashells, and that is confirmed by peaks that appeared at 2θ = 23.1°, 29.4°, 36.1°, 39.4°, 4.31°, 47.5°, 48.5° and 60.6° (Janković *et al.* 2022). The presence of CaO is confirmed by the peaks in 2θ = 64.6° and 54.3° (Jung *et al.* 2000; Ouafi *et al.* 2021). $Ca(OH)_2$ was observed in the peaks 2θ = 47.5°, 64.7° and 84.7° (Bulut *et al.* 2018). For the calcined eggshell (CE), peaks at 2θ = 29.5°, 32.2°, 47.6°, 64.7° and 67.3° are characteristics of calcium oxide (Ayodeji *et al.* 2018; Bharadwaj *et al.* 2019). Whereas for eggshells (ES) there were traces of $CaCO_3$, this was observed in the peaks 2θ = 29.4°, 36.1°, 39.0°, 47.5° and 48.4° (Ayodeji *et al.* 2018).

The peaks at 2θ = 19.4º, 28.3º, 28.4º, 37.5, 40.52º, 58.6 º and 66.4º, in calcined banana peels (CB) can be attributed to the presence of tetragonal structured potassium, which was found to be a major phase of catalyst. These peaks also confirm the presence of minerals such as hexagonal structured calcium and silicon, and cubic structured magnesium (Balajii *et al.* 2019, 2020; Jitjamnong *et al.* 2021). The peaks observed at 2θ = 31º and 31.4º can be attributed to the presence of the compound K_2O. While the peaks at 2θ = 33.8º and 37.5º indicate the presence of K_2CO_3 and CaO, respectively and the presence of aluminum oxide (Al_2O_3) is represented in 2θ = 25.9º (Fan *et al.* 2019; Daimary *et al.* 2022; Husin *et al.* 2023). In banana peels it was observed that a minimum number of peaks was observed between 2θ = 10º and 90º and this is because of the presence of cellulose-hemicellulose-lignin matrix (Fan *et al.* 2019; Balajii *et al.* 2020).

4.2 Feasibility study: contaminant removal using synthesised bio-coagulants

This section assesses the treatability of wastewater using a variety of synthetic bio-coagulants, including banana peels (BP), eggshells (ES), seashells (SS), calcined banana peels (CBP), calcined eggshells (CES), and calcined seashells (CSS). The mixing speed, mixing time, and settling time were all held constant at 150 rpm (rapid mixing), 30 rpm (slow mixing), 15 minutes (mixing time), and 30 minutes (settling time), respectively (Precious Sibiya *et al.* 2021). The findings collected are shown and described in the graphs below. The wastewater properties before and after coagulation treatment were analysed using established procedures (APHA 2007, APHA 2012), as shown in Table 3-2.

The bio-coagulants were employed in a series of studies to determine the optimum bio-coagulant for wastewater treatment. Turbidity and COD removal, which define a sample's organic composition, were evaluated. Figures 4-5 and 4-6 show the impact of uncalcined and calcined bio-coagulants on turbidity reduction at dosages of 0.2 g, 0.4 g, 0.6 g, 0.8 g, 2 g, 4 g, 6 g, and 8 g of bio-coagulant. The uncalcined bio-coagulants at doses of 0.2 g, 0.4 g, and 0.6 g showed turbidity removal efficiencies of less than 80% at 8,96%, 30,62%, and 50,398% for banana peels, 46,91%, 48,65%, and 63,98% for eggshells, and 38,17%, 46,62%, and 54,18% for seashells, respectively. This could be attributed to underdosage which is insufficient dose of coagulant for the successful binding to the pollutants in the wastewater, thus requiring higher doses of coagulant to reach the optimal removal efficiency of >80%. Additional coagulants were needed to reach the optimal condition. At a dose of 0.8 g, banana peels and eggshells removed more than 80% of the turbidity, at 82.69% and 83.35%, respectively, however, seashells removed just 60.84%.

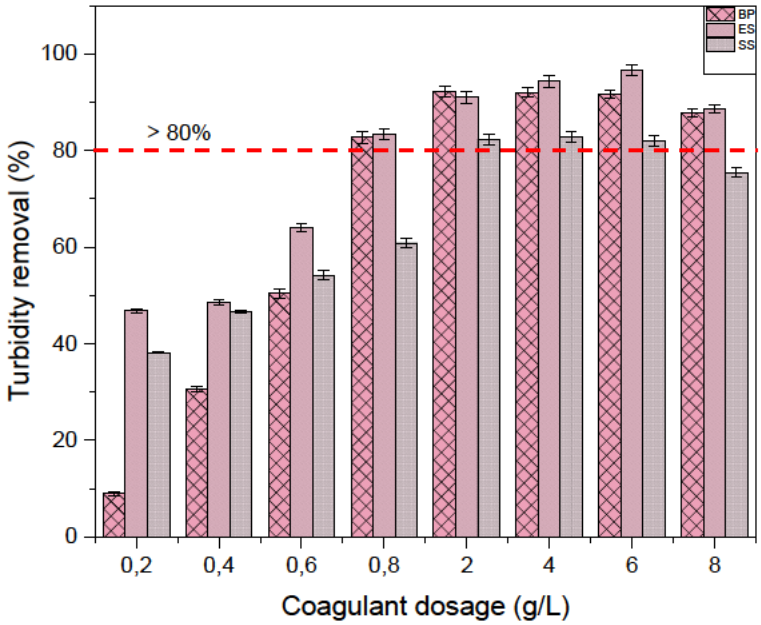

Figure 4-5: Turbidity removal using the coagulation process using banana peel (BP), eggshell (ES) and seashell (SS) with coagulant dosage of 0.2-8 g/L.

Dosages of 2 g, 4 g, and 6 g indicate substantial increases for all bio-coagulants at 92.23%, 92.01%, and 91.61% for banana peels, 90.99%, 94.32%, and 96.58% for eggshells, and 82.3%, 82.86% dose of 8 g, there was a drop in turbidity removal, and 81.93% for seashells (Khader *et al.* 2018; Husen *et al.* 2024). Turbidity removal efficiency decreased at 8 g, however banana peels and eggshells remained over 80%, while seashells fell short at 75.43%. This reduction might be caused by excess coagulants that did not combine with the oppositely charged colloidal particles, which had previously been flocculated, resulting in increased turbidity in the water.

The coagulants that were calcined showed an improvement in the removal of turbidity; however, the dosages 0.2 g, 0.4 g and 0.6 g still had a removal efficiency lower than 80% at 28,32%, 51,36% and 73,26% for CBP, 32,46%, 55,71%, and 78,32% for CES and 44,36%, 48,63%, and 70,18% for CSS. Adding more coagulants into the wastewater will increase the number of active coagulant sites, enhancing their ability to attract and absorb contaminants. The dosage from 0.8 g to 8 g shows high removal percentages of over 80%; adding more coagulants exceeding the optimum dosage will only pollute the wastewater, as shown in CBP. Excess coagulant saturates the surface of colloids, which saturates the coagulant, causing particle destabilisation, producing a repulsive attraction between contaminants, preventing floc formation (Wang *et al.* 2021a).

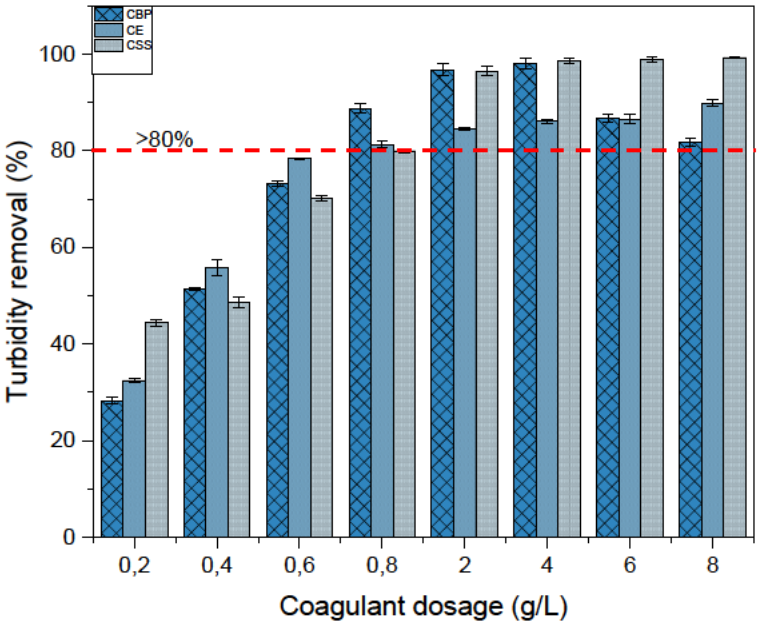

Figure 4-6: Turbidity removal using the coagulation process using calcined banana peel (CBP), calcined eggshell (CE) and calcined seashell (CSS) with coagulant dosage of 0.2-8 g/L.

The COD removal efficiency was evaluated at various dosages listed above to determine the most suitable bio-coagulant, as shown in Figure 4-7 and Figure 4-8. The uncalcined bio-coagulant results showed that SS had the highest removal of 84% at a dosage of 6 g/L, whereas BP had the lowest removal efficiency, with an optimum efficiency of 44% at 4 g/L. The calcined bio-coagulants showed the opposite of the uncalcined, where the CB had the highest removal of 90,62% at a dosage of 2 g, and CS had the highest removal of 57,07% at 2g. CBP had a COD percentage removal between the 0.8 – 8 g/L dosage. However, there was a slight deterioration after a dosage of 2 g. The CE performed better than CB and CS at a COD removal percentage of 91,72% at a dosage of 4 g (Khader *et al.* 2018). The results obtained from the feasibility study confirmed that calcination does alter the morphology of the bio-coagulant and increases the surface dynamics of the bio-material, hence improving treatability.

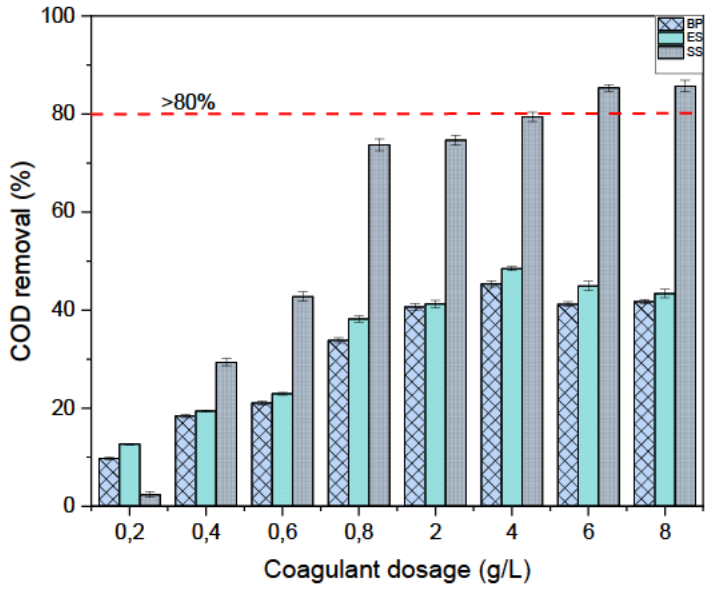

Figure 4-7: COD removal using the coagulation process using banana peel (BP), eggshell (ES) and seashell (SS) with coagulant dosage of 0.2-8 g/L.

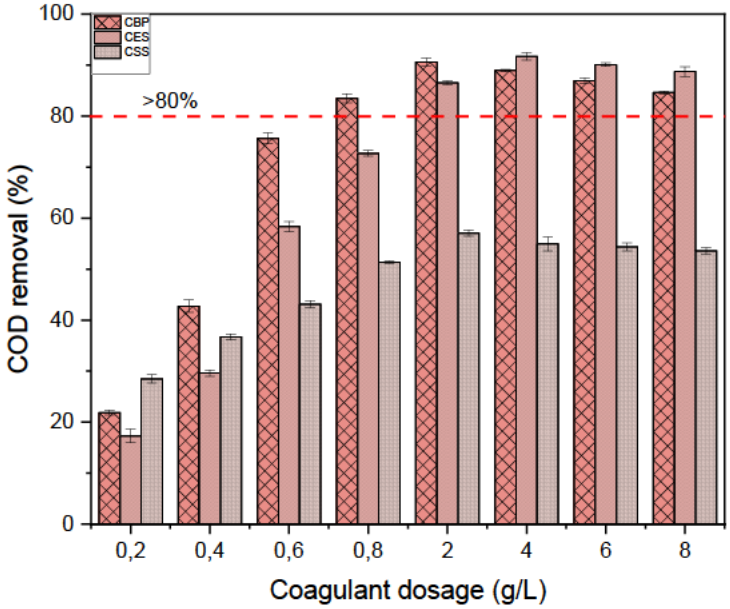

Figure 4-8: COD removal using the coagulation process using calcined banana peel (CBP), calcined eggshell (CE) and calcined seashell (CSS) with coagulant dosage of 0.2-8 g/L.

All the bio-coagulants performed well, however, the calcined banana peels were determined to be the best bio-coagulant. This was determined by observing the bio-coagulants with the highest removal for turbidity and COD at the low dosage. The range that will be used to optimise is between 1 – 6 g/L of the BP.

4.3 The development of a predictive model

This section focuses on the results which are in line with objective two. The findings presented below focus on the development of a predictive model and the optimisation of the coagulation system using the calcined banana peel.

4.3.1 The optimisation of the coagulation process using the calcined banana peel as a coagulant

The design of the experiment, coupled with the Box-Behnken design, was used for statistical analysis and data modelling. An investigation of various operational parameters, including speed (30 – 50 rpm), Dosage (1 – 6 g), mixing time (2 – 15 min) and settling time (20 – 120 min) and the interaction effects between them was done as shown in Table 4-3. The experimental data of the response and predicted results, which include colour, turbidity and COD, are also represented in the table below. These operating conditions were evaluated to obtain the optimum conditions for wastewater treatment. The initial data for colour and COD were measured using the DR 3900 Hach spectrophotometer, and turbidity was measured using the turbidity meter. The experimental data was calculated using equation 3-1, whereas the predicted values were computed from the model.

Table 4-3: Table showing the actual vs predicted results of the matrix for colour, turbidity and COD percentage removal.

	Factor 1	Factor 2	Factor 3	Factor 4	Colour		Turbidity		COD	
Run	A: Speed	B: Dosage	C: Mixing time	D: Settling time	**Actual Value**	**Predicted Value**	**Actual Value**	**Predicted Value**	**Actual Value**	**Predicted Value**
	min	g/L	Min	min						
1	150	3.5	15	70	69.72	69.75	81.17	80.53	89.54	89.64
2	150	6	8.5	70	66.12	65.75	81.03	80.34	88.43	88.52
3	90	1	8.5	20	87.05	87.06	93.98	94.34	87.22	87.38
4	30	3.5	8.5	20	87.51	86.36	92.49	90.94	89.52	89.61
5	30	3.5	8.5	120	93.12	92.83	90.06	88.86	91.85	91.91
6	90	6	2	70	80.73	80.65	90.30	89.76	89.71	89.81
7	30	6	8.5	70	82.72	82.54	84.55	83.66	89.91	89.97
8	150	1	8.5	70	84.41	83.94	93.91	92.82	89.04	89.05
9	90	1	15	70	84.40	85.20	88.49	88.49	90.60	90.44
10	150	3.5	2	70	82.06	81.35	94.59	94.28	90.67	90.74
11	90	3.5	8.5	70	81.07	82.22	85.63	87.07	88.65	88.31
12	90	6	8.5	120	76.78	77.38	78.60	79.79	87.76	87.59
13	90	1	2	70	95.95	96.81	98.99	99.76	88.34	88.29
14	30	1	8.5	70	96.92	96.65	95.47	96.14	90.02	90.00

15	150	3.5	8.5	20	70.91	71.61	85.87	87.62	90.33	90.21
16	90	3.5	2	20	86.01	85.49	96.33	95.04	89.41	89.33
17	90	3.5	2	120	92.05	91.97	94.51	94.48	90.25	90.31
18	30	3.5	2	70	95.57	96.10	96.21	97.60	90.59	90.49
19	90	3.5	15	120	81.79	80.36	78.40	79.22	90.02	90.17
20	90	1	8.5	120	94.72	93.53	94.69	92.27	90.02	90.08
21	30	3.5	15	70	82.99	84.50	82.28	83.85	92.38	92.30
22	90	6	8.5	20	70.79	70.90	81.35	81.87	89.38	89.31
23	150	3.5	8.5	120	77.12	78.08	84.57	85.54	89.05	88.90
24	90	3.5	8.5	70	81.84	82.22	86.15	87.07	87.98	88.31
25	90	3.5	15	20	74.47	73.89	83.26	82.81	90.17	90.18
26	90	6	15	70	69.39	69.05	74.85	73.54	88.39	88.37

The analysis of variance (ANOVA) for the modified model used to estimate the removal percentage of colour, turbidity and COD using calcined banana peels can be seen in Equation 4-1, to Equation 4-6, indicating the suitability of the model to predict the removal percentage. It can be observed that the removal of colour and turbidity are affected by the mixing time and settling time whereas COD removal is also affected by the speed. A positive value represents an effect that favours the optimisation, while a negative value an inverse relationship between the factors and the responses. For colour and turbidity and COD, significant effects were obtained for linear and quadratic terms, where the quadratic terms indicate the presence of curvatures. This indicates that an increase in mixing time, settling time and mixing speed will increase the removal efficiency; however, after reaching the optimum removal, it will start to decrease.

$$Y1 = 82.2191 - 7.37462A - 8.07749B - 5.80213C + 3.2379D - 1.02162AB + 0.707951C^2$$

Equation 4-1

$$Y1 = 106.709 - 0.0990724A - 2.61802B - 1.17749C + 0.064758D - 0.00681083AB + 0.0167562C^2$$

Equation 4-1

$$Y2 = 87.0675 - 1.65994A - 6.23869B - 6.87349C - 1.03786D - 1.2357BC - 0.75975CD + 1.17517A^2 + 0.820717C^2$$

Equation 4-2

$$Y2 = 109.127 - 0.0864241A - 1.84911B - 0.9579C - 0.000886782D - 0.0760431BC - 0.00233769CD + 0.000326435A^2 + 0.0194253C^2$$

Equation 4-3

$$Y3 = 88.3149 - 0.60095A - 0.138217B + 0.177892C + 0.244792D - 0.125025AB - 0.728375AC - 0.90385AD - 0.89665BC - 1.10458\,BD - 0.2452CD + 1.31795A^2 - 0.246379B^2 + 1.15928C^2 + 0.522858D^2$$

Equation 4-4

$$Y3 = 86.4794 - 0.0360312A + 1.38325B - 0.0250658C + 0.0400723D - 0.0008335AB - 0.00186763AC - 0.000301283AD - 0.0551785BC - 0.0088366BD - 0.000754462CD + 0.000366096A^2 - 0.0394207B^2 + 0.0274387C^2 + 0.000209143D^2$$

Equation 4-5

4.3.2 Model fitting and statistical analysis

Table 4-4 (Colour removal %), and Table 4-5 (Turbidity removal %) represent analysis of variance for statistical significance of a modified model, whereas Table 4-6 (COD removal %) shows the ANOVA of a quadratic model. The Fishers test (F-value) is used to measure the significance of the means between operating conditions. An F-value of 454.84, 74.52 and 61.46 shows that these regression models are significant for the removal of colour, turbidity and COD. The probability value (P-value) is an important statistical parameter that evaluates the model fitness quality (Ghafari *et al.* 2009; Rifi *et al.* 2022). Model terms are considered significant when their p-values are less than 0.0500 and not significant if the values are over 0.1000. For these models, colour model terms A, B, C, D, AB and C^2 have considerable significance, for turbidity removal terms A, B, C, D and A^2 are significant and A, B, C, D, AC, AD, BC, BD, CD, A^2, B^2, C^2 and D^2 for COD are also significant.

Table 4-4: ANOVA for Reduced quadratic model, Response 1, Colour removal

Source	Sum of Squares	df	Mean Square	F-value	p-value	
Model	1972.77	6	328.79	454.84	< 0.0001	significant
A-Speed	652.62	1	652.62	902.81	< 0.0001	
B-Dosage	782.95	1	782.95	1083.10	< 0.0001	
C-Mixing time	403.98	1	403.98	558.84	< 0.0001	
D-Settling time	125.81	1	125.81	174.04	< 0.0001	
AB	4.17	1	4.17	5.78	0.0266	
C^2	3.24	1	3.24	4.48	0.0477	
Residual	13.73	19	0.7229			
Lack of Fit	13.44	18	0.7467	2.54	0.4621	not significant
Pure Error	0.2945	1	0.2945			
Cor Total	1986.50	25				

Table 4-5: ANOVA for Reduced quadratic model Response 2: Turbidity (Removal %)

Source	Sum of Squares	df	Mean Square	F-value	p-value	
Model	1098.71	8	137.34	74.52	< 0.0001	significant
A-Speed	33.06	1	33.06	17.94	0.0006	
B-Dosage	467.06	1	467.06	253.42	< 0.0001	
C-Mixing time	566.94	1	566.94	307.61	< 0.0001	
D-Settling time	12.93	1	12.93	7.01	0.0169	
BC	6.11	1	6.11	3.31	0.0863	
CD	2.31	1	2.31	1.25	0.2786	

A^2	8.42	1	8.42	4.57	0.0474	
C^2	4.11	1	4.11	2.23	0.1539	
COr Total	31.33	17	1.84			
Lack of Fit	31.20	16	1.95	14.34	0.2049	not significant
Pure Error	0.1359	1	0.1359			
Cor Total	1130.04	25				

Table 4-6: ANOVA for quadratic model, Response 3: COD (Removal %)

Source	Sum of Squares	df	Mean Square	F-value	p-value	
Model	35.10	14	2.51	61.46	< 0.0001	significant
A-Speed	4.33	1	4.33	106.21	< 0.0001	
B-Dosage	0.2292	1	0.2292	5.62	0.0371	
C-Mixing time	0.3797	1	0.3797	9.31	0.0110	
D-Settling time	0.7191	1	0.7191	17.62	0.0015	
AB	0.0625	1	0.0625	1.53	0.2415	
AC	2.12	1	2.12	52.01	< 0.0001	
AD	3.27	1	3.27	80.09	< 0.0001	
BC	3.22	1	3.22	78.82	< 0.0001	
BD	4.88	1	4.88	119.61	< 0.0001	
CD	0.2405	1	0.2405	5.89	0.0335	
A^2	7.58	1	7.58	185.77	< 0.0001	
B^2	0.2649	1	0.2649	6.49	0.0271	
C^2	5.86	1	5.86	143.73	< 0.0001	
D^2	1.19	1	1.19	29.24	0.0002	
Residual	0.4488	11	0.0408			
Lack of Fit	0.2256	10	0.0226	0.1011	0.9896	not significant
Pure Error	0.2232	1	0.2232			
Cor Total	35.55	25				

The determination coefficient (R^2) is used for evaluation of the quality of the polynomial fitting. R^2 considers all effects, and adjusted R^2 considers only square effects and interaction effects between two input variables (Kassem *et al.* 2021). The predicted R^2 and adjusted R^2 in this study were 0.9931 and 0.9909 for colour removal, 0.9723 and 0.9592 for turbidity removal, and 0.9874 and 0.9713 for COD removal, with a difference of less than 2% between the actual and adjusted R^2, which demonstrates good accordance between the calculated and observed results. The adequate precision "Adeq Precision" measures the signal-to-noise ratio, quantifying the range in predicted response relative to its associated error, and a ratio greater than 4 is desirable. The colour, turbidity and COD ratios in this study were 70.4085, 32.8326

and 32.0618, respectively, indicating an adequate and reliable signal. The design's accuracy level is quantified by the coefficient of variation (C.V) and standard deviation (Std. Dev.). A low coefficient of variation and standard deviation indicate that the experiment was done with a high level of accuracy. In this study, the Std. Dev. for colour, turbidity and COD were 0.8502, 1.36 and 0.2020, respectively, and the C.V (%) was 1.03, 1.54 and 0.2255.

Table 4-7: ANOVA fit statistics

	Colour removal (%)	**Turbidity removal (%)**	**COD removal (%)**
Std. Dev.	0.8502	1.36	0.2020
Mean	82.55	87.99	89.59
C.V. %	1.03	1.54	0.2255
R^2	0.9931	0.9723	0.9874
Adjusted R^2	0.9909	0.9592	0.9713
Predicted R^2	0.9878	0.9364	0.9383
Adeq Precision	70.4085	32.8326	32.0618

The diagnostic plot of the predicted versus actual values is represented in Figure 4.9. These plots aid with the analysis of the model generated by the system, and the experimental results agree. The predicted versus actual value plots of the effectiveness of calcined banana peels in the removal of Figure 4-9 (a) colour, Figure 4-9 (b) turbidity and Figure 4-9 (c) COD. These plots indicate an adequate agreement between real data and the ones obtained from the models. The data points are closely spread on the 45^o line and indicate a good agreement between experimental and predicted values of colour, turbidity and COD removal. Thus, indicating that the model provides an acceptable fit for the experimental data. These plots indicate an adequate agreement between real data and the ones obtained from the models. This agrees with the adequate precision values higher than four (Table 4-7) for all the responses, confirming that all predicted models can be used to navigate the design space defined by the BBD.

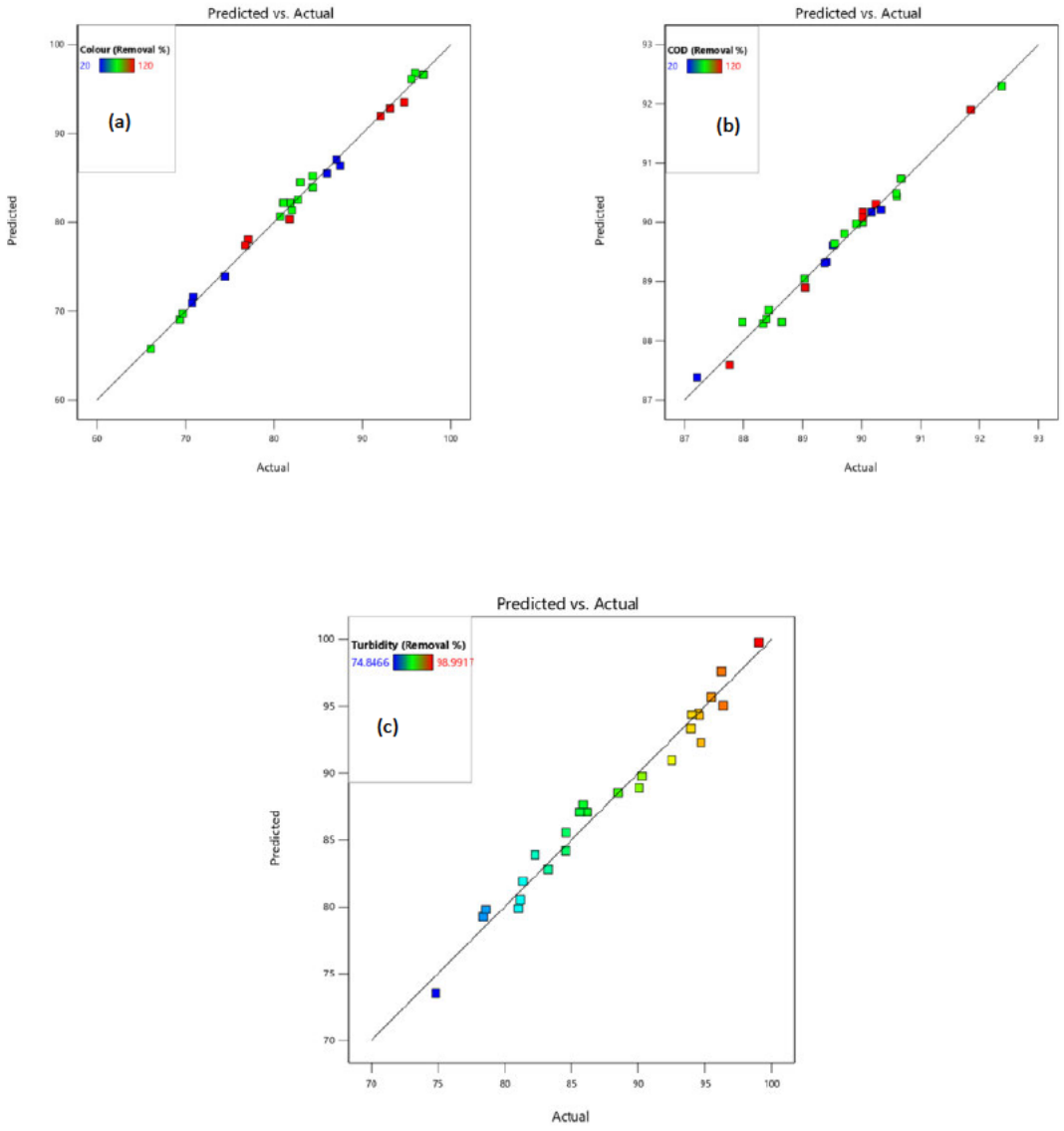

Figure 4-9: Graph showing actual vs predicted plot for (a) which represents colour, (b) representing turbidity and (c) representing COD

The 3D surface plots determined by the regression model equations for the removal efficiencies of colour, turbidity and COD are represented in Figure 4-10 to Figure 4-12; these results are coupled with their corresponding contour plots. The response surface and contour plots are the graphical representative of the model used to visualize the relationship between the response and experimental data. The response graphs show a clear relationship between coagulant dosage and mixing speed. It is clearly shown that the removal of colour, turbidity and COD are greatly affected by the Mixing speed and coagulant dosage. The response graphs show a clear curve, which implies that the optimal conditions for obtaining maximum response values are achieved and are attributed to the mixing speed and coagulant dosage in the design space. The maximum colour removal for colour using calcined banana peels as bio-coagulants was over

90% at a coagulant dosage ranging from 1 – 3 g/L at a speed of 30 rpm to 90 rpm. The same observation can be made for the removal efficiency of turbidity, where a 90% removal percentage was achieved. The removal efficiency of COD shows that the lower mixing rates and dosages between 1 to 5 g/L increase the efficiency of COD removal.

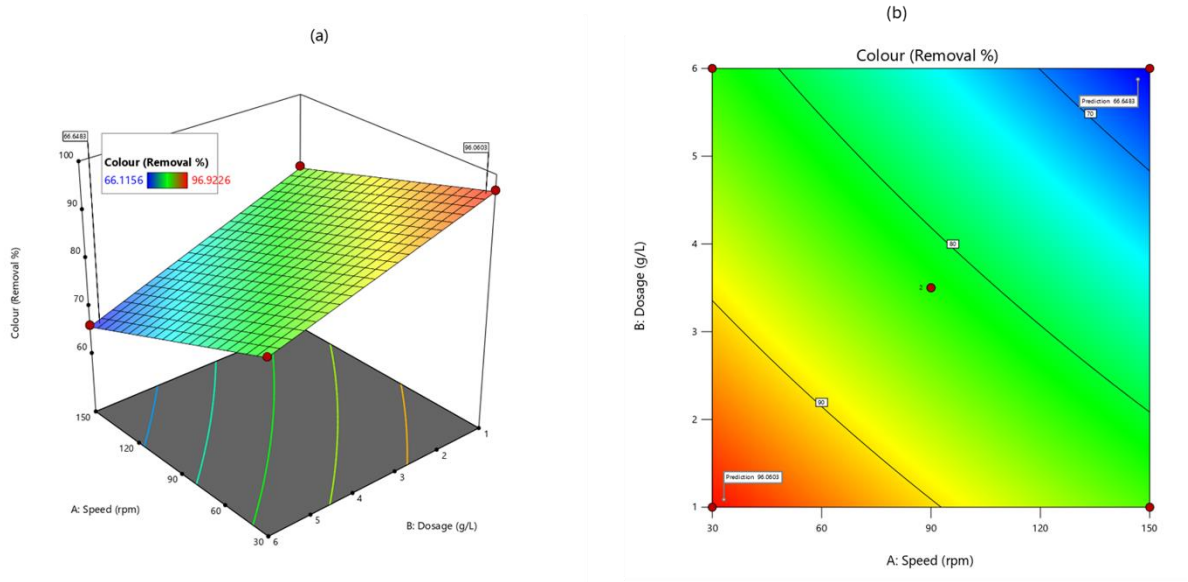

Figure 4-10: Plots showing the colour removal (%) cross factor interactions between speed (rpm) and dosage (g/L); (a) 3D plot (b) contour plot

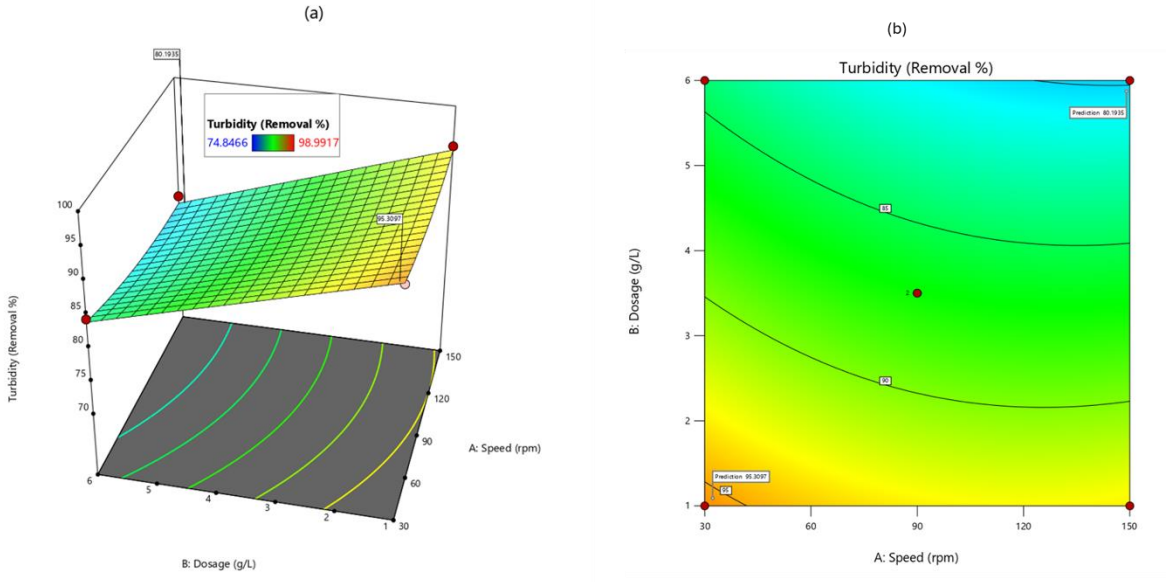

Figure 4-11 : Plots showing the turbidity removal (%) cross factor interactions between speed (rpm) and dosage (g/L); (a) 3D plot (b) contour plot

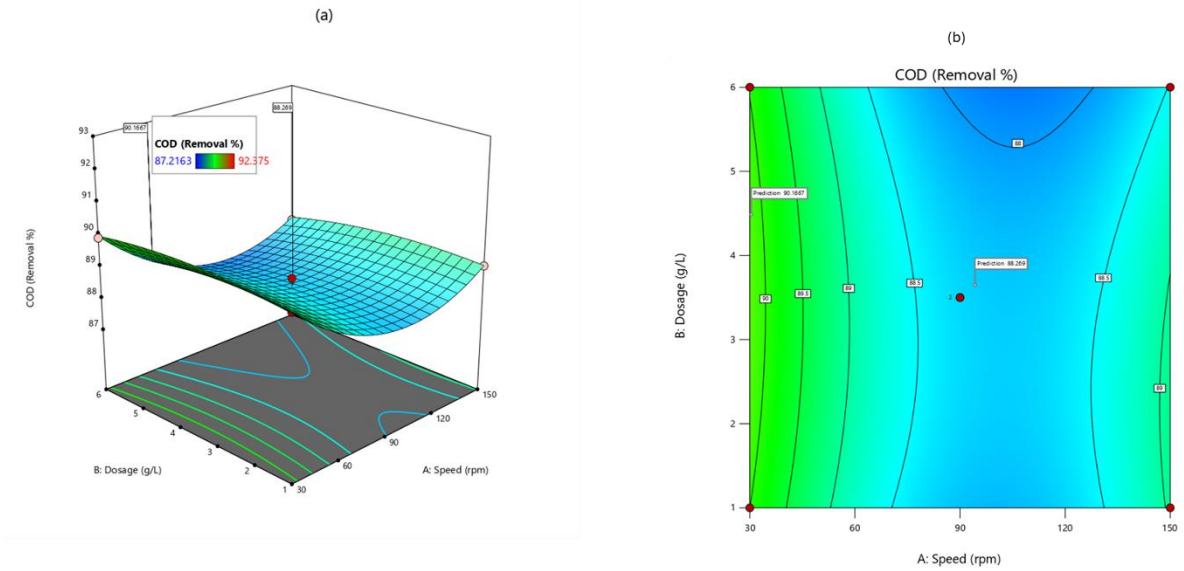

Figure 4-12: Plots showing the COD removal (%) cross factor interactions between speed (rpm) and dosage (g/L); (a) 3D plot (b) contour plot

4.3.3 Optimisation and validation of the coagulation process using BBD

The numerical optimization tool in RSM was used to optimize the four operational coagulation variables. Table 4-8 indicates that all responses in the process were maximised while the input variables (coagulant dosage, mixing speed, mixing time, and settling time) were maintained within the specified range. Figure 4-14 represents the ramp plots that show the optimal operating conditions, and the desirability obtained. With a coagulant dosage, mixing time, mixing speed and settling time of 5.451 g/L, 6.643 min, 48.148 rpm and 56.631 min, respectively, and with a desirability performance of 100%, the COD, turbidity and colour removals were achieved at 89.299% 86.466% 82.466% respectively. The validity and predicting efficacy of the models under optimal conditions were determined using triplicated experimental runs, as described in section 4.4.

Table 4-8: Optimum conditions of CBP for the coagulation system

Number	Speed	Dosage	Mixing time	Settling time	Colour (Removal %)	Turbidity (Removal %)	COD (Removal %)	Desirability	
1	**48.148**	**5.451**	**6.643**	**56.631**	**82.466**	**86.722**	**89.299**	**1.000**	**Selected**
2	90.000	1.000	15.000	70.000	85.202	88.489	90.441	1.000	
3	141.000	5.625	7.850	77.500	69.420	81.505	88.298	1.000	
4	90.000	1.000	2.000	70.000	96.807	99.765	88.291	1.000	
5	30.000	3.500	8.500	120.000	92.832	88.865	91.905	1.000	
6	90.000	1.000	8.500	20.000	87.059	94.344	87.380	1.000	
7	90.000	3.500	15.000	120.000	80.363	79.217	90.174	1.000	
8	30.000	3.500	15.000	70.000	84.500	83.850	92.299	1.000	
9	150.000	3.500	8.500	20.000	71.607	87.621	90.214	1.000	
10	90.000	3.500	2.000	20.000	85.491	95.040	89.329	1.000	

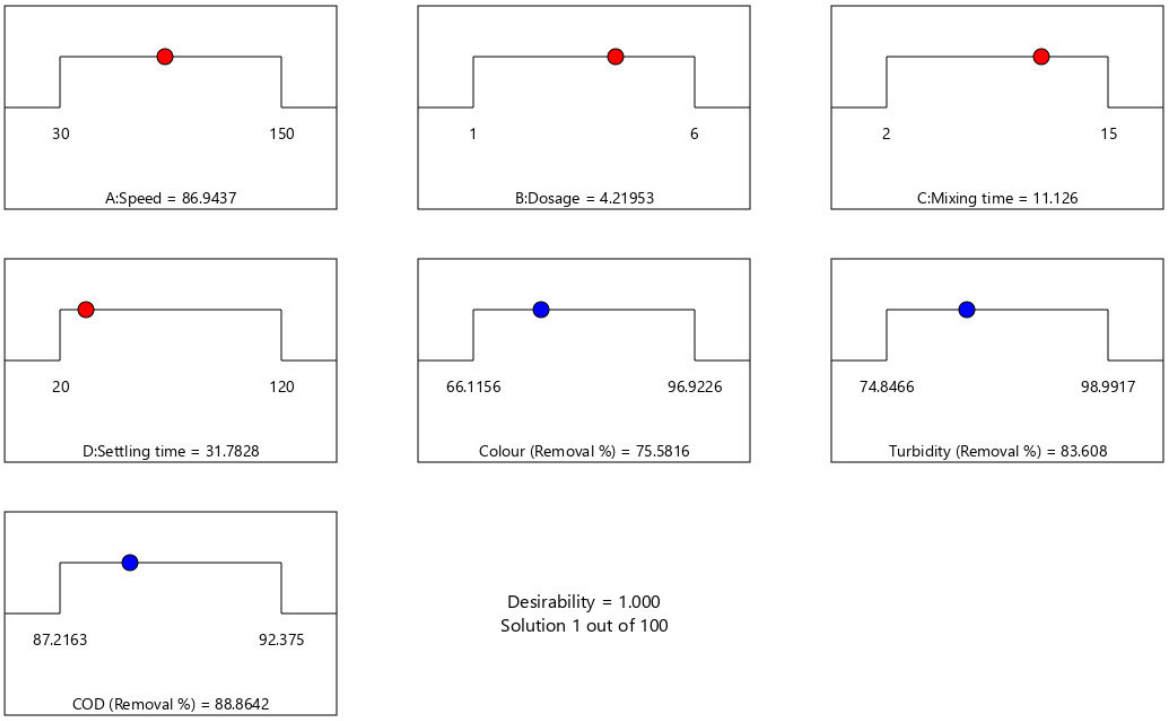

Figure 4-13: Plot showing the ramps of the optimum conditions of the coagulation process with a desirability of 100%

4.3.4 Coagulation kinetic study for turbidity removal

To better understand the dynamic and the aggregation formed in the coagulation/flocculation process, coagulation kinetics were conducted. Coagulation kinetics are conducted to enhance the understanding of the coagulation process throughout time. To achieve this the optimum conditions for turbidity removal and varying settling time (10 min – 100 min) were used. The experimental data was fitted on the pseudo first order model and pseudo second order model for the assessment of the kinetics of the coagulation experimental data as shown in Figure 4-15 and Figure 4-16.

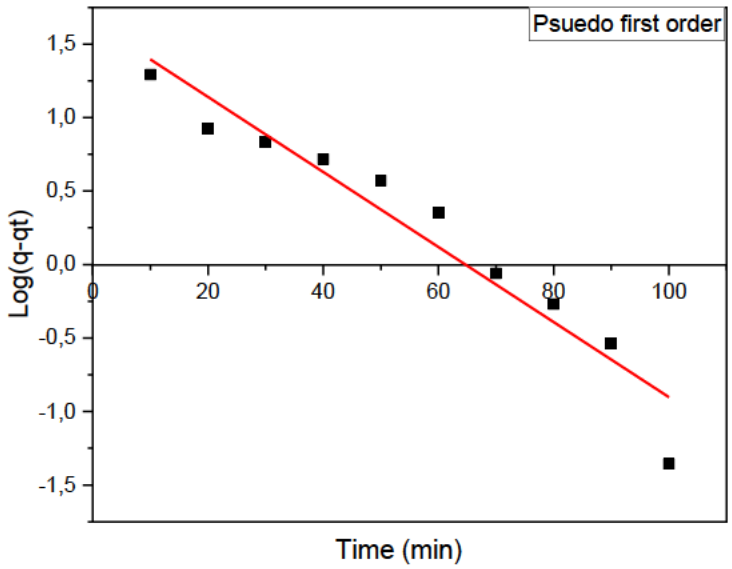

Figure 4-14: Psuedo first order model of coagulation kinetics

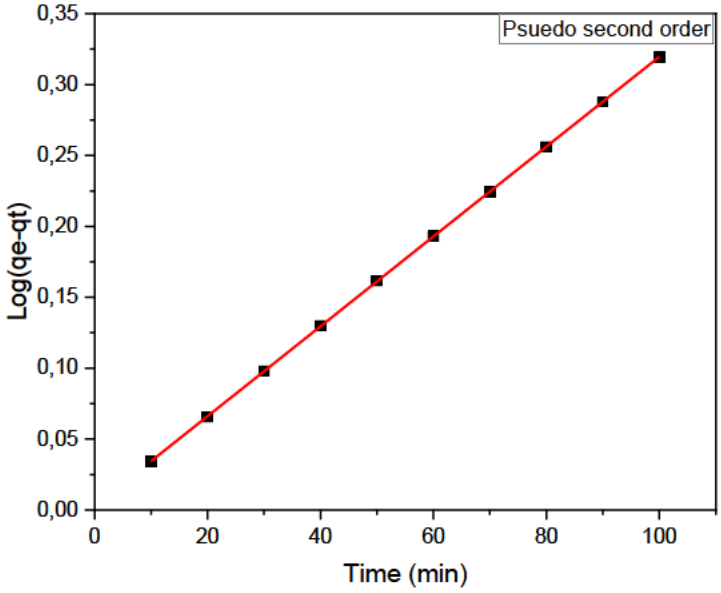

Figure 4-15: Psuedo second order model of coagulation kinetics

Table 4-9 shows the summary for the kinetic study where the pseudo first order had a correlation coefficient (R^2) of 0.93062, in contrast to the pseudo second order which had a better R^2 of 0.9999. The second-order kinetics had a lower reaction rate (K) of 0.004 L/mol/s compared to the first-order reaction, which was 0.026 L/mol/s. This confirms that the coagulation process is an excellent fit for a second order process with a higher R^2 and lower K value (Obiora-Okafo *et al.* 2022).

Table 4-9: Psuedo first order and pseudo second order kinetic parameters.

Kinetics parameters	First order kinetics	Second order kinetics
R^2	0,93062	0,99999
Adjusted R^2	0,92194	0,99999
qe	5.211	315.458
K (L/mol/s)	0.026	0.004
Residual Sum of Squares	0,40079	$1{,}01x10^{-06}$

4.3.5 Coagulation isotherm study

Figure 4-17 and 4-18 illustrates the Langmuir and Freundlich isotherm models for the removal of turbidity from wastewater using optimised conditions from CBP. Using the intercept and slope values, the Langmuir constant and the maximum coagulation values were calculated and found to be 0,18224 L/g and 5,487269535 respectively. The Freundlich constant was calculated to be 2.4016 L/g. The coefficient of determination values (R^2) is represented In Table 4-10. The R^2 values for the Langmuir isotherm model was 0,98219, which was higher than the Freundlich isotherm model of 0,908. The R^2 for both the Langmuir and Freundlich isotherms were over 0.9, which showed that both isotherms fit with the experimental data. However, the higher R^2 of the Langmuir isotherm model implies that it is the best fit for the data provided for the removal of turbidity using CBP as a bio-coagulant, it also describes the monolayer and a physical sorption mechanism (Edet *et al.* 2020).

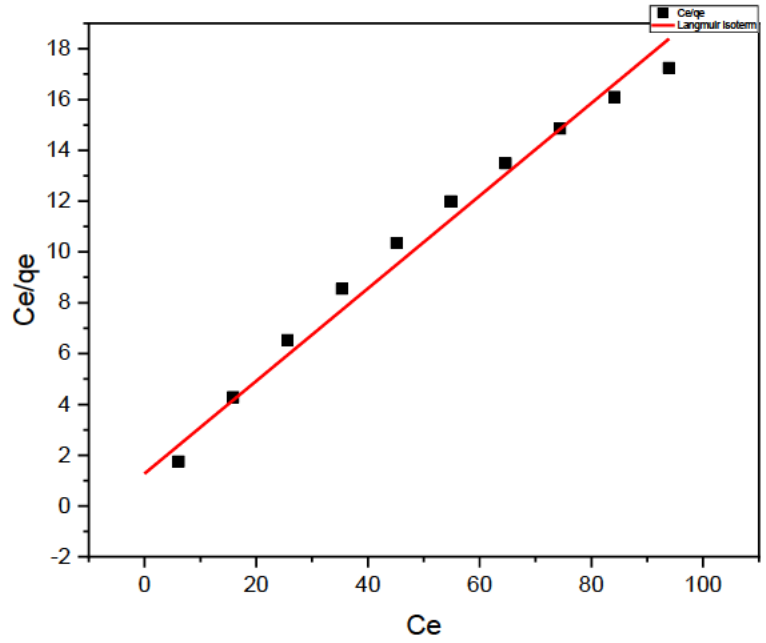

Figure 4-16: Langmuir isotherm model for turbidity removal from wastewater using CBP as bio-coagulant

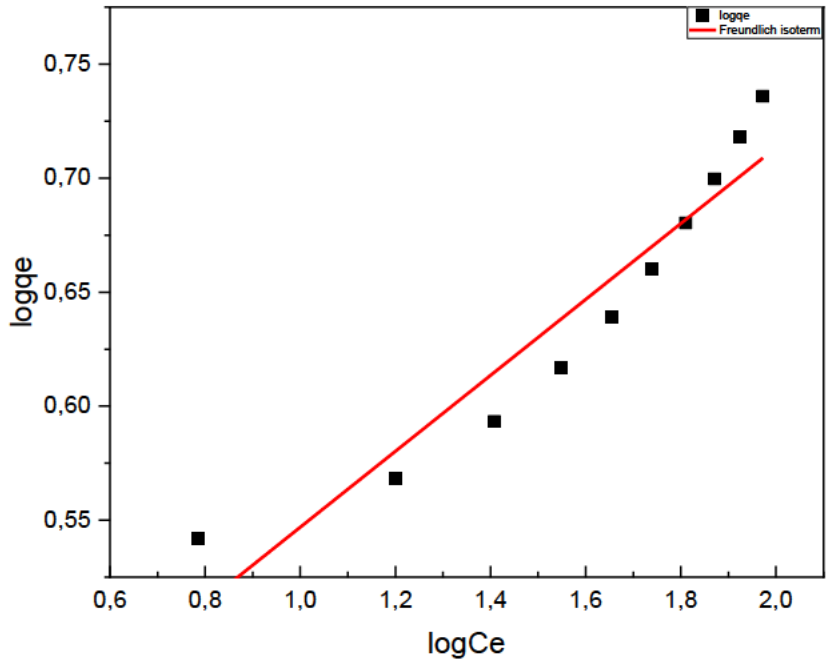

Figure 4-17: Freundlich isotherm model for turbidity removal from wastewater using CBP as bio-coagulant

Table 4-10: Langmuir and Freundlich isotherm evaluations

	Langmuir	Freundlich
k	0.143	2.402

q	0.003	--
n	--	0.167
Residual Sum of Squares	6,09589	0,0035
R^2	0,98219	0,908
Adj. R^2	0,98022	0,8965

4.4 Comparative study

This section presents the results obtained, which align with objective three. The optimised conditions of the conventional coagulant (poly-aluminium chloride) will be compared to that of the calcined banana peel and the various bio-coagulants used in this study.

4.4.1 The optimization of Poly Aluminium Chloride (PAC) and its comparison with calcined banana peel (CBP) in wastewater treatment.

The optimisation of poly-aluminium chloride was conducted for the comparison of natural bio-coagulants to the commercial coagulants used for the treatment of wastewater. This investigation aimed to see if there would be a major difference in the optimum conditions obtained and the effect of the commercial coagulants. The six bio-coagulants had the same design matrix as presented in Table 4-3; however, through experimental work and research on literature, it was determined that PAC requires a lower dosage to be more effective in wastewater treatment. An increase in the dosage of PAC causes colloidal particles to become saturated with positively charged ions which creates a repulsive effect which hinders agglomeration and causes increased turbidity and colour levels (Islam *et al.* 2020; Nti *et al.* 2021). The dosage of PAC was reduced to a range of 0.1 – 0.6 g/L, the design matrix is represented in Table 4-11, the mixing speed (150 -30 rpm), mixing time (2 -15 mins) and settling time (20 – 120 min) corresponded with the design matrix presented in Table 4-3. Table 4-11 also shows the correlation between the predicted results and the experimental results of colour, COD and turbidity removal percentages. The results show that for all the results there is a difference in result that is under 2%, which shows a good correlation between the experimental and the predicted data results. This indicates that the models are appropriately aligned to establish a relationship between the independent and dependent variables during the coagulation process. The ANOVA, diagnostics and graphical representations of the results obtained for the BBD will be in the appendices.

.

Table 4-11: BBD design showing the actual vs predicted results of the matrix for colour, turbidity and COD percentage removal

Factor					Response					
Run	A:Speed	B:Dosage	C:Mixing time	D:Settling time	Colour		Turbidity		COD	
	rpm	g/L	Min	min	% Removal					
1	30	0.35	2	70	97.12	97.65	97.58	97.32	44.97	45.12
2	90	0.35	8.5	70	96.95	97.06	95.32	95.73	45.36	45.00
3	90	0.35	8.5	70	97.17	97.06	96.14	95.73	44.64	45.00
4	90	0.35	2	20	95.67	95.05	92.40	92.35	36.75	35.96
5	90	0.35	15	120	97.45	97.99	97.24	97.16	43.13	42.93
6	90	0.6	2	70	81.36	80.76	88.80	88.93	30.84	31.46
7	90	0.6	8.5	120	96.84	97.44	98.32	98.08	41.67	41.08
8	90	0.1	8.5	20	97.17	96.49	96.56	96.82	41.23	41.92
9	90	0.1	8.5	120	79.76	79.50	95.42	95.46	41.08	41.82
10	90	0.1	2	70	98.56	99.67	99.92	100.20	41.88	41.93
11	150	0.1	8.5	70	97.56	97.53	95.99	95.58	38.34	37.40
12	90	0.35	2	120	95.51	95.50	98.08	98.00	50.16	49.97
13	30	0.35	8.5	120	97.06	96.59	97.50	97.66	46.59	46.66
14	30	0.1	8.5	70	82.84	81.92	96.67	96.51	45.00	44.19
15	90	0.6	15	70	97.01	96.05	98.09	97.91	44.82	45.68
16	150	0.35	15	70	95.01	94.39	93.25	93.53	47.24	47.19
17	150	0.6	8.5	70	75.83	76.66	89.14	89.16	38.64	38.45
18	90	0.1	15	70	81.98	82.75	92.50	92.48	38.99	39.28
19	30	0.35	8.5	20	92.07	92.64	97.21	97.14	48.40	49.13
20	30	0.35	15	70	97.67	98.00	97.85	97.89	48.21	48.14
21	150	0.35	2	70	96.78	96.37	92.87	92.84	38.47	38.65
22	150	0.35	8.5	120	94.34	93.94	96.71	96.90	46.43	46.61
23	30	0.6	8.5	70	97.23	97.18	96.80	97.08	39.12	39.07
24	90	0.35	15	20	91.01	90.93	94.50	94.45	55.36	54.55

25	90	0.6	8.5	20	72.77	72.94	88.37	88.35	39.23	38.59
26	150	0.35	8.5	20	89.75	90.39	89.12	89.06	40.92	41.76

The optimization process was done to find out the values of the optimal variables that would provide high removal efficiency of colour, turbidity and COD in wastewater using PAC as coagulants and the results are presented below. The ramp plots shows the optimised conditions of the coagulation process as well as the desirability that was achieved, as seen in Figure 4-19. To achieve this, the input variables (coagulant dose, mixing speed, mixing time, and settling time) were kept within their respective ranges and the responses (colour, COD and turbidity) were maximized to target 95% confidence predicted levels. From the optimisation process, 100 conditional solutions were achieved, where the optimum condition with a desirability of 93.4% was achieved at 4.897 g/L coagulant dosage, 15 min of mixing time, mixing speed of 30 rpm and a settling time of4 3.384 min. These conditions obtained a maximum removal efficiency of colour, turbidity and COD of 98.562, 99.491 and 51.611, respectively. Validation runs were done in triplicates, and the results are presented in Figure 4-20.

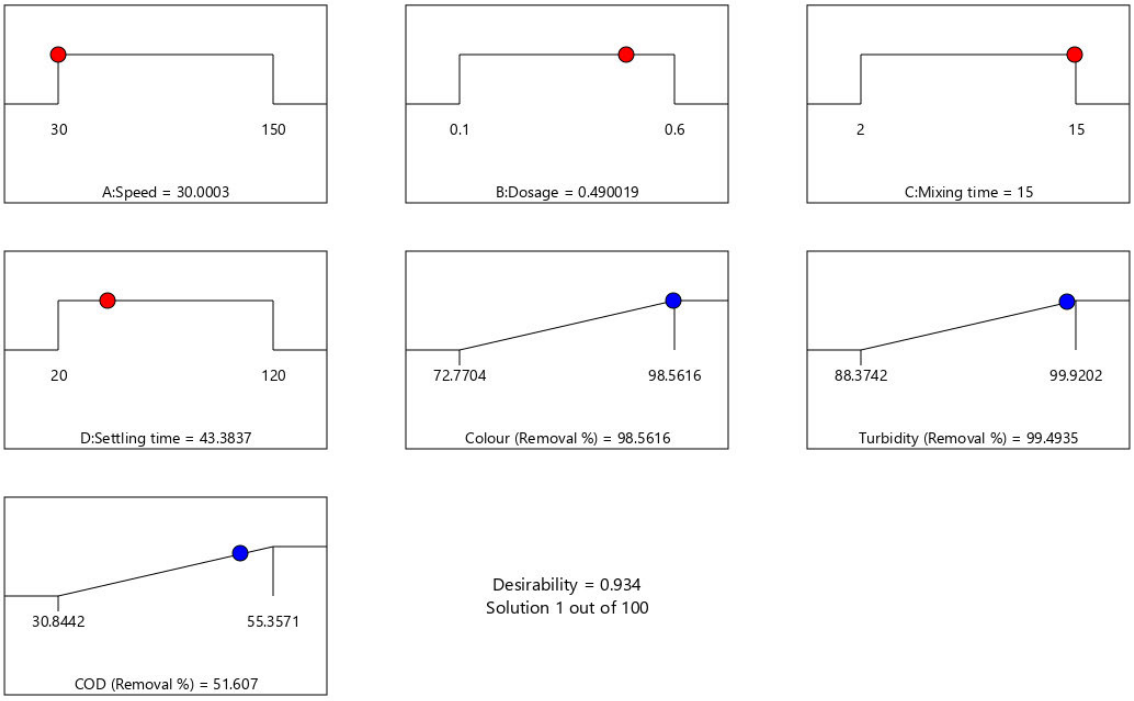

Figure 4-18: Plot showing the ramps of the optimum conditions of the coagulation process with a desirability of 93.4%

Table 4-12: BBD optimisation solutions for PAC-coagulation system

Speed	Dosage	Mixing time	Settling time	Colour	Turbidity	COD	Desirability	
30.000	**0.490**	**15.000**	**43.384**	**98.562**	**99.493**	**51.607**	**0.934**	**Selected**
30.000	0.492	15.000	43.336	98.561	99.509	51.578	0.934	
30.000	0.487	15.000	43.456	98.561	99.472	51.646	0.934	
30.000	0.499	15.000	43.222	98.562	99.558	51.473	0.934	
30.007	0.512	15.000	42.935	98.511	99.656	51.237	0.933	
30.001	0.487	14.934	43.650	98.562	99.449	51.540	0.932	
31.017	0.478	15.000	44.069	98.561	99.353	51.684	0.932	
30.000	0.471	14.947	44.193	98.554	99.327	51.734	0.931	
30.000	0.461	15.000	43.844	98.396	99.257	51.977	0.931	
30.000	0.525	15.000	43.194	98.562	99.759	50.900	0.931	

To assess the validity of the optimum condition presented by the BBD-RSM optimisation analysis and the validity of the suggested models, experimental runs were done in triplicates. This was done to see if the experimental data would correlate with those that were predicted, and the results are presented in Figure 4-20. At a coagulant dosage, mixing speed, mixing time and settling time of 0.49 g/L, 30 rpm, 15 mins and 43.38 mins, the coagulation process obtained an average colour, turbidity and COD removal of 96.13%, 98.23% and 53,21%, respectively. The results showed a strong correlation between the predicted and experimental results. The standard deviation was found to be less than 2%; this indicates the models were well fitted. The models showed acceptable ability for the prediction of the performance of the coagulation process. This shows the variability of the coagulation system with a 95% confidence level and 93.4% desirability.

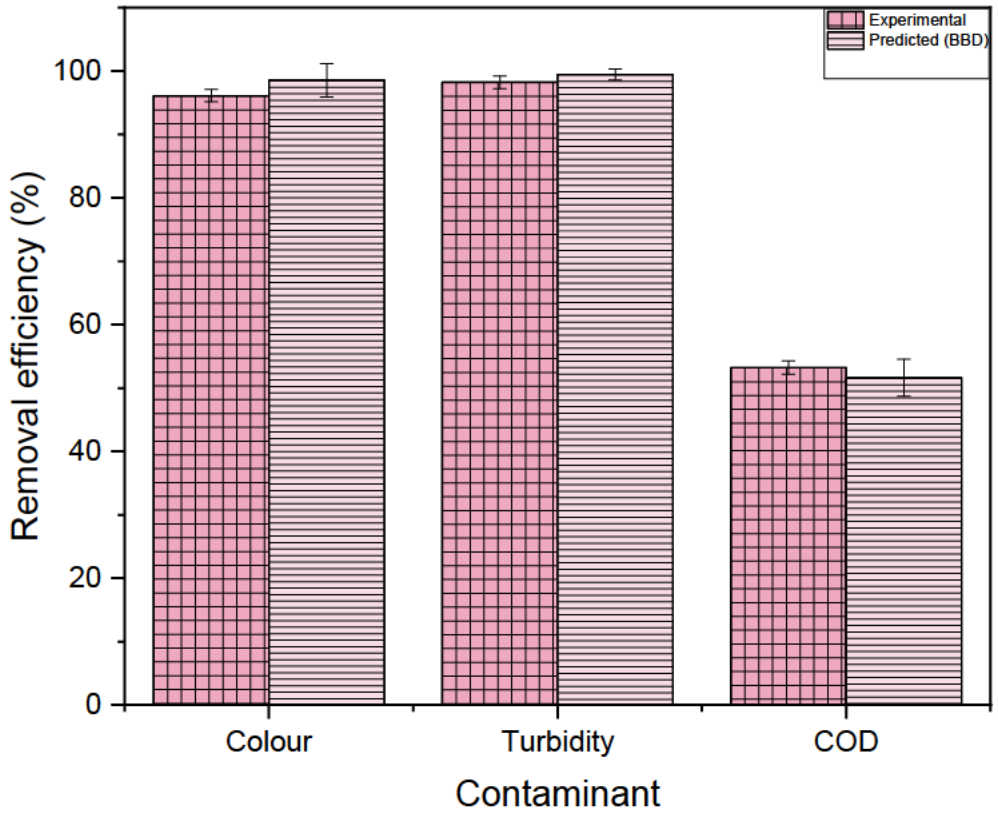

Figure 4-19: The comparison of the RSM predicted values to the actual experimental data

A comparative study was done on PAC and CBP, comparing the removal efficiencies of colour, turbidity and COD found on the RSM matrix, as shown in Figure 4-21. The optimum conditions for both PAC and CBP were used for the respective coagulants; this was done to observe if using bio-coagulants was plausible in the treatment of wastewater and to see if similar results would be observed when comparing the optimum conditions of PAC with the bio-coagulants.

The CBP showed to have a removal efficiency that was over the baseline of 80% at its optimum with a coagulant dosage, mixing speed, mixing time and coagulant dosage of 5.451 g/L, 48.148 rpm, 6.643 mins, and 56.631 mins yielding a removal efficiency of 82.466%, 86.722% and 89.299% for colour, turbidity and COD. The coagulant dosage, mixing speed, mixing time and settling time of 0.49 g/L, 30 rpm, 15 mins and 43.38 mins of PAC yielded results for colour, turbidity and COD at 98.562%, 99.493% and 51.607%. The results, which were previously discussed, showed that CBP has a significant effect on the treatment of wastewater, achieving a contaminant removal of over 80% for colour, turbidity and COD. PAC fell under the 80% bar for COD removal; therefore, it was concluded that CBP can be a viable substitute for chemical coagulants.

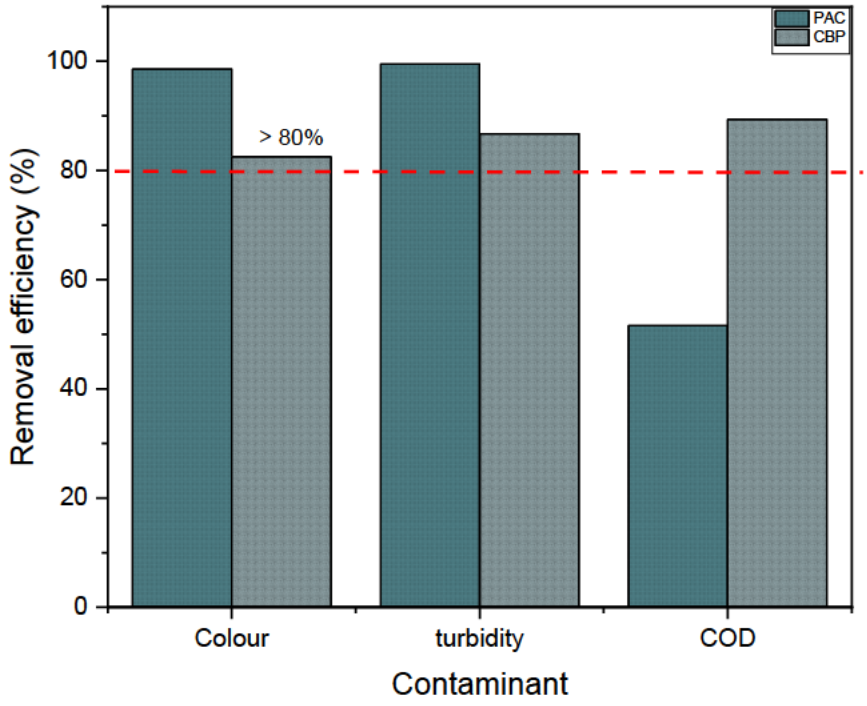

Figure 4-20: Comparative study between PAC and CBP

Further studies were carried out with various other bio-coagulants and were investigated to see the effect they would have in the treatment of wastewater. The same matrix from Table 4-3 was used to generate a predictive model. The bio-coagulants that were used were banana peels, eggshells, seashells, calcined banana peels, calcined eggshells and calcined seashells; the first three optimum solutions are presented in Table 4-13. The results showed that bio-coagulants have the potential to be used as alternatives to conventional coagulants. Where all the bio-coagulants had a desirability of over 90%. In terms of the treatability of colour removal and turbidity removal, it was observed that the removal percentages were over 70% for all the bio-

coagulants. However, there was a variation in results when it came to the removal of COD content. Seashells, calcined eggshells and calcined banana peels showed a high removal in COD content of over 80% and calcined seashells, banana peels, and eggshells had a removal of less than 65%.

Table 4-13: BBD optimisation solutions of various bio-coagulants

Coagulants	Speed				Dosage			Desirability	
	Speed	Dosage	Mixing time	Settling time	Colour	Turbidity	COD		
Banana peels	**56.378**	**3.927**	**3.394**	**29.262**	**89.427**	**96.046**	**37.344**	**1.000**	**Selected**
	90.000	3.500	15.000	20.000	91.396	97.039	38.051	1.000	
	30.000	3.500	15.000	70.000	79.591	95.585	39.357	1.000	
Eggshells	**74.305**	**1.534**	**10.246**	**108.498**	**90.235**	**97.435**	**40.964**	**1.000**	**Selected**
	30.000	6.000	8.500	70.000	75.279	95.621	34.926	1.000	
	90.000	1.000	15.000	70.000	90.406	97.482	40.875	1.000	
Seashell	**38.754**	**1.573**	**14.179**	**82.649**	**89.759**	**69.120**	**88.201**	**1.000**	**Selected**
	90.000	6.000	15.000	70.000	92.335	70.671	69.362	1.000	
	30.000	3.500	15.000	70.000	91.731	72.231	83.212	1.000	
Calcined banana peel	**48.148**	**5.451**	**6.643**	**56.631**	**82.466**	**86.722**	**89.299**	**1.000**	**Selected**
	90.000	1.000	15.000	70.000	85.202	88.489	90.441	1.000	
	141.000	5.625	7.850	77.500	69.420	81.505	88.298	1.000	
Calcined eggshell	**30.324**	**1.564**	**9.219**	**29.896**	**80.410**	**87.507**	**90.355**	**1.000**	**Selected**
	90.000	1.000	15.000	70.000	85.776	93.745	91.139	1.000	
	39.000	3.250	9.475	27.500	79.531	86.420	89.558	1.000	
Calcined Seashell	**120.329**	**1.329**	**5.485**	**56.370**	**86.460**	**97.681**	**54.463**	**1.000**	**Selected**
	90.000	1.000	8.500	20.000	82.705	95.211	53.393	1.000	
	90.000	1.000	8.500	120.000	86.146	98.492	54.478	1.000	

4.5 The removal of contaminants in wastewater

The results presented in this section are in line with objective four, where the removal of phenol, phosphate, nitrate and ammonia will be discussed. The removal efficiency of the calcined bio-coagulants will be compared to that of PAC.

4.5.1 The comparative study of calcined bio-coagulants and PAC for the removal contaminants

In order to assess the impact of the bio-coagulant use, it was judicious to examine the quality of the treated water after having obtained the optimal conditions for the removal of colour, turbidity and COD, and confirmed the predicted values of the three responses considered. The optimal for the various bio-coagulants, as presented in Tables 4-12 and 4-13, were used to test the ability of the bio-coagulants to remove other pollutants such as phosphate, nitrates, ammonia, and phenols. Figure 4-22 shows that calcined banana peels had a removal efficiency of over 80% for only phenols. However, the removal of phosphates and nitrates is over 60%, with ammonia removal being less than 40%. Calcined seashells were shown to be the most promising bio-coagulant in the removal of contaminants, with phosphate, phenols and ammonia having a removal efficiency of over 80% and over 50% for the removal of nitrate.

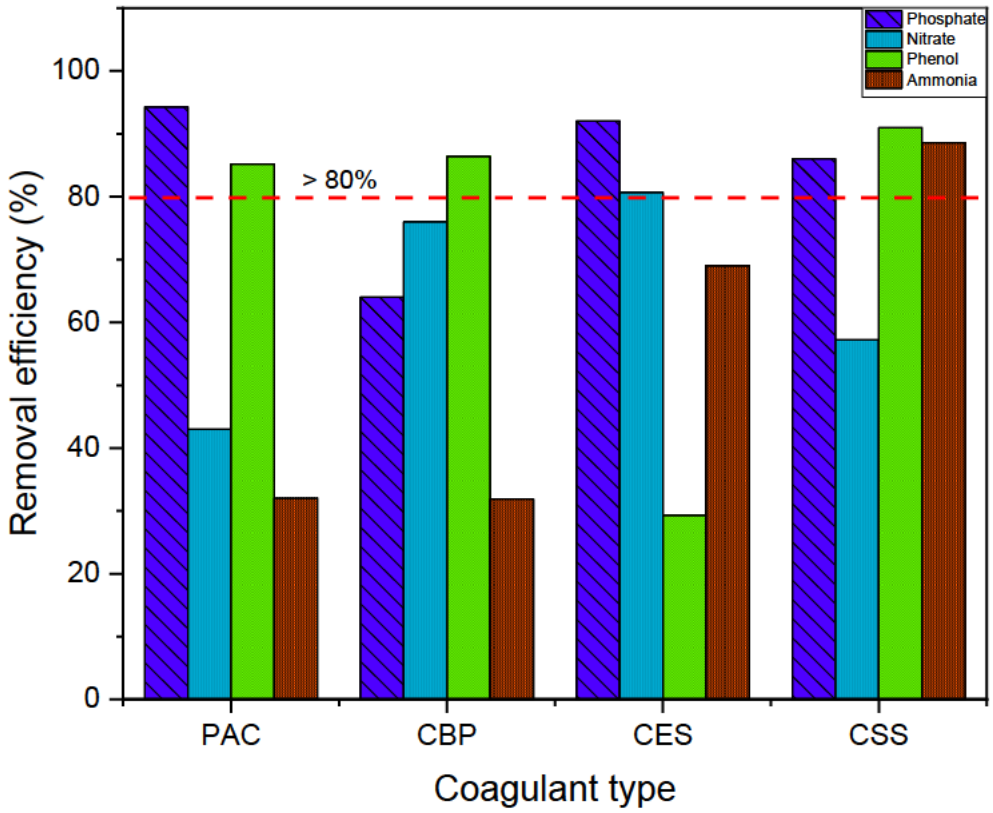

Figure 4-21: The removal of phenol, phosphate, nitrate and ammonia using PAC, calcined banana peel, calcined seashell and calcined eggshell in wastewater

4.6 Summary

In this study, six bio-coagulants were synthesised for the treatment of wastewater; this was done to find an alternative to chemical coagulants that are currently used in industry. The best coagulant was chosen based on its ability to remove turbidity and COD. The calcined banana peel was chosen to be the most effective bio-coagulant with a COD and turbidity removal efficiency of over 80% at a coagulant dosage range of 0.8 g/L to 8 g/L. Design of experiment (BBD) was used for the optimisation of this process. A comparative study was done to evaluate the treatability of the wastewater between calcined banana peels and poly-aluminium chloride. The CBP showed to have a higher removal efficiency at its optimum with a coagulant dosage, mixing speed, mixing time and coagulant dosage of 1.12 g/L, 30.00 rpm, 2.00 mins, and 119.79 mins yielding a removal efficiency of 82.466%, 86.722% and 89.299% for colour, turbidity and COD. for colour, turbidity and COD. Validation tests were conducted in triplicates to determine if the optimum conditions were consistent with the experimental runs and if the results were in conjunction with those of the predicted model. However further studies of the various bio-coagulants are recommended. This is essential for a better understanding of natural

biowaste materials as substitutes for traditional coagulants in the coagulation process of wastewater.

Chapter 5: Conclusion and Recommendations

This chapter focuses on the outcomes and observations made on this study and recommendations for future research are made. This research was focused on the synthesis of six bio-coagulants (banana peels (BP), calcined banana peel (CBP), eggshells (ES), calcined eggshells (CES), seashells (SS) and calcined seashells (CSS)), as a possible substitute of poly-aluminium chloride in the treatment of wastewater. Physical, chemical and morphological characteristics were done using SEM/EDX, FTIR, BET AND XRD for the bio-coagulants.

Specific objectives:

The objectives of this study were:

1. To synthesize and characterize the natural coagulants (eggshells, seashells, and banana peels) and conduct a feasibility study.
2. To develop a predictive model for evaluating the coagulation treatment process with various operating conditions (mixing time, coagulant dosage, speed and settling time).
3. To apply and evaluate the coagulation treatment efficiency of using the synthesized and natural coagulants in comparison to that of PAC at optimized conditions.
4. To evaluate the removal of phosphates, phenols, ammonia and nitrates in industrial wastewater at the optimized conditions using the best coagulant.

5.1 Conclusion

Bio-coagulants which include banana peel (BP), eggshells (ES), and seashells (SS), were prepared and synthesised via the calcination process, which requires an exposure of the biomaterials to high temperatures at a specific time. The banana peels were calcined at $600^{O}C$ for a period of 2 hours, and the seashells and eggshells were calcined at $800^{O}C$ for a period of three hours. The following observations were made on the findings of the characterisation and application of the bio-coagulants on the coagulation process with the aid of a jar tester.

Scanning electron microscopy (SEM) combined with energy-dispersive X-ray (EDX) spectroscopy, Fourier-transform infrared (FTIR) spectroscopy, Brunauer–Emmett– Teller (BET) analyzer, and X-ray diffraction (XRD) analyzer, analysis were done to analyse the surface morphology, elemental composition, functional grouping, surface area and crystal structure of the bio-materials. The SEM/EDX confirmed that the calcined bio-coagulants had more voids and were more agglomerated compared to their uncalcined counterparts, which

shows that the calcination process enhanced the bio-coagulants. Furthermore, the FTIR showed that the biomaterials had functional groups such as O-H stretching and O-H bending, which are essential for the coagulation process. The BET showed that calcining the biomaterials changed their surface area. The banana peel had a surface area of 2.7190 m^2/g before calcination and 4.3889 m^2/g after. All the bio-waste materials were successfully synthesised and could be used as bio-coagulants. A feasibility study was conducted on the calcined and uncalcined bio-coagulants after successful characterisation. This was done to obtain the range of the dosage for the bio-coagulant and, to find the best-performing bio-coagulant. The results showed that the calcined banana peels performed the best with a removal efficiency of over 80% between the ranges 0.8 g/L – 6 g/L. The range that would generate the best results would be between 1 g – and 6g.

The Box-Behnken design adopted from the response surface methodology was used to optimise and evaluate the process for the bio-coagulants and the PAC. Coagulant dosage, mixing time, mixing speed and settling time were the input variables, and the output variables were colour, turbidity and COD removal. The design model was quadratic for the CBP. To assess the model's suitability, the ANOVA was analysed, and the results showed that the regression coefficient for colour, turbidity and COD for CBP were 0.9931, 0.9723 and 0.9874, respectively. This was followed by the optimisation of the process, which determined that the best results would be obtained at 48.148 rpm (mixing speed), 5.451 g/L (dosage), 6.643 min (mixing time), and 56.631 min (settling time). The optimisation of PAC showed that the optimum results would be obtained at 15 min (mixing time), 4.897 g/L (dosage), 30 rpm (mixing speed), and 43.384 min (settling time). The results showed that CBP can be a viable replacement for PAC.

The bio-coagulants significantly impacted the removal of phenol, phosphate, nitrate, and ammonia. CSS had the best bio-coagulant performance, with an efficiency of over 60% for phenol, phosphate, and ammonia removal and a percentage removal of nitrate under 60%.

Based on the study conducted, biowaste materials are a sustainable and economical substitute to conventional coagulants. This technology also assists in decreasing landfill mining and adding value to waste.

5.2 Recommendations

The results obtained in this research show great potential for large-scale experimentation. However, more investigation needs to be done on the efficiency of the bio-coagulants in various

wastewater samples i.e. river water, agricultural water. The removal of contaminants when the bio-coagulants are mixed with PAC at various ratios should also be studied. Also, for future research, more focus should be on cost-benefit analysis and life cycle analysis, to assist in the upscaling of this project.

References

Abdelfattah, A., Ali, S. S., Ramadan, H., El-Aswar, E. I., Eltawab, R., Ho, S.-H., Elsamahy, T., Li, S., El-Sheekh, M. M. and Schagerl, M. 2023. Microalgae-based wastewater treatment: Mechanisms, challenges, recent advances, and future prospects. *Environmental Science and Ecotechnology*, 13: 100205.

Abdullah, F., Bakar, N. A. and Bakar, M. A. 2022. Current advancements on the fabrication, modification, and industrial application of zinc oxide as photocatalyst in the removal of organic and inorganic contaminants in aquatic systems. *Journal of Hazardous Materials*, 424: 127416.

Abdullah I, A., Ighalo, J., Ajala, O. and Ayika, S. 2020. Physicochemical analysis and heavy metals remediation of pharmaceutical industry effluent using bentonite clay modified by H2SO4 and HCl. *Journal of the Turkish chemical society section A: chemistry*, 7 (3): 727-744.

Abidin, Z. Z., Shamsudin, N. S. M., Madehi, N. and Sobri, S. 2013. Optimisation of a method to extract the active coagulant agent from Jatropha curcas seeds for use in turbidity removal. *Industrial Crops and Products*, 41: 319-323.

Abraham, S., Joslyn, S. and Suffet, I. 2015. Treatment of odor by a seashell biofilter at a wastewater treatment plant. *Journal of the Air & Waste Management Association*, 65 (10): 1217-1228.

Abujazar, M. S. S., Karaağaç, S. U., Abu Amr, S. S., Alazaiza, M. Y. D. and Bashir, M. J. K. 2022. Recent advancement in the application of hybrid coagulants in coagulation-flocculation of wastewater: A review. *Journal of Cleaner Production*, 345: 131133.

Adelagun, R., Ngana, O. and Ezekiel, E. 2016. Evaluation of egg shell as a coagulant aid in dye removal from aqueous system. *FUW: Trends Sci Technol J*, 1 (2): 591-594.

Ahmad, A., Sumathi, S. and Hameed, B. 2006. Coagulation of residue oil and suspended solid in palm oil mill effluent by chitosan, alum and PAC. *Chemical Engineering Journal*, 118 (1-2): 99-105.

Ajala, E., Eletta, O. and Oyeniyi, S. 2018. Characterization and evaluation of chicken eggshell for use as a bio-resource. Article ID.

Ajiboye, T. O., Oyewo, O. A. and Onwudiwe, D. C. 2021. Simultaneous removal of organics and heavy metals from industrial wastewater: A review. *Chemosphere*, 262: 128379.

Akhtar, N., Syakir Ishak, M. I., Bhawani, S. A. and Umar, K. 2021. Various natural and anthropogenic factors responsible for water quality degradation: A review. *Water*, 13 (19): 2660.

Akpor, O. B., Ohiobor, G. O. and Olaolu, D. 2014a. Heavy metal pollutants in wastewater effluents: sources, effects and remediation. *Advances in Bioscience and Bioengineering*, 2 (4): 37-43.

Akpor, O. B., Otohinoyi, D., Olaolu, D. and Aderiye, B. 2014b. Pollutants in wastewater effluents: impacts and remediation processes. *International Journal of Environmental Research and Earth Science*, 3 (3): 050-059.

Al-Hazmi, H. E., Mohammadi, A., Hejna, A., Majtacz, J., Esmaeili, A., Habibzadeh, S., Saeb, M. R., Badawi, M., Lima, E. C. and Mąkinia, J. 2023. Wastewater treatment for reuse in agriculture: Prospects and challenges. *Environmental Research*, Article ID: 116711.

Albu, D. 2021. The sustainable development goals report 2021. *Drepturile Omului*, Article ID: 115.

Ali, A., Zhang, N. and Santos, R. M. 2023. Mineral characterization using scanning electron microscopy (SEM): a review of the fundamentals, advancements, and research directions. *Applied Sciences*, 13 (23): 12600.

Amo-Duodu, G., Tetteh, E. K., Rathilal, S., Armah, E. K., Adedeji, J., Chollom, M. N. and Chetty, M. 2021. Effect of engineered biomaterials and magnetite on wastewater treatment: Biogas and kinetic evaluation. *Polymers*, 13 (24): 4323.

Amuda, O. and Amoo, I. 2007. Coagulation/flocculation process and sludge conditioning in beverage industrial wastewater treatment. *Journal of Hazardous Materials*, 141 (3): 778-783.

Anane, I. 2023. Considerations on pollution at European level. *Technium Social Sciences Journal*, 46: 171-187.

Anjaneyulu, Y., Sreedhara Chary, N. and Samuel Suman Raj, D. 2005. Decolourization of industrial effluents–available methods and emerging technologies–a review. *Reviews in Environmental Science and Bio/Technology*, 4: 245-273.

Antao, S. M. and Hassan, I. 2010. Temperature dependence of the structural parameters in the transformation of aragonite to calcite, as determined from in situ synchrotron powder X-ray-diffraction data. *The Canadian Mineralogist*, 48 (5): 1225-1236.

Aslan, N. and Cebeci, Y. 2007. Application of Box–Behnken design and response surface methodology for modeling of some Turkish coals. *Fuel*, 86 (1-2): 90-97.

Asthana, M., Kumar, A. and Sharma, B. 2017. Wastewater treatment. *Principles and applications of environmental biotechnology for a sustainable future*, Article ID: 173-232.

Ayodeji, A. A., Modupe, O. E., Rasheed, B. and Ayodele, J. M. 2018. Data on CaO and eggshell catalysts used for biodiesel production. *Data in Brief*, 19: 1466-1473.

Bahrodin, M. B., Zaidi, N. S., Hussein, N., Sillanpää, M., Prasetyo, D. D. and Syafiuddin, A. 2021. Recent Advances on Coagulation-Based Treatment of Wastewater: Transition from Chemical to Natural Coagulant. *Current Pollution Reports*, 7 (3): 379-391.

Balajii, M. and Niju, S. 2019. A novel biobased heterogeneous catalyst derived from Musa acuminata peduncle for biodiesel production–Process optimization using central composite design. *Energy Conversion and Management*, 189: 118-131.

Balajii, M. and Niju, S. 2020. Banana peduncle–A green and renewable heterogeneous base catalyst for biodiesel production from Ceiba pentandra oil. *Renewable Energy*, 146: 2255-2269.

Balls, M. 2014. Relationships between floc properties and NOM removal using a moorland water source. Article IDUCL (University College London).

Barchiesi, M., Chiavola, A., Di Marcantonio, C. and Boni, M. R. 2021. Presence and fate of microplastics in the water sources: focus on the role of wastewater and drinking water treatment plants. *Journal of Water Process Engineering*, 40: 101787.

Bashir, L., Ossai, P., Shittu, O., Abubakar, A. and Caleb, T. 2015. Comparison of the nutritional value of egg yolk and egg albumin from domestic chicken, guinea fowl and hybrid chicken. *American journal of experimental agriculture*, 6 (5): 310-316.

Bhamidipati, S. H., Vadlamudi, D. P. and Moka, S. 2021. Polymers as Coagulants for Wastewater Treatment. In: *Advanced Materials and Technologies for Wastewater Treatment*. CRC Press, 85-114.

Bharadwaj, A. S., Singh, M., Niju, S., Begum, K. M. S. and Anantharaman, N. 2019. Biodiesel production from rubber seed oil using calcium oxide derived from eggshell as catalyst–optimization and modeling studies. *Green Processing and Synthesis*, 8 (1): 430-442.

Bhat, S. U. and Qayoom, U. 2021. Implications of sewage discharge on freshwater ecosystems. Article ID.

Boczkaj, G. and Fernandes, A. 2017. Wastewater treatment by means of advanced oxidation processes at basic pH conditions: A review. *Chemical Engineering Journal*, 320: 608-633.

Bolong, N., Ismail, A., Salim, M. R. and Matsuura, T. 2009. A review of the effects of emerging contaminants in wastewater and options for their removal. *Desalination*, 239 (1-3): 229-246.

Bratby, J. 2016. *Coagulation and flocculation in water and wastewater treatment*. IWA publishing.

Brown, M. A., Bossa, G. V. and May, S. 2015. Emergence of a stern layer from the incorporation of hydration interactions into the Gouy–Chapman model of the electrical double layer. *Langmuir*, 31 (42): 11477-11483.

Buenaño, B., Vera, E. and Aldás, M. 2019. Study of coagulating/flocculating characteristics of organic polymers extracted from biowaste for water treatment. *Ingeniería e investigación*, 39 (1): 24-35.

Bukhari, A. A. 2008. Investigation of the electro-coagulation treatment process for the removal of total suspended solids and turbidity from municipal wastewater. *Bioresource technology*, 99 (5): 914-921.

Bulut, A., Yusan, S., Aytas, S. and Sert, S. 2018. The use of sea shell (Donax trunculus) powder to remove Sr (II) ions from aqueous solutions. *Water science and Technology*, 78 (4): 827-836.

Capa-Cobos, L. F., Jaramillo-Fierro, X. and González, S. 2021. Computational study of the adsorption of phosphates as wastewater pollutant molecules on faujasites. *Processes*, 9 (10): 1821.

Chao, H.-P. and Chang, C.-C. 2012. Adsorption of copper (II), cadmium (II), nickel (II) and lead (II) from aqueous solution using biosorbents. *Adsorption*, 18: 395-401.

Chartres, C. and Varma, S. 2010. *Out of water: from abundance to scarcity and how to solve the world's water problems*. FT Press.

Chaudhry, F. N. and Malik, M. 2017. Factors affecting water pollution: a review. *J. Ecosyst. Ecography*, 7 (1): 225-231.

Chollom, M. N., Rathilal, S., Swalaha, F. M., Bakare, B. F. and Tetteh, E. K. 2020. Removal of antibiotics during the anaerobic digestion of slaughterhouse wastewater. *Planning*, 15 (3): 335-343.

Chou, M.-Y., Lee, T.-A., Lin, Y.-S., Hsu, S.-Y., Wang, M.-F., Li, P.-H., Huang, P.-H., Lu, W.-C. and Ho, J.-H. 2023. On the removal efficiency of copper ions in wastewater using calcined waste eggshells as natural adsorbents. *Scientific Reports*, 13 (1): 437.

Chu, B., Biriukov, D., Bischoff, M., Předota, M., Roke, S. and Marchioro, A. 2023. Evolution of the electrical double layer with electrolyte concentration probed by second harmonic scattering. *Faraday Discussions*, 246: 407-425.

Collivignarelli, M. C., Abbà, A., Carnevale Miino, M. and Damiani, S. 2019. Treatments for color removal from wastewater: State of the art. *Journal of environmental management*, 236: 727-745.

Crini, G. and Lichtfouse, E. 2019. Advantages and disadvantages of techniques used for wastewater treatment. *Environmental Chemistry Letters*, 17: 145-155.

Cripps, S. J. and Bergheim, A. 2000. Solids management and removal for intensive land-based aquaculture production systems. *Aquacultural engineering*, 22 (1-2): 33-56.

Cruz, R. C., Segadães, A. M., Oberacker, R. and Hoffmann, M. J. 2017. Double layer electrical conductivity as a stability criterion for concentrated colloidal suspensions. *Colloids and Surfaces A: Physicochemical and Engineering Aspects*, 520: 9-16.

Daimary, N., Boruah, P., Eldiehy, K. S., Pegu, T., Bardhan, P., Bora, U., Mandal, M. and Deka, D. 2022. Musa acuminata peel: A bioresource for bio-oil and by-product utilization as a sustainable source of renewable green catalyst for biodiesel production. *Renewable Energy*, 187: 450-462.

Dampang, S., Purwanti, E., Destyorini, F., Kurniawan, S. B., Abdullah, S. R. S. and Imron, M. F. 2021. Analysis of optimum temperature and calcination time in the production of CaO using seashells waste as CaCO3 source. *Journal of Ecological Engineering*, 22 (5): 221-228.

Dayarathne, H., Angove, M. J., Jeong, S., Aryal, R., Paudel, S. R. and Mainali, B. 2022. Effect of temperature on turbidity removal by coagulation: Sludge recirculation for rapid settling. *Journal of Water Process Engineering*, 46: 102559.

Dehghani, M. H., Omrani, G. A. and Karri, R. R. 2021. Solid waste—sources, toxicity, and their consequences to human health. In: *Soft computing techniques in solid waste and wastewater management*. Elsevier, 205-213.

Deshmukh, R. A., Joshi, K., Bhand, S. and Roy, U. 2016. Recent developments in detection and enumeration of waterborne bacteria: a retrospective minireview. *MicrobiologyOpen*, 5 (6): 901-922.

Diver, D., Nhapi, I. and Ruziwa, W. R. 2023. The potential and constraints of replacing conventional chemical coagulants with natural plant extracts in water and wastewater treatment. *Environmental Advances*, Article ID: 100421.

Dmochowska, A., Czajkowska, J., Jędrzejewski, R., Stawiński, W., Migdał, P. and Fiedot-Toboła, M. 2020. Pectin based banana peel extract as a stabilizing agent in zinc oxide nanoparticles synthesis. *International Journal of Biological Macromolecules*, 165: 1581-1592.

Duan, J. and Gregory, J. 2003. Coagulation by hydrolysing metal salts. *Advances in colloid and interface science*, 100: 475-502.

Edet, U. A. and Ifelebuegu, A. O. 2020. Kinetics, Isotherms, and Thermodynamic Modeling of the Adsorption of Phosphates from Model Wastewater Using Recycled Brick Waste. *Processes*, 8 (6): 665.

Edokpayi, J. N., Enitan-Folami, A. M., Adeeyo, A. O., Durowoju, O. S., Jegede, A. O. and Odiyo, J. O. 2020. Recent trends and national policies for water provision and wastewater treatment in South Africa. In: *Water conservation and wastewater treatment in BRICS nations*. Elsevier, 187-211.

El-taweel, R. M., Mohamed, N., Alrefaey, K. A., Husien, S., Abdel-Aziz, A. B., Salim, A. I., Mostafa, N. G., Said, L. A., Fahim, I. S. and Radwan, A. G. 2023. A review of coagulation explaining its definition, mechanism, coagulant types, and optimization models; RSM, and ANN. *Current Research in Green and Sustainable Chemistry*, 6: 100358.

Ellerbrock, R. H. and Gerke, H. H. 2021. FTIR spectral band shifts explained by OM–cation interactions. *Journal of Plant Nutrition and Soil Science*, 184 (3): 388-397.

Eyjolfsson, R. 2015. Chapter One - Introduction. In: Eyjolfsson, R. ed. *Design and Manufacture of Pharmaceutical Tablets*. Boston: Academic Press, 1-28. Available: https://www.sciencedirect.com/science/article/pii/B9780128021828000015 (Accessed

Ezekannagha, C. B., Onukwuli, O. D., Obibuenyi, J. I. and Udunwa, D. I. 2023. Kinetic modeling of papaya seed triglyceride transesterification catalyzed by calcined banana peel ash in methyl ester production. *Chemical Engineering Research and Design*, 200: 256-265.

Fan, M., Wu, H., Shi, M., Zhang, P. and Jiang, P. 2019. Well-dispersive K2OKCl alkaline catalyst derived from waste banana peel for biodiesel synthesis. *Green Energy & Environment*, 4 (3): 322-327.

Farmer, A. 2018. Phosphate pollution: A global overview of the problem. *Phosphorus: Polluter and Resource of the Future—Removal and Recovery from Wastewater; Schaum, C., Ed*, Article ID: 35-55.

Ferraz, E., Gamelas, J. A., Coroado, J., Monteiro, C. and Rocha, F. 2019. Recycling waste seashells to produce calcitic lime: characterization and wet slaking reactivity. *Waste and biomass valorization*, 10: 2397-2414.

Gan, Y., Ding, C., Xu, B., Liu, Z., Zhang, S., Cui, Y., Wu, B., Huang, W. and Song, X. 2023. Antimony (Sb) pollution control by coagulation and membrane filtration in water/wastewater treatment: A comprehensive review. *Journal of Hazardous Materials*, 442: 130072.

Gao, F., Guo, X., Cui, H., Wang, J., Liu, J., Wu, Y., Wan, L., Zhang, C. and Xu, G. 2023. Preparation of magnetic ZnFe2O4 nanosphere photocatalyst for high concentration ammonia nitrogen wastewater treatment. *Journal of Environmental Chemical Engineering*, 11 (5): 110894.

Ghafari, S., Aziz, H. A., Isa, M. H. and Zinatizadeh, A. A. 2009. Application of response surface methodology (RSM) to optimize coagulation–flocculation treatment of leachate using poly-aluminum chloride (PAC) and alum. *Journal of Hazardous Materials*, 163 (2): 650-656.

Ghaly, A., Ananthashankar, R., Alhattab, M. and Ramakrishnan, V. V. 2014. Production, characterization and treatment of textile effluents: a critical review. *J Chem Eng Process Technol*, 5 (1): 1-19.

Ghernaout, D. and Ghernaout, B. 2012. Sweep flocculation as a second form of charge neutralisation—a review. *Desalination and Water Treatment*, 44 (1-3): 15-28.

Girish, C. 2017. Various isotherm models for multicomponent adsorption: A review. *Int. J. Civ. Eng. Technol*, 8 (10): 80-86.

Govenment, S. A. 1956. *Water Act (Act 54 of 1956)* Available: https://soer.environment.gov.za/soer/UploadLibraryImages/UploadDocuments/270123104026_water%20act%20of%201956.pdf (Accessed

Govenment, S. A. 1998. *National Water Act 36 of 1998*. Available: https://www.gov.za/documents/national-water-act (Accessed

Gumbi, N. 2020. The effectiveness of domestic water treatment processes, North West Province, South Africa. Article IDNorth-West University (South Africa).

Gupta, V. K., Ali, I., Saleh, T. A., Nayak, A. and Agarwal, S. 2012. Chemical treatment technologies for waste-water recycling—an overview. *Rsc Advances*, 2 (16): 6380-6388.

Hai, F. I., Yamamoto, K. and Fukushi, K. 2007. Hybrid treatment systems for dye wastewater. *Critical Reviews in Environmental Science and Technology*, 37 (4): 315-377.

Halkos, G. and Gkampoura, E.-C. 2021. Where do we stand on the 17 Sustainable Development Goals? An overview on progress. *Economic Analysis and Policy*, 70: 94-122.

Hamada, H. M., Abed, F., Tayeh, B., Al Jawahery, M. S., Majdi, A. and Yousif, S. T. 2023. Effect of recycled seashells on concrete properties: A comprehensive review of the recent studies. *Construction and Building Materials*, 376: 131036.

Hamdi, M. 1996. Anaerobic digestion of olive mill wastewaters. *Process Biochemistry*, 31 (2): 105-110.

Hamed, M. M., Khalafallah, M. G. and Hassanien, E. A. 2004. Prediction of wastewater treatment plant performance using artificial neural networks. *Environmental Modelling & Software*, 19 (10): 919-928.

Hamilton, R. 1986. The microstructure of the hen's egg shell-a short review. *Food Structure*, 5 (1): 13.

Hanlon, J. B. 1954. Screenings and Grit Complicate Starting Operations at Nut Island Sewage Treatment Plant. *Sewage and Industrial Wastes*, Article ID: 1290-1301.

Hassan, L., Abdullah, N., Abdullah, S., Ghazali, S., Sobri, N., Hashim, N., Yahya, N. and Muslim, W. 2022. The Effectiveness of Chitosan Extraction from Crustaceans' Shells as a natural coagulant. In: Proceedings of *Journal of Physics: Conference Series*. IOP Publishing, 012002.

He, W., Nan, J., Li, H. and Li, S. 2012. Characteristic analysis on temporal evolution of floc size and structure in low-shear flow. *Water Research*, 46 (2): 509-520.

Hogg, R. 2005. Flocculation and dewatering of fine-particle suspensions. *Coagulation and flocculation: Second Edition (FL): CRC Press, Boca Raton*, Article ID: 805-850.

Hoslett, J., Massara, T. M., Malamis, S., Ahmad, D., van den Boogaert, I., Katsou, E., Ahmad, B., Ghazal, H., Simons, S. and Wrobel, L. 2018. Surface water filtration using granular media and membranes: A review. *Science of The Total Environment*, 639: 1268-1282.

Hossain, M. S., Omar, F., Asis, A. J., Bachmann, R. T., Islam Sarker, M. Z. and Ab Kadir, M. O. 2019a. Effective treatment of palm oil mill effluent using FeSO4.7H2O waste from titanium oxide industry: Coagulation adsorption isotherm and kinetics studies. *Journal of Cleaner Production*, 219: 86-98.

Hossain, M. S., Omar, F., Asis, A. J., Bachmann, R. T., Sarker, M. Z. I. and Ab Kadir, M. O. 2019b. Effective treatment of palm oil mill effluent using FeSO4. 7H2O waste from titanium oxide industry: Coagulation adsorption isotherm and kinetics studies. *Journal of Cleaner Production*, 219: 86-98.

Hsiang, S. M., Burke, M. and Miguel, E. 2013. Quantifying the influence of climate on human conflict. *Science*, 341 (6151): 1235367.

Hu, Q., Pang, S. and Wang, D. 2022. In-depth insights into mathematical characteristics, selection criteria and common mistakes of adsorption kinetic models: A critical review. *Separation & Purification Reviews*, 51 (3): 281-299.

Husen, A. K., Bidira, F., Desta, W. M. and Asaithambi, P. 2024. COD, color, and turbidity reduction from surface water using natural coagulants: Investigation and optimization. *Progress in Engineering Science*, 1 (2-3): 100007.

Husin, H., Riza, M. and Faisal, M. 2023. Biodiesel production using waste banana peel as renewable base catalyst. *Materials Today: Proceedings*, Article ID.

Ighalo, J. O. and Adeniyi, A. G. 2020. A mini-review of the morphological properties of biosorbents derived from plant leaves. *SN Applied Sciences*, 2 (3): 509.

Ince, M. and Ince, O. K. 2019. Heavy metal removal techniques using response surface methodology: water/wastewater treatment. In: *Biochemical Toxicology-Heavy Metals and Nanomaterials*. IntechOpen.

Islam, M. R. and Mostafa, M. 2020. Characterization of textile dyeing effluent and its treatment using polyaluminum chloride. *Applied Water Science*, 10 (5): 1-10.

Iwuozor, K. O. 2019. Prospects and challenges of using coagulation-flocculation method in the treatment of effluents. *Advanced Journal of Chemistry-Section A*, 2 (2): 105-127.

Janković, B., Manić, N., Jović, M. and Smičiklas, I. 2022. Kinetic and thermodynamic analysis of thermo-oxidative degradation of seashell powders with different particle size fractions: compensation effect and iso-equilibrium phenomena. *Journal of Thermal Analysis and Calorimetry*, 147 (3): 2305-2334.

Jitjamnong, J., Thunyaratchatanon, C., Luengnaruemitchai, A., Kongrit, N., Kasetsomboon, N., Sopajarn, A., Chuaykarn, N. and Khantikulanon, N. 2021. Response surface optimization of biodiesel synthesis over a novel biochar-based heterogeneous catalyst from cultivated (Musa sapientum) banana peels. *Biomass Conversion and Biorefinery*, 11: 2795-2811.

Jung, J. H., Shon, B. H., Yoo, K. S. and Oh, K. J. 2000. Physicochemical characteristics of waste sea shells for acid gas cleaning absorbent. *Korean Journal of Chemical Engineering*, 17: 585-592.

Kamsonlian, S., Suresh, S., Majumder, C. and Chand, S. 2011. Characterization of banana and orange peels: biosorption mechanism. *International Journal of Science Technology & Management*, 2 (4): 1-7.

Karri, R. R., Sahu, J. N. and Chimmiri, V. 2018. Critical review of abatement of ammonia from wastewater. *Journal of Molecular Liquids*, 261: 21-31.

Kassem, Y., Gökçekuş, H., Çamur, H. and Esenel, E. 2021. Application of artificial neural network, multiple linear regression, and response surface regression models in the estimation of monthly rainfall in Northern Cyprus. *Desalination and Water Treatment*, 215: 328-346.

Keraita, B. 2010. Extent and implications of agricultural reuse of untreated, partly treated and diluted wastewater in developing countries. *Cab Reviews: Perspectives in Agriculture, Veterinary Science, Nutrition and Natural Resources*, 3.

Kestioğlu, K., Yonar, T. and Azbar, N. 2005. Feasibility of physico-chemical treatment and Advanced Oxidation Processes (AOPs) as a means of pretreatment of olive mill effluent (OME). *Process Biochemistry*, 40 (7): 2409-2416.

Khader, E., Mohammed, T. and Mirghaffari, N. 2018. Use of natural coagulants for removal of COD, oil and turbidity from produced waters in the petroleum industry. *J. Pet. Environ. Biotechnol*, 9 (3): 1-7.

Khattri, S. and Singh, M. 2000. Colour removal from synthetic dye wastewater using a bioadsorbent. *Water, Air, and Soil Pollution*, 120: 283-294.

Khazaie, A., Mazarji, M., Samali, B., Osborne, D., Minkina, T., Sushkova, S., Mandzhieva, S. and Soldatov, A. 2022. A review on coagulation/flocculation in dewatering of coal slurry. *Water*, 14 (6): 918.

Khiadani, M., Kolivand, R., Ahooghalandari, M. and Mohajer, M. 2014. Removal of turbidity from water by dissolved air flotation and conventional sedimentation systems using poly aluminum chloride as coagulant. *Desalination and Water Treatment*, 52 (4-6): 985-989.

Khumalo, J. L. 2011. Overview of the National Environmental Management Act 107 of 1998. Article IDUniversity of Limpopo (Turfloop Campus).

Khuri, A. I. and Mukhopadhyay, S. 2010. Response surface methodology. *Wiley Interdisciplinary Reviews: Computational Statistics*, 2 (2): 128-149.

Kilag, O. K. T., Miñoza, J. L., Ledesma, E. N. B., Dosdos, B. V. C., Poloyapoy, B. N. M. and Lisao, C. Y. 2023. Shepherding nature: The environmental degradation. *Science and Education*, 4 (1): 129-147.

Kleitz, F. 2009. Ordered Microporous and Mesoporous Materials. *Nanoscale Materials in Chemistry*, Article ID: 243-329.

Koga, N., Kasahara, D. and Kimura, T. 2013. Aragonite crystal growth and solid-state aragonite–calcite transformation: A physico–geometrical relationship via thermal dehydration of included water. *Crystal growth & design*, 13 (5): 2238-2246.

Kordbacheh, F. and Heidari, G. 2023. Water pollutants and approaches for their removal. *Materials Chemistry Horizons*, 2 (2): 139-153.

Koul, B., Bhat, N., Abubakar, M., Mishra, M., Arukha, A. P. and Yadav, D. 2022. Application of natural coagulants in water treatment: A sustainable alternative to chemicals. *Water*, 14 (22): 3751.

Kumar, J., Choudhary, M., Dikshit, P. K. and Kumar, S. 2024. Recent advancements in utilizing plant-based approaches for water and wastewater treatment technologies. *Cleaner Water*, Article ID: 100030.

Kurniawan, S. B., Abdullah, S. R. S., Imron, M. F., Said, N. S. M., Ismail, N. I., Hasan, H. A., Othman, A. R. and Purwanti, I. F. 2020. Challenges and opportunities of biocoagulant/bioflocculant application for drinking water and wastewater treatment and its potential for sludge recovery. *International journal of environmental research and public health*, 17 (24): 9312.

Kurniawan, S. B., Imron, M. F., Chik, C. E. N. C. E., Owodunni, A. A., Ahmad, A., Alnawajha, M. M., Rahim, N. F. M., Said, N. S. M., Abdullah, S. R. S. and Kasan, N. A. 2022. What compound inside biocoagulants/bioflocculants is contributing the most to the coagulation and flocculation processes? *Science of the Total Environment*, 806: 150902.

Kurwadkar, S., Dane, J., Kanel, S. R., Nadagouda, M. N., Cawdrey, R. W., Ambade, B., Struckhoff, G. C. and Wilkin, R. 2022. Per-and polyfluoroalkyl substances in water and wastewater: A critical review of their global occurrence and distribution. *Science of The Total Environment*, 809: 151003.

Kweinor Tetteh, E. and Rathilal, S. 2020. Evaluating pre-and post-coagulation configuration of dissolved air flotation using response surface methodology. *Processes*, 8 (4): 383.

Landrigan, P. J., Stegeman, J. J., Fleming, L. E., Allemand, D., Anderson, D. M., Backer, L. C., Brucker-Davis, F., Chevalier, N., Corra, L. and Czerucka, D. 2020. Human health and ocean pollution. *Annals of global health*, 86 (1).

Lawler, D. F. 1986. Removing particles in water and wastewater. *Environmental Science & Technology*, 20 (9): 856-861.

Lin-Vien, D., Colthup, N. B., Fateley, W. G. and Grasselli, J. G. 1991. *The handbook of infrared and Raman characteristic frequencies of organic molecules*. Elsevier.

Lin, D., Huang, Y., Zhao, J., Wu, Z., Liu, S., Qin, W., Wu, D., Chen, H. and Zhang, Q. 2020. Evaluation of seed nitrate assimilation and stimulation of phenolic-linked antioxidant on pentose phosphate pathway and nitrate reduction in three feed-plant species. *BMC Plant Biology*, 20: 1-12.

Lin, J.-L., Pan, J. R. and Huang, C. 2013. Enhanced particle destabilization and aggregation by flash-mixing coagulation for drinking water treatment. *Separation and Purification Technology*, 115: 145-151.

Liu, C., Ngo, H. H., Guo, W. and Tung, K.-L. 2012. Optimal conditions for preparation of banana peels, sugarcane bagasse and watermelon rind in removing copper from water. *Bioresource technology*, 119: 349-354.

Liu, D. H. and Lipták, B. G. 2020. *Wastewater treatment*. CRC Press.

Mahallati, M. N. 2020. Advances in modeling saffron growth and development at different scales. In: *Saffron*. Elsevier, 139-167.

Makarigakis, A. K. and Jimenez-Cisneros, B. E. 2019. UNESCO's contribution to face global water challenges. *Water*, 11 (2): 388.

Maphela, B. and Cloete, F. 2020. Johannesburg's implementation of the National Water Act, 1998 in Soweto, South Africa. *Development Southern Africa*, 37 (4): 535-552.

Marques Correia, L., Cecilia, J. A., Rodríguez-Castellón, E., Cavalcante, C. L. and Vieira, R. S. 2017. Relevance of the physicochemical properties of calcined quail eggshell (CaO) as a catalyst for biodiesel production. *Journal of Chemistry*, 2017.

Mat Yasin, N. M. F., Hossain, M. S., HPS, A. K., Zulkifli, M., Al-Gheethi, A., Asis, A. J. and Yahaya, A. N. A. 2020. Treatment of palm oil refinery effluent using tannin as a polymeric coagulant: Isotherm, kinetics, and thermodynamics analyses. *Polymers*, 12 (10): 2353.

McBride, M. B. 1997. A critique of diffuse double layer models applied to colloid and surface chemistry. *Clays and Clay minerals*, 45: 598-608.

Medhi, K. 2021. Chapter 14 - Integrated assessment of ammonia-nitrogen in water environments and its exposure to ecology and human health. In: Ahamad, A., Siddiqui, S. I. and Singh, P. eds. *Contamination of Water*. Academic Press, 199-216. Available: https://www.sciencedirect.com/science/article/pii/B9780128240588000244 (Accessed

Memon, J. R., Memon, S. Q., Bhanger, M., Memon, G. Z., El-Turki, A. and Allen, G. C. 2008. Characterization of banana peel by scanning electron microscopy and FT-IR spectroscopy and its use for cadmium removal. *Colloids and Surfaces B: Biointerfaces*, 66 (2): 260-265.

Mittal, A., Teotia, M., Soni, R. and Mittal, J. 2016. Applications of egg shell and egg shell membrane as adsorbents: a review. *Journal of Molecular Liquids*, 223: 376-387.

Mogbo, O. N., Iorwua, M. B., Duweni, E. C. and Tiza, M. T. 2020. A study on the efficacy of bio-coagulants for turbid and waste water treatment. *J. Crit. Rev*, 7: 1307-1315.

Mohammed, N. A., Saeed, L. I. and Mhemid, R. K. S. 2023. Sustainable Production of an Iron-Eggshell Nanocomposite and Investigating its Catalytic Potential for Phenol Removal. *Ecological Chemistry and Engineering S*, 30 (3): 387-403.

Mohammed, R. R. and Chong, M. F. 2014. Treatment and decolorization of biologically treated Palm Oil Mill Effluent (POME) using banana peel as novel biosorbent. *Journal of environmental management*, 132: 237-249.

Mohd-Salleh, S. N. A., Mohd-Zin, N. S. and Othman, N. 2019. A review of wastewater treatment using natural material and its potential as aid and composite coagulant. *Sains Malaysiana*, 48 (1): 155-164.

Mokgawa, M. P. 2020. The health and survival of fish exposed to wastewater from Motetema wastewater treatment plant, Sekhukhune District. Article ID.

Mousazadeh, M., Kabdaşlı, I., Khademi, S., Sandoval, M. A., Moussavi, S. P., Malekdar, F., Gilhotra, V., Hashemi, M. and Dehghani, M. H. 2022. A critical review on the existing wastewater treatment methods in the COVID-19 era: What is the potential of advanced oxidation processes in combatting viral especially SARS-CoV-2? *Journal of Water Process Engineering*, Article ID: 103077.

Mphuthi, B. R. 2021. Assessing the pollutant removal efficiency of a wetland as a polishing treatment for municipal wastewater. Article IDVaal University of Technology.

Muhamad, N., Juhari, N. and Mohamad, I. 2020. Efficiency of Natural Plant-Based Coagulants for Water Treatment. *IOP Conference Series: Earth and Environmental Science*, 616: 012075.

Musah, M., Azeh, Y., Mathew, J. T., Umar, M. T., Abdulhamid, Z. and Muhammad, A. I. 2022. Adsorption kinetics and isotherm models: a review. *CaJoST*, 4 (1): 20-26.

Mustafa, S., Bhatti, H. N., Maqbool, M. and Iqbal, M. 2021. Microalgae biosorption, bioaccumulation and biodegradation efficiency for the remediation of wastewater and carbon dioxide mitigation: Prospects, challenges and opportunities. *Journal of Water Process Engineering*, 41: 102009.

Myers, R. H., Montgomery, D. C. and Anderson-Cook, C. M. 2016. *Response surface methodology: process and product optimization using designed experiments*. John Wiley & Sons.

Nan, J., Yao, M., Chen, T., Li, S., Wang, Z. and Feng, G. 2016. Breakage and regrowth of flocs formed by sweep coagulation using additional coagulant of poly aluminium chloride and non-ionic polyacrylamide. *Environmental Science and Pollution Research*, 23: 16336-16348.

Narain, V. 2009. Water as a fundamental right: A perspective from India. *Vt. L. Rev.*, 34: 917.

Nath, A., Mishra, A. and Pande, P. P. 2021. A review natural polymeric coagulants in wastewater treatment. *Materials Today: Proceedings*, 46: 6113-6117.

Ngteni, R., Hossain, M. S., Ab Kadir, M. O., Asis, A. J. and Tajudin, Z. 2020. Kinetics and isotherm modeling for the treatment of rubber processing effluent using iron (II) sulphate waste as a coagulant. *Water*, 12 (6): 1747.

Nimesha, S., Hewawasam, C., Jayasanka, D., Murakami, Y., Araki, N. and Maharjan, N. 2022. Effectiveness of natural coagulants in water and wastewater treatment. *Global Journal of Environmental Science and Management*, 8 (1): 101-116.

Nnaji, N., Ani, J., Aneke, L., Onukwuli, O., Okoro, U. and Ume, J. 2014. Modelling the coag-flocculation kinetics of cashew nut testa tannins in an industrial effluent. *Journal of Industrial and Engineering Chemistry*, 20 (4): 1930-1935.

Nordin, N., Hamzah, Z., Hashim, O., Kasim, F. H. and Abdullah, R. 2015. Effect of temperature in calcination process of seashells. *Malaysian Journal of Analytical Sciences*, 19 (1): 65-70.

Nti, S. O., Buamah, R. and Atebiya, J. 2021. Polyaluminium chloride dosing effects on coagulation performance: case study, Barekese, Ghana. *Water Practice & Technology*, 16 (4): 1215-1223.

Nyambura, J. W. 2023. EFFICACY OF TREATING WASTEWATER FROM WASTEPAPER RECYCLING MILL USING A BLEND OF Moringa oleifera Lam AND SYNTHETIC COAGULANTS. Article IDUniversity of Eldoret.

Obiora-Okafo, I. A., Onukwuli, O. D., Igwegbe, C. A., Onu, C. E. and Omotioma, M. 2022. Enhanced performance of natural polymer coagulants for dye removal from wastewater: coagulation kinetics, and mathematical modelling approach. *Environmental Processes*, 9 (2): 20.

Oladipo, A. A., Ahaka, E. O. and Gazi, M. 2019. High adsorptive potential of calcined magnetic biochar derived from banana peels for Cu2+, Hg2+, and Zn2+ ions removal in single and ternary systems. *Environmental Science and Pollution Research*, 26 (31): 31887-31899.

Olaolu, D., Akpor, O. B. and Akor, C. O. 2014. Pollution indicators and pathogenic microorganisms in wastewater treatment: implication on receiving water bodies. *International Journal of environmental protection and policy*, 2 (6): 205-212.

Oller, I., Malato, S. and Sánchez-Pérez, J. A. 2011. Combination of Advanced Oxidation Processes and biological treatments for wastewater decontamination—A review. *Science of The Total Environment*, 409 (20): 4141-4166.

Ouafi, R., Ibrahim, A., Mehdaoui, I., Asri, M., Taleb, M. and Rais, Z. 2021. Spectroscopic analysis of chemical compounds derived from the calcination of snail shells waste at different temperatures. *Chemistry Africa*, 4: 923-933.

Owodunni, A. A., Ismail, S., Kurniawan, S. B., Ahmad, A., Imron, M. F. and Abdullah, S. R. S. 2023. A review on revolutionary technique for phosphate removal in wastewater using green coagulant. *Journal of Water Process Engineering*, 52: 103573.

Popa, V. 2006. ANALYTICAL METHODS FOR LIGNIN CHARACTERIZATION. II. SPECTROSCOPIC STUDIES CARMEN-MIHAELA POPESCU, CORNELIA VASILE, MARIA-CRISTINA POPESCU, GH. SINGUREL*, V. I. POPA** and B. S. MUNTEANU*. *Cellulose Chemistry and Technology*, 40 (8), 597-621 (2006: 597-621.

Precious Sibiya, N., Rathilal, S. and Kweinor Tetteh, E. 2021. Coagulation treatment of wastewater: kinetics and natural coagulant evaluation. *Molecules*, 26 (3): 698.

Rangabhashiyam, S., Anu, N., Giri Nandagopal, M. S. and Selvaraju, N. 2014. Relevance of isotherm models in biosorption of pollutants by agricultural byproducts. *Journal of Environmental Chemical Engineering*, 2 (1): 398-414.

Reddy, D. H. K., Ramana, D., Seshaiah, K. and Reddy, A. 2011. Biosorption of Ni (II) from aqueous phase by Moringa oleifera bark, a low cost biosorbent. *Desalination*, 268 (1-3): 150-157.

Renou, S., Givaudan, J., Poulain, S., Dirassouyan, F. and Moulin, P. 2008. Landfill leachate treatment: Review and opportunity. *Journal of hazardous materials*, 150 (3): 468-493.

Rezai, B. and Allahkarami, E. 2021. Wastewater treatment processes—techniques, technologies, challenges faced, and alternative solutions. In: *Soft Computing Techniques in Solid Waste and Wastewater Management*. Elsevier, 35-53.

Rifi, S. K., Souabi, S., El Fels, L., Driouich, A., Nassri, I., Haddaji, C. and Hafidi, M. 2022. Optimization of coagulation process for treatment of olive oil mill wastewater using Moringa oleifera as a natural coagulant, CCD combined with RSM for treatment optimization. *Process Safety and Environmental Protection*, 162: 406-418.

Rocha, C. G., Zaia, D. A. M., da Silva Alfaya, R. V. and da Silva Alfaya, A. A. 2009. Use of rice straw as biosorbent for removal of Cu (II), Zn (II), Cd (II) and Hg (II) ions in industrial effluents. *Journal of Hazardous Materials*, 166 (1): 383-388.

Rodríguez-Vidal, F. J., García-Valverde, M., Ortega-Azabache, B., González-Martínez, Á. and Bellido-Fernández, A. 2020. Characterization of urban and industrial wastewaters using excitation-emission matrix (EEM) fluorescence: Searching for specific fingerprints. *Journal of environmental management*, 263: 110396.

Roets, Y. 2020. Bioaugmentation with Bacillus spp. for bioremediation of synthetic wastewater using a fluidized-bed reactor. Article ID.

Sahu, O. and Chaudhari, P. 2013. Review on chemical treatment of industrial waste water. *Journal of Applied Sciences and Environmental Management*, 17 (2): 241-257.

Said, K. A. M., Ismail, A. F., Karim, Z. A., Abdullah, M. S. and Hafeez, A. 2021. A review of technologies for the phenolic compounds recovery and phenol removal from wastewater. *Process Safety and Environmental Protection*, 151: 257-289.

Saifuddin, N. and Dinara, S. 2011a. Pretreatment of palm oil mill effluent (POME) using magnetic chitosan. *Journal of Chemistry*, 8: S67-S78.

Saifuddin, N. and Dinara, S. 2011b. Pretreatment of palm oil mill effluent (POME) using magnetic chitosan. *E-Journal of Chemistry*, 8 (S1): S67-S78.

Salah-Tazdaït, R. and Tazdaït, D. 2023. Aerated Constructed Wetlands for Treatment of Food Industry Wastewater. In: *Recent Trends in Constructed Wetlands for Industrial Wastewater Treatment*. Springer, 139-160.

Saleh, T. A. 2021. Protocols for synthesis of nanomaterials, polymers, and green materials as adsorbents for water treatment technologies. *Environmental Technology & Innovation*, 24: 101821.

Saleh, T. A., Tuzen, M. and Sarı, A. 2021. Evaluation of poly (ethylene diamine-trimesoyl chloride)-modified diatomite as efficient adsorbent for removal of rhodamine B from wastewater samples. *Environmental Science and Pollution Research*, 28 (39): 55655-55666.

Salvestrini, S. 2018. Analysis of the Langmuir rate equation in its differential and integrated form for adsorption processes and a comparison with the pseudo first and pseudo second order models. *Reaction Kinetics, Mechanisms and Catalysis*, 123 (2): 455-472.

SANS-241. 2015. South Africa National Standard 2015. Drinking wate; part 1: Microbiological, physical,

aesthetic and chemical determinands. *South African National standards*, Article ID.

Saravanan, A., Kumar, P. S., Jeevanantham, S., Karishma, S., Tajsabreen, B., Yaashikaa, P. and Reshma, B. 2021. Effective water/wastewater treatment methodologies for toxic pollutants removal: Processes and applications towards sustainable development. *Chemosphere*, 280: 130595.

Saxena, K., Brighu, U. and Choudhary, A. 2018. Parameters affecting enhanced coagulation: a review. *Environmental Technology Reviews*, 7 (1): 156-176.

Scheufele, F. B., Módenes, A. N., Borba, C. E., Ribeiro, C., Espinoza-Quiñones, F. R., Bergamasco, R. and Pereira, N. C. 2016. Monolayer–multilayer adsorption phenomenological model: Kinetics, equilibrium and thermodynamics. *Chemical Engineering Journal*, 284: 1328-1341.

Schneider, C., Hanisch, M., Wedel, B., Jusufi, A. and Ballauff, M. 2011. Experimental study of electrostatically stabilized colloidal particles: Colloidal stability and charge reversal. *Journal of colloid and interface science*, 358 (1): 62-67.

Shahwan, T. 2014. Sorption kinetics: obtaining a pseudo-second order rate equation based on a mass balance approach. *Journal of Environmental Chemical Engineering*, 2 (2): 1001-1006.

Shanmuganathan, S., Loganathan, P., Kazner, C., Johir, M. and Vigneswaran, S. 2017. Submerged membrane filtration adsorption hybrid system for the removal of organic micropollutants from a water reclamation plant reverse osmosis concentrate. *Desalination*, 401: 134-141.

Shao, Q., Zhang, Y., Liu, Z., Long, L., Liu, Z., Chen, Y., Hu, X.-M., Lu, M. and Huang, L.-Z. 2022. Phosphorus and nitrogen recovery from wastewater by ceramsite: Adsorption mechanism, plant cultivation and sustainability analysis. *Science of The Total Environment*, 805: 150288.

Shukri, A. S., Baharudin, F., Kassim, J., Mohd Kamil, N. A. F. and Hamzah, N. 2023. Performance of plant-based coagulants in removing turbidity and chemical oxygen demand (COD) in industrial wastewater: a systematic review and meta-analysis. *Journal of Sustainable Civil Engineering & Technology (JSCET)*, 2 (2): 91-103.

Sibiya, N. P. 2023. Treatment of industrial effluent using specialized, magnetized coagulants. Article ID.

Sibiya, N. P., Amo-Duodu, G., Tetteh, E. K. and Rathilal, S. 2022. Magnetic Field Effect on Coagulation Treatment of Wastewater Using Magnetite Rice Starch and Aluminium Sulfate. *Polymers*, 15 (1): 10.

Sigurdarson, J. J., Svane, S. and Karring, H. 2018. The molecular processes of urea hydrolysis in relation to ammonia emissions from agriculture. *Reviews in Environmental Science and Bio/Technology*, 17 (2): 241-258.

Simate, G. S., Cluett, J., Iyuke, S., Musapatika, E., Ndlovu, S., Walubita, L. and Alvarez, A. 2011. The treatment of brewery wastewater for reuse: State of the art. *Desalination*, 273: 235 to 247.

Simate, G. S. and Ndlovu, S. 2015. The removal of heavy metals in a packed bed column using immobilized cassava peel waste biomass. *Journal of Industrial and Engineering Chemistry*, 21: 635-643.

Singh, S., Anil, A. G., Kumar, V., Kapoor, D., Subramanian, S., Singh, J. and Ramamurthy, P. C. 2022. Nitrates in the environment: A critical review of their distribution, sensing techniques, ecological effects and remediation. *Chemosphere*, 287: 131996.

Sonal, S. and Mishra, B. K. 2021. Role of coagulation/flocculation technology for the treatment of dye wastewater: trend and future aspects. *Water pollution and management practices*, Article ID: 303-331.

Sukmana, H., Bellahsen, N., Pantoja, F. and Hodur, C. 2021. Adsorption and coagulation in wastewater treatment–Review. *Progress in Agricultural Engineering Sciences*, 17 (1): 49-68.

Tamjidi, S. and Ameri, A. 2020. A review of the application of sea material shells as low cost and effective bio-adsorbent for removal of heavy metals from wastewater. *Environmental Science and Pollution Research*, 27 (25): 31105-31119.

Tatsi, A., Zouboulis, A., Matis, K. and Samaras, P. 2003. Coagulation–flocculation pretreatment of sanitary landfill leachates. *Chemosphere*, 53 (7): 737-744.

Teh, C. Y., Budiman, P. M., Shak, K. P. Y. and Wu, T. Y. 2016. Recent advancement of coagulation–flocculation and its application in wastewater treatment. *Industrial & Engineering Chemistry Research*, 55 (16): 4363-4389.

Teh, C. Y., Wu, T. Y. and Juan, J. C. 2014. Optimization of agro-industrial wastewater treatment using unmodified rice starch as a natural coagulant. *Industrial Crops and Products*, 56: 17-26.

Tempelhoff, J. 2017. The Water Act, No. 54 of 1956 and the first phase of apartheid in South Africa (1948–1960). *Water History*, 9: 189-213.

Tetteh, E. K. and Rathilal, S. 2019a. Application of organic coagulants in water and wastewater treatment. *Org. Polym*, 1: 51-68.

Tetteh, E. K. and Rathilal, S. 2019b. Application of organic coagulants in water and wastewater treatment. *Org. Polym*, Article ID.

Tetteh, E. K. and Rathilal, S. 2021. Application of magnetized nanomaterial for textile effluent remediation using response surface methodology. *Materials Today: Proceedings*, 38: 700-711.

Tetteh, E. K., Rathilal, S., Chetty, M., Armah, E. K. and Asante-Sackey, D. 2019c. Treatment of water and wastewater for reuse and energy generation-emerging technologies. *Water and wastewater treatment*, Article ID: 53-80.

Tisti, H. J. and Ghawi, A. H. 2020. Performance improvement of package water treatment plant by using static mixer and natural Coagulant. *J. Green Eng*, 10: 3717-3744.

Tofail, S. A. and Bauer, J. 2016. Electrically polarized biomaterials. *Advanced Materials*, 28 (27): 5470-5484.

Tolkou, A. K., Meez, E., Kyzas, G. Z., Torretta, V., Collivignarelli, M. C., Caccamo, F. M., Deliyanni, E. A. and Katsoyiannis, I. A. 2021. A mini review of recent findings in cellulose-, polymer-and graphene-based membranes for fluoride removal from drinking water. *C*, 7 (4): 74.

Tom, A. P. 2021. Nanotechnology for sustainable water treatment—A review. *Mater. Today Proc*, 10: 16-78.

Tran, C. Q., Chantler, C. and de Jonge, M. 2024. Energy calibration for X-ray spectroscopy using powder and single-crystal standards. Article ID.

Tripathy, T. and De, B. R. 2006. Flocculation: a new way to treat the waste water. Article ID.

Tyagi, S., Sharma, B., Singh, P. and Dobhal, R. 2013. Water quality assessment in terms of water quality index. *American Journal of water resources*, 1 (3): 34-38.

Tzoupanos, N. and Zouboulis, I. 2008. Coagulation-flocculation processes in water/wastewater treatment: the application of new generation of chemical reagents. In: Proceedings of *6th IASME/WSEAS international conference on heat transfer, thermal engineering and environment (HTE'08), August 20th–22nd, Rhodes, Greece*. 309-317.

Ugya, A. Editors: Ugya AY, Imam, TS Book: Wastewater Remediation Using Plant Techniques. Article ID.

United Nations. 2015. *Transforming our world: the 2030 Agenda for Sustainable Development*. Available: https://sdgs.un.org/2030agenda (Accessed

Van Haandel, A. and Van Der Lubbe, J. 2007. *Handbook biological waste water treatment-design and optimisation of activated sludge systems*. Webshop Wastewater Handbook.

Vepsäläinen, M. and Sillanpää, M. 2020. Electrocoagulation in the treatment of industrial waters and wastewaters. In: *Advanced water treatment*. Elsevier, 1-78.

Verma, A. K., Dash, R. R. and Bhunia, P. 2012. A review on chemical coagulation/flocculation technologies for removal of colour from textile wastewaters. *Journal of environmental management*, 93 (1): 154-168.

Vikrant, K., Kim, K.-H., Ok, Y. S., Tsang, D. C. W., Tsang, Y. F., Giri, B. S. and Singh, R. S. 2018. Engineered/designer biochar for the removal of phosphate in water and wastewater. *Science of The Total Environment*, 616-617: 1242-1260.

Wang, J. and Guo, X. 2020a. Adsorption isotherm models: Classification, physical meaning, application and solving method. *Chemosphere*, 258: 127279.

Wang, J. and Guo, X. 2020b. Adsorption kinetic models: Physical meanings, applications, and solving methods. *Journal of Hazardous Materials*, 390: 122156.

Wang, K.-J., Wang, P.-S. and Nguyen, H.-P. 2021a. A data-driven optimization model for coagulant dosage decision in industrial wastewater treatment. *Computers & Chemical Engineering*, 152: 107383.

Wang, L. K., Vaccari, D. A., Li, Y. and Shammas, N. K. 2005. Chemical precipitation. In: *Physicochemical treatment processes*. Springer, 141-197.

Wang, L. K., Wang, M.-H. S., Shammas, N. K. and Hahn, H. H. 2021b. Physicochemical treatment consisting of chemical coagulation, precipitation, sedimentation, and flotation. *Integrated natural resources research*, Article ID: 265-397.

Weerasooriya, R., Liyanage, L., Rathnappriya, R., Bandara, W., Perera, T., Gunarathna, M. and Jayasinghe, G. 2021. Industrial water conservation by water footprint and sustainable development goals: a review. *Environment, Development and Sustainability*, Article ID: 1-49.

Wei, H., Gao, B., Ren, J., Li, A. and Yang, H. 2018. Coagulation/flocculation in dewatering of sludge: A review. *Water Research*, 143: 608-631.

Weralupitiya, C., Wanigatunge, R., Joseph, S., Athapattu, B. C., Lee, T.-H., Biswas, J. K., Ginige, M. P., Lam, S. S., Kumar, P. S. and Vithanage, M. 2021. Anammox bacteria in treating ammonium rich wastewater: Recent perspective and appraisal. *Bioresource technology*, 334: 125240.

WHO. 2004. Guidelines for drinking-water quality. *World health organisation*, Article ID.

Wolff, S., Weber, F., Kerpen, J., Winklhofer, M., Engelhart, M. and Barkmann, L. 2020. *Elimination of Microplastics by Downstream Sand Filters in Wastewater Treatment. Water 2021, 13, 33*: s Note: MDPI stays neu-tral with regard to jurisdictional clai-ms in ….

Wu, B., Wan, J., Zhang, Y., Pan, B. and Lo, I. M. C. 2020. Selective Phosphate Removal from Water and Wastewater using Sorption: Process Fundamentals and Removal Mechanisms. *Environmental Science & Technology*, 54 (1): 50-66.

Xia, K., Liu, X., Wang, W., Yang, X. and Zhang, X. 2020a. Synthesis of modified starch/polyvinyl alcohol composite for treating textile wastewater. *Polymers*, 12 (2): 289.

Xia, Y., Zhang, M., Tsang, D. C., Geng, N., Lu, D., Zhu, L., Igalavithana, A. D., Dissanayake, P. D., Rinklebe, J. and Yang, X. 2020b. Recent advances in control technologies for non-point source pollution with nitrogen and phosphorous from agricultural runoff: current practices and future prospects. *Applied Biological Chemistry*, 63: 1-13.

Xiao, F., Ma, J., Yi, P. and Huang, J.-C. H. 2008. Effects of low temperature on coagulation of kaolinite suspensions. *Water Research*, 42 (12): 2983-2992.

Xu, D., Li, Y., Yin, L., Ji, Y., Niu, J. and Yu, Y. 2018. Electrochemical removal of nitrate in industrial wastewater. *Frontiers of environmental science & engineering*, 12: 1-14.

Yang, R., Li, H., Huang, M., Yang, H. and Li, A. 2016. A review on chitosan-based flocculants and their applications in water treatment. *Water Research*, 95: 59-89.

Yang, X., Wan, Y., Zheng, Y., He, F., Yu, Z., Huang, J., Wang, H., Ok, Y. S., Jiang, Y. and Gao, B. 2019. Surface functional groups of carbon-based adsorbents and their roles in the removal of heavy metals from aqueous solutions: a critical review. *Chemical engineering journal*, 366: 608-621.

Yaqoob, A. A., Parveen, T., Umar, K. and Mohamad Ibrahim, M. N. 2020. Role of nanomaterials in the treatment of wastewater: A review. *Water*, 12 (2): 495.

Yoshioka, S. and Kitano, Y. 1985. Transformation of aragonite to calcite through heating. *Geochemical Journal*, 19 (4): 245-249.

Zahrim, A. and Hilal, N. 2013. Treatment of highly concentrated dye solution by coagulation/flocculation–sand filtration and nanofiltration. *Water resources and industry*, 3: 23-34.

Zainal-Abideen, M., Aris, A., Yusof, F., Abdul-Majid, Z., Selamat, A. and Omar, S. 2012. Optimizing the coagulation process in a drinking water treatment plant–comparison between traditional and statistical experimental design jar tests. *Water science and Technology*, 65 (3): 496-503.

Zanacic, E., Stavrinides, J. and McMartin, D. W. 2016. Field-analysis of potable water quality and ozone efficiency in ozone-assisted biological filtration systems for surface water treatment. *Water Research*, 104: 397-407.

Zhang, M., Song, G., Gelardi, D. L., Huang, L., Khan, E., Mašek, O., Parikh, S. J. and Ok, Y. S. 2020. Evaluating biochar and its modifications for the removal of ammonium, nitrate, and phosphate in water. *Water Research*, 186: 116303.

Zhao, C., Zhou, J., Yan, Y., Yang, L., Xing, G., Li, H., Wu, P., Wang, M. and Zheng, H. 2021. Application of coagulation/flocculation in oily wastewater treatment: A review. *Science of The Total Environment*, 765: 142795.

Zhao, Y., Yang, H., Xia, S. and Wu, Z. 2022. Removal of ammonia nitrogen, nitrate, and phosphate from aqueous solution using biochar derived from Thalia dealbata Fraser: effect of carbonization temperature. *Environmental Science and Pollution Research*, 29 (38): 57773-57789.

Zheng, J.-C., Feng, H.-M., Lam, M. H.-W., Lam, P. K.-S., Ding, Y.-W. and Yu, H.-Q. 2009. Removal of Cu (II) in aqueous media by biosorption using water hyacinth roots as a biosorbent material. *Journal of hazardous materials*, 171 (1-3): 780-785.

Zinicovscaia, I. 2016. Conventional methods of wastewater treatment. *Cyanobacteria for bioremediation of wastewaters*, Article ID: 17-25.

Appendix A: General protocols

Figure 6-1: (a) HACH spectrophotometer used for contaminant analysis (DR3900), and (b) COD digester

Figure 6-2: ELGA PURELAB Option-Q water deionizer

Figure 6-3: Calcination furnace

Figure 6-4: ELGA PURELAB Option-Q water deionizer

Figure 6-5: Hach 2100N turbidimeter

Figure 6-6: Jar tester with (a) Samples during coagulation process (b) Sample after settling.

Figure 6-7: Sampling of the effluent

6.1 Appendix C: RSM Raw DATA

6.1.1 PAC-Coagulation optimisation

Table 6-1: ANOVA fit statistics for colour, turbidity and COD

	Colour	Turbidity	COD
Std. Dev.	0.8698	0.3161	0.8265
Mean	92.02	95.09	42.98
C.V. %	0.9453	0.3324	1.92
R^2	0.9944	0.9959	0.9881
Adjusted R^2	0.9873	0.9908	0.9729
Predicted R^2	0.9678	0.9788	0.9320
Adeq Precision	40.4590	49.3714	36.7786

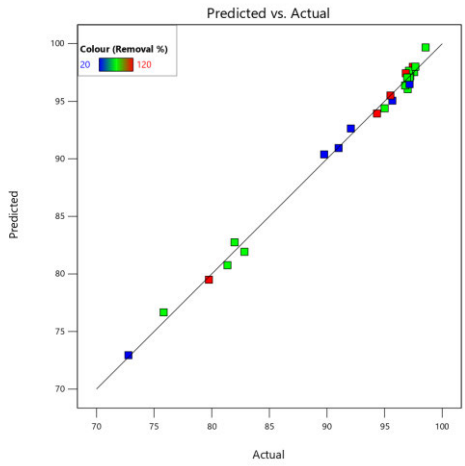

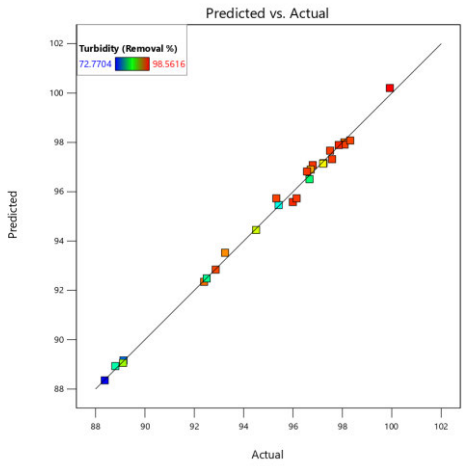

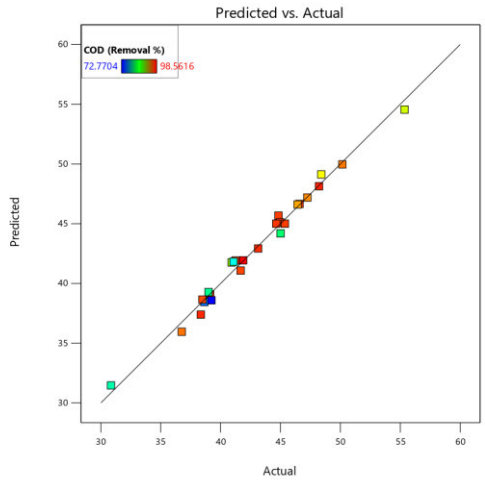

Figure 6-8: Graph showing actual vs predicted plot for (a) which represents colour, (b) representing turbidity and (c) representing COD

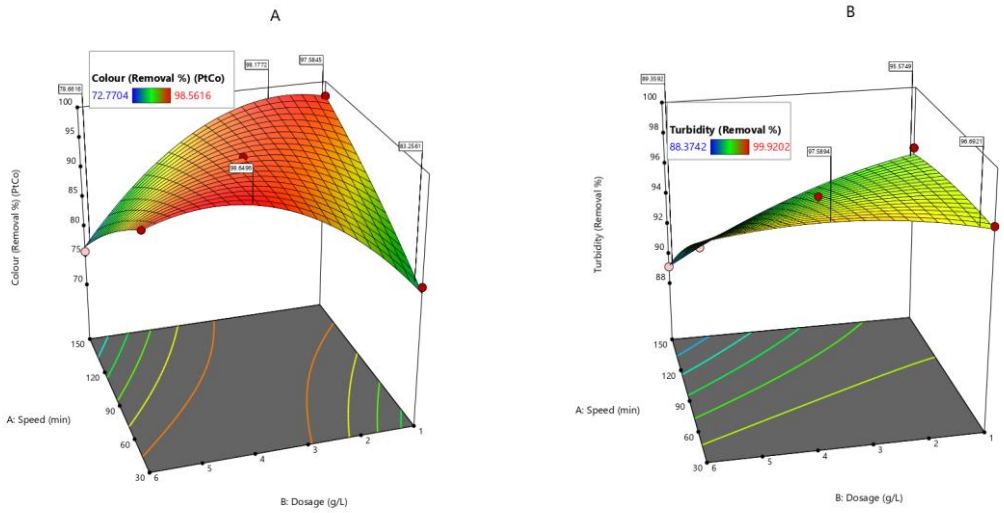

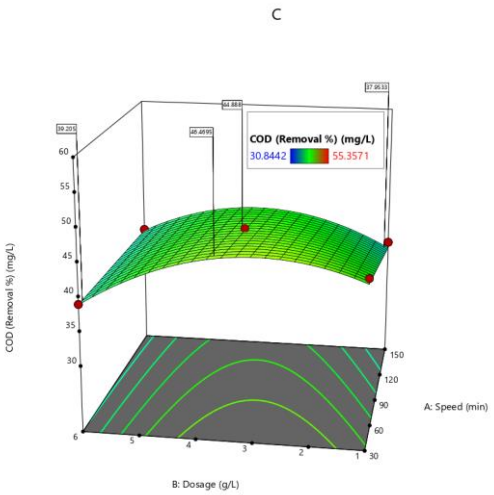

Figure 6-9: Response surface plots showing 3D plots for (a) Colour removal (%), (b) Turbidity removal (%) and (c) COD removal (%)

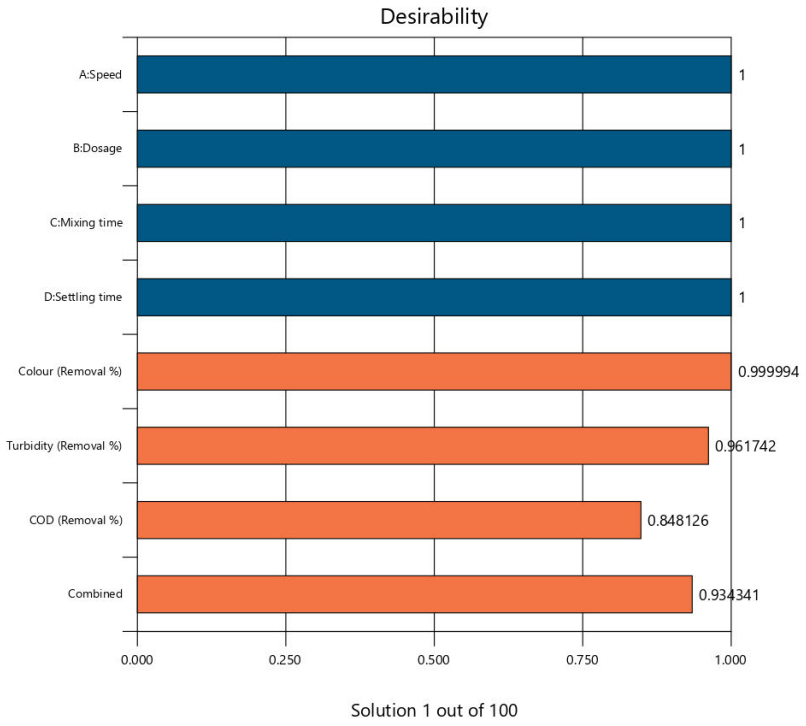

Figure 6-10: Solutions of the optimisation of PAC-Coagulation process

6.1.2 Banana peel – Coagulation system optimisation

Table 6-2: Table showing the actual vs predicted results of the matrix for colour, turbidity and COD percentage removal.

Factor					Response					
Run	A:Speed	B:Dosage	C:Mixing time	D:Settling time	Colour		Turbidity		COD	
	rpm	g/L	Min	min	% Removal					
1	90	1	15	70	84.67	84.76	97.37	97.34	41.24	41.18
2	30	6	8.5	70	81.12	81.14	93.70	93.69	35.33	35.33
3	150	1	8.5	70	91.93	91.82	96.33	96.29	38.37	38.31
4	90	6	8.5	20	92.86	92.79	95.36	95.29	39.33	39.28
5	90	6	2	70	87.55	87.48	96.37	96.33	42.33	42.34
6	150	6	8.5	70	92.29	92.28	98.58	98.61	44.86	44.82
7	150	3.5	2	70	92.98	92.99	97.17	97.17	43.48	43.50
8	90	3.5	15	20	91.33	91.40	96.99	97.04	38.04	38.05
9	90	6	15	70	85.93	85.93	96.00	95.96	37.87	37.81
10	30	3.5	2	70	81.94	81.96	94.99	95.00	33.13	33.11
11	90	3.5	2	20	93.84	93.91	96.52	96.52	40.33	40.32
12	30	3.5	8.5	20	87.16	87.19	96.69	96.66	36.50	36.39
13	150	3.5	8.5	20	98.05	98.11	96.95	96.90	42.10	41.98
14	90	1	8.5	120	79.65	79.72	94.94	94.92	36.43	36.36
15	90	3.5	2	120	81.03	81.04	95.70	95.65	36.33	36.29
16	90	3.5	8.5	70	86.47	86.41	96.36	96.37	38.97	38.90
17	90	3.5	15	120	79.29	79.30	96.27	96.27	40.97	40.94
18	30	1	8.5	70	80.50	80.41	96.98	96.90	37.17	37.14
19	150	3.5	8.5	120	85.98	85.98	98.00	98.00	41.19	41.15

20	90	1	2	70	87.44	87.47	95.87	95.85	34.27	34.27
21	90	3.5	8.5	70	86.33	86.41	95.84	96.37	38.10	38.90
22	90	6	8.5	120	80.56	80.62	97.07	97.00	40.96	40.87
23	90	1	8.5	20	92.58	92.52	98.29	98.27	39.12	39.09
24	30	3.5	8.5	120	74.39	74.36	93.90	93.93	36.10	36.08
25	30	3.5	15	70	79.65	79.59	95.61	95.59	39.33	39.36
26	150	3.5	15	70	91.17	91.11	97.76	97.72	39.56	39.63

Table 6-3: ANOVA fit statistics for colour, turbidity and COD

	Colour	Turbidity	COD
Std. Dev.	0.0761	0.1458	0.2186
Mean	86.41	96.37	38.90
C.V. %	0.0881	0.1513	0.5619
R^2	0.9999	0.9912	0.9964
Adjusted R^2	0.9998	0.9854	0.9940
Predicted R^2	0.9997	0.9883	0.9954
Adeq Precision	479.6605	51.8559	82.3679

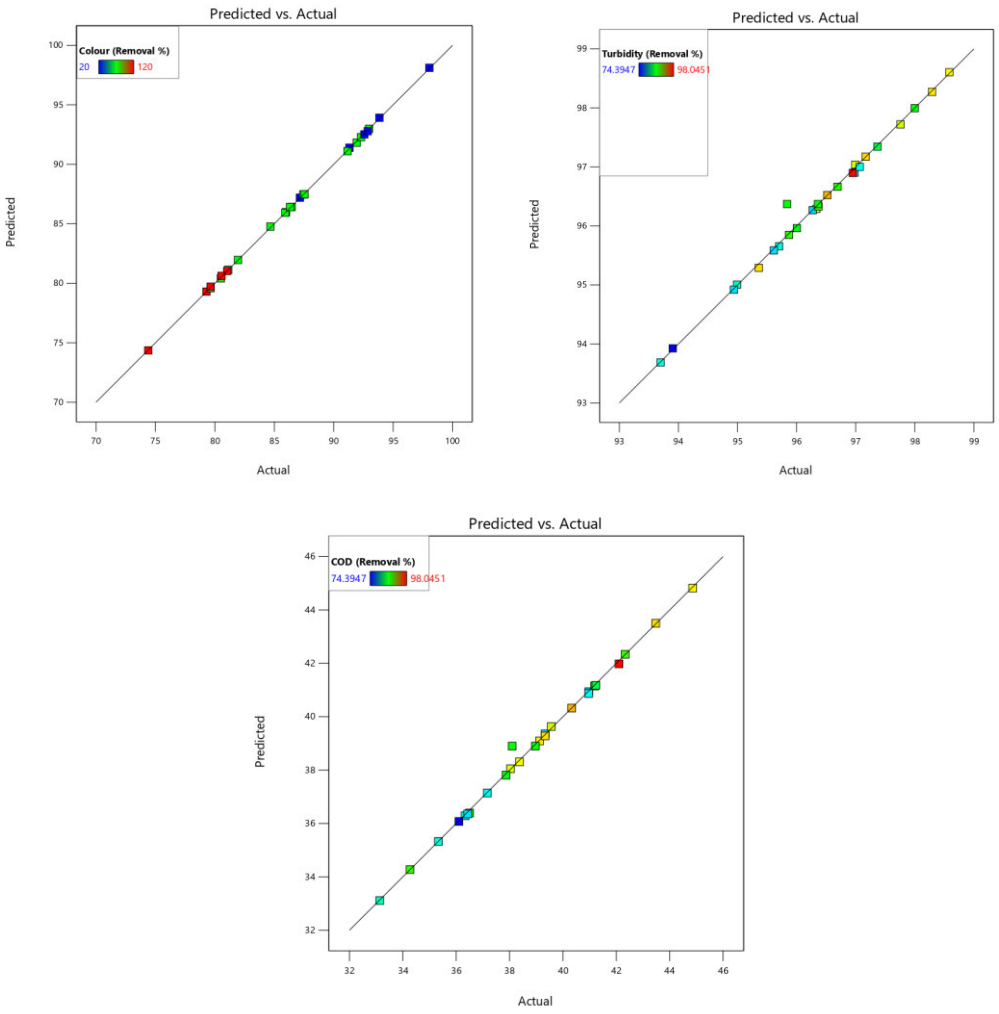

Figure 6-11: Graph showing actual vs predicted plot for (a) which represents colour, (b) representing turbidity and (c) representing COD

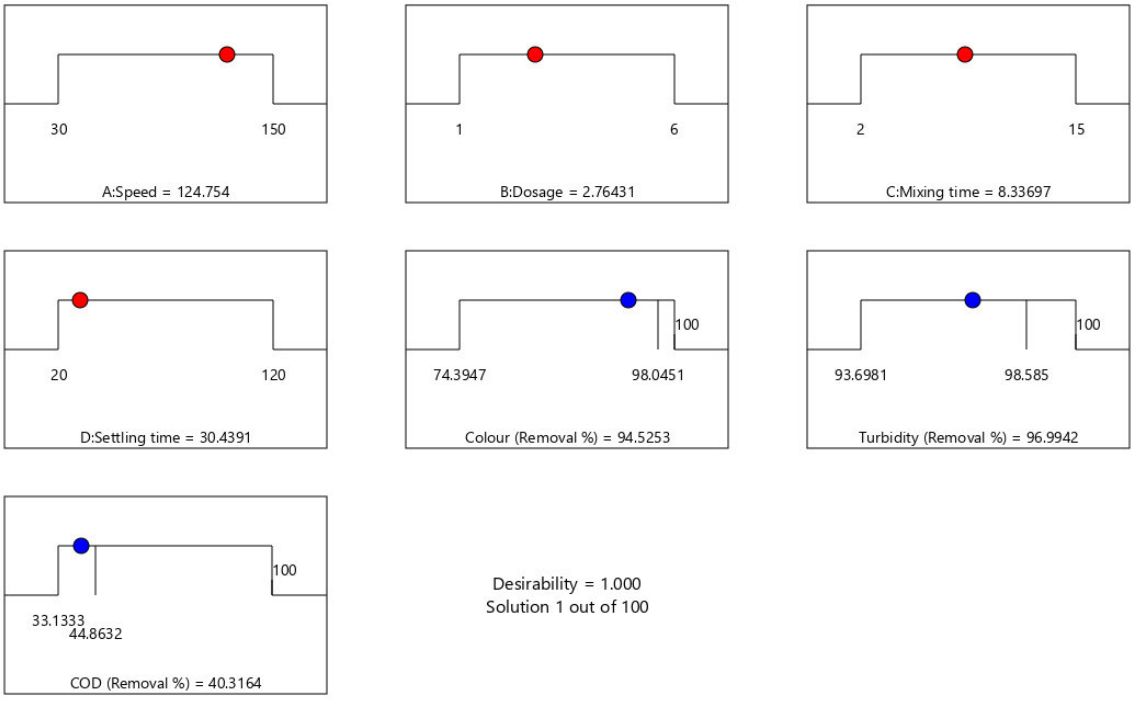

Figure 6-12: Plot showing the ramps of the optimum conditions of the coagulation process with a desirability of 100%

Table 6-4Optimum conditions of BP for the coagulation system

Number	Speed	Dosage	Mixing time	Settling time	Colour (Removal %)	Turbidity (Removal %)	COD (Removal %)	Desirability	
1	**124.754**	**2.764**	**8.337**	**30.439**	**94.525**	**96.994**	**40.316**	**1.000**	**Selected**
2	150.000	1.000	8.500	70.000	91.817	96.289	38.309	1.000	
3	90.000	3.500	2.000	120.000	81.037	95.655	36.288	1.000	
4	150.000	3.500	8.500	20.000	98.113	96.898	41.982	1.000	
5	90.000	3.500	8.500	70.000	86.411	96.371	38.900	1.000	
6	90.000	3.500	15.000	20.000	91.396	97.039	38.051	1.000	
7	90.000	3.500	2.000	20.000	93.910	96.523	40.323	1.000	
8	43.500	5.438	7.525	68.750	82.609	94.547	36.434	1.000	
9	30.000	1.000	8.500	70.000	80.413	96.903	37.141	1.000	
10	90.000	6.000	15.000	70.000	85.932	95.962	37.812	1.000	

6.1.3 Eggshells – Coagulation System Optimisation

Table 6-5: Table showing the actual vs predicted results of the matrix for colour, turbidity and COD percentage removal.

Factor					Response					
Run	A:Speed	B:Dosage	C:Mixing time	D:Settling time	Colour		Turbidity		COD	
	rpm	g/L	Min	min	% Removal					
1	90	3.5	2	20	80.44	79.53	95.87	96.00	35.67	35.93
2	150	6	8.5	70	89.98	89.03	96.50	96.26	39.59	39.65
3	90	3.5	8.5	70	86.10	85.53	97.00	96.30	39.76	38.73
4	30	6	8.5	70	76.65	75.28	95.61	95.62	34.83	34.93
5	150	3.5	8.5	120	95.58	96.89	99.77	100.03	43.88	44.11
6	150	3.5	15	70	93.05	93.91	97.95	97.95	42.90	42.96
7	30	3.5	15	70	78.42	80.16	95.70	95.80	36.33	36.26
8	90	6	2	70	79.86	80.65	95.36	95.61	36.33	36.23
9	150	3.5	2	70	91.17	90.89	96.76	96.60	39.56	39.69
10	90	1	15	70	91.56	90.41	97.56	97.48	40.96	40.88
11	150	3.5	8.5	20	88.53	87.92	94.13	94.52	38.57	38.55
12	150	1	8.5	70	95.29	95.77	98.48	98.29	42.86	43.00
13	90	1	8.5	20	84.73	84.41	95.00	94.75	37.87	37.85
14	90	1	8.5	120	93.84	93.38	98.52	98.57	42.33	42.49
15	90	3.5	8.5	70	86.98	85.53	96.29	96.30	38.82	38.73
16	90	6	8.5	20	76.03	77.67	96.70	96.51	35.33	35.28
17	90	3.5	2	120	89.33	88.50	95.49	95.44	39.94	39.76

18	30	3.5	8.5	120	83.94	83.13	93.99	93.91	37.33	37.67
19	90	6	15	70	84.55	83.67	96.37	96.27	38.33	38.35
20	90	6	8.5	120	84.89	86.64	95.27	95.38	39.17	39.29
21	90	3.5	15	120	92.67	91.52	98.37	98.50	42.24	42.02
22	90	1	2	70	86.47	87.38	95.56	95.83	39.67	39.46
23	30	3.5	2	70	76.39	77.14	94.90	94.85	36.00	36.00
24	90	3.5	15	20	81.55	82.55	94.94	95.25	37.00	37.21
25	30	3.5	8.5	20	75.16	74.16	96.69	96.73	34.50	34.59
26	30	1	8.5	70	80.50	82.02	94.98	95.03	37.17	37.33

Table 6-6: ANOVA fit statistics for colour, turbidity and COD

	colour	Turbidity	COD
Std. Dev.	1.18	0.2902	0.3302
Mean	85.53	96.30	38.73
C.V. %	1.38	0.3013	0.8527
R^2	0.9707	0.9761	0.9908
Adjusted R^2	0.9651	0.9601	0.9846
Predicted R^2	0.9548	0.9408	0.9829
Adeq Precision	43.8180	32.4223	44.3238

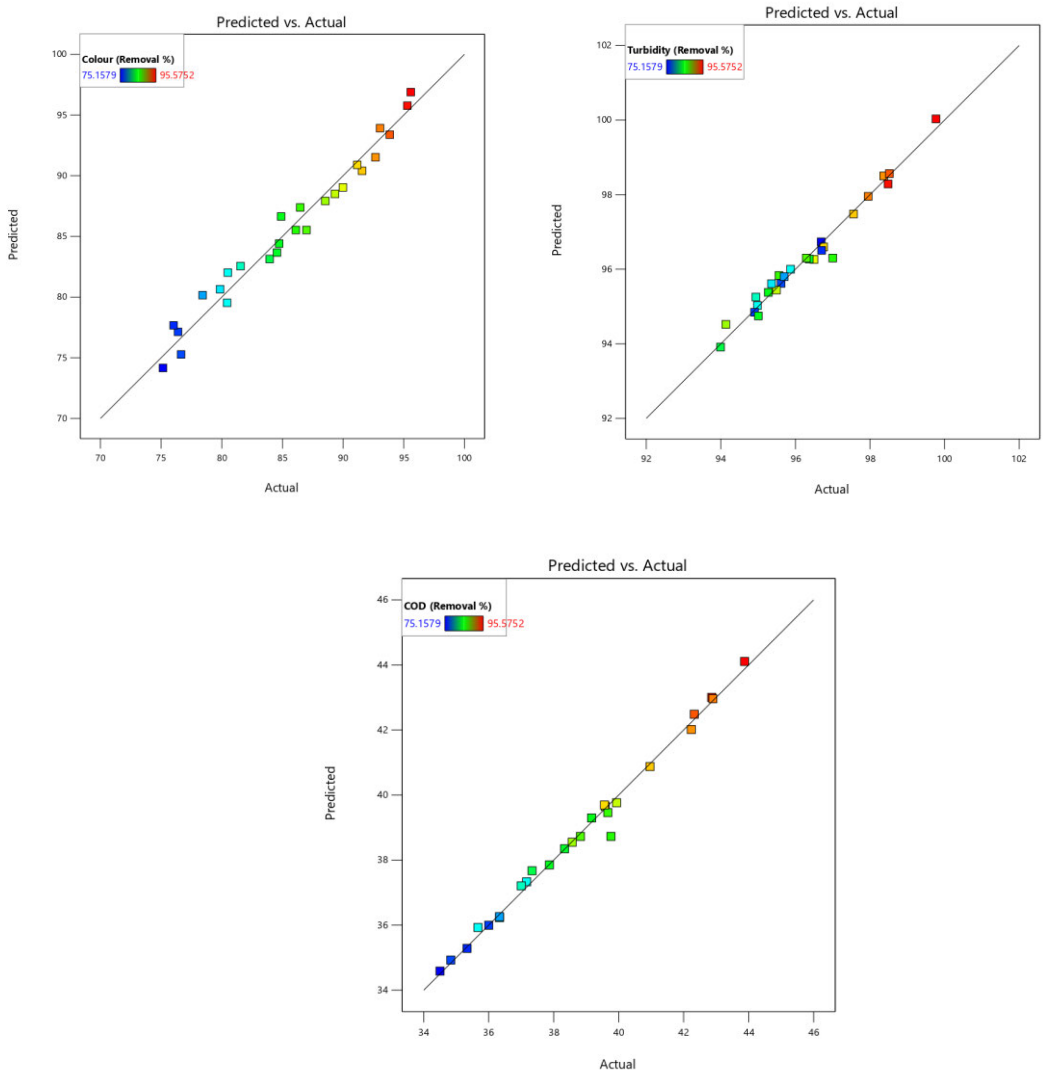

Figure 6-13: Graph showing actual vs predicted plot for (a) which represents colour, (b) representing turbidity and (c) representing COD

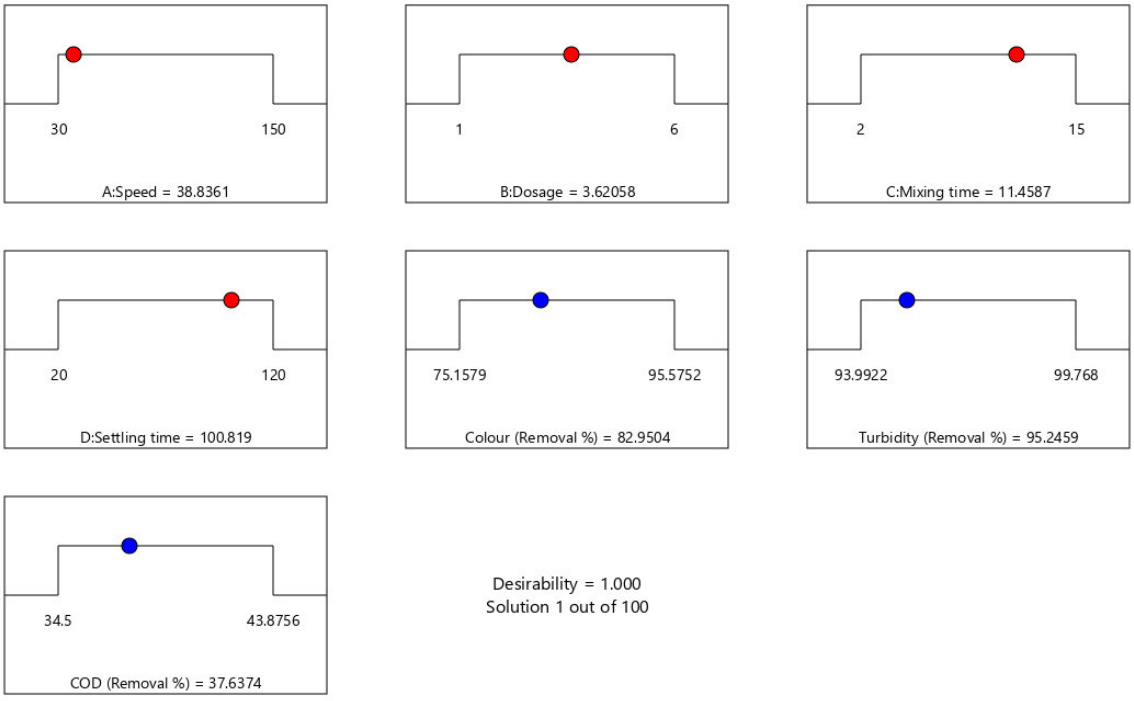

Figure 6-14: Plot showing the ramps of the optimum conditions of the coagulation process with a desirability of 100%

Table 6-7: Optimum conditions of ES for the coagulation system

Number	Speed	Dosage	Mixing time	Settling time	Colour (Removal %)	Turbidity (Removal %)	COD (Removal %)	Desirability	
1	**38.836**	**3.621**	**11.459**	**100.819**	**82.950**	**95.246**	**37.637**	**1.000**	**Selected**
2	30.000	6.000	8.500	70.000	75.279	95.621	34.926	1.000	
3	90.000	6.000	15.000	70.000	83.668	96.274	38.349	1.000	
4	150.000	3.500	2.000	70.000	90.891	96.598	39.694	1.000	
5	90.000	3.500	8.500	70.000	85.525	96.300	38.729	1.000	
6	90.000	6.000	8.500	20.000	77.672	96.507	35.284	1.000	
7	39.000	3.250	9.475	112.500	84.055	94.821	38.112	1.000	
8	150.000	3.500	8.500	20.000	87.918	94.520	38.548	1.000	
9	90.000	1.000	8.500	20.000	84.410	94.748	37.851	1.000	
10	30.000	1.000	8.500	70.000	82.017	95.026	37.333	1.000	

6.1.4 Seashell – Coagulation System Optimisation

Table 6-8: Table showing the actual vs predicted results of the matrix for colour, turbidity and COD percentage removal.

Factor					Response					
Run	A:Speed	B:Dosage	C:Mixing time	D:Settling time	Colour		Turbidity		COD	
	rpm	g/L	Min	min	% Removal					
1	30	3.5	15	70	91.54	91.73	72.14	72.23	83.15	83.21
2	90	3.5	8.5	70	94.42	94.78	75.14	74.84	67.75	67.52
3	90	1	2	70	97.12	96.72	71.89	71.72	67.75	68.05
4	30	6	8.5	70	88.55	88.60	73.72	73.71	65.38	65.57
5	90	6	8.5	120	95.65	94.98	68.63	68.16	70.17	70.58
6	150	3.5	15	70	84.68	84.87	71.29	71.45	71.56	72.34
7	90	6	2	70	89.85	89.91	68.91	69.01	71.60	71.92
8	30	3.5	8.5	20	89.96	89.68	75.65	75.75	66.13	66.58
9	150	1	8.5	70	83.94	83.65	74.93	74.74	71.80	71.95
10	90	6	15	70	92.14	92.34	70.52	70.67	69.98	69.36
11	90	3.5	2	120	96.74	96.85	75.37	75.52	66.25	66.62
12	90	3.5	8.5	70	95.14	94.78	74.54	74.84	67.29	67.52
13	30	3.5	8.5	120	93.82	93.99	74.13	74.31	68.83	68.35
14	90	1	8.5	20	87.93	89.06	66.16	66.86	72.50	72.06
15	150	3.5	8.5	120	90.59	90.65	78.20	78.08	72.26	71.49
16	30	1	8.5	70	92.40	92.00	69.62	69.20	70.44	71.01
17	150	3.5	8.5	20	83.58	83.18	75.12	74.93	58.94	59.10
18	90	1	15	70	85.75	85.47	67.20	67.08	90.98	90.35
19	30	3.5	2	70	93.93	94.20	71.39	71.46	65.46	64.65

20	90	3.5	15	20	86.91	86.55	73.53	73.18	69.44	69.41
21	90	1	8.5	120	90.62	90.87	78.10	78.30	73.38	73.42
22	90	3.5	15	120	94.27	94.34	71.64	71.72	88.23	88.66
23	150	6	8.5	70	86.96	87.11	70.90	71.12	60.50	60.27
24	150	3.5	2	70	90.95	91.22	75.06	75.20	71.26	71.17
25	90	3.5	2	20	93.17	92.86	72.64	72.36	71.79	71.71
26	90	6	8.5	20	84.80	85.01	77.86	77.89	57.85	57.78

Table 6-9: ANOVA fit statistics for colour, turbidity and COD

	colour	Turbidity	COD
Std. Dev.	0.5538	0.3884	0.6435
Mean	90.59	72.86	70.41
C.V. %	0.6113	0.5331	0.9140
R^2	0.9919	0.9936	0.9968
Adjusted R^2	0.9815	0.9854	0.9927
Predicted R^2	0.9542	0.9642	0.9817
Adeq Precision	32.5020	38.7603	66.6286

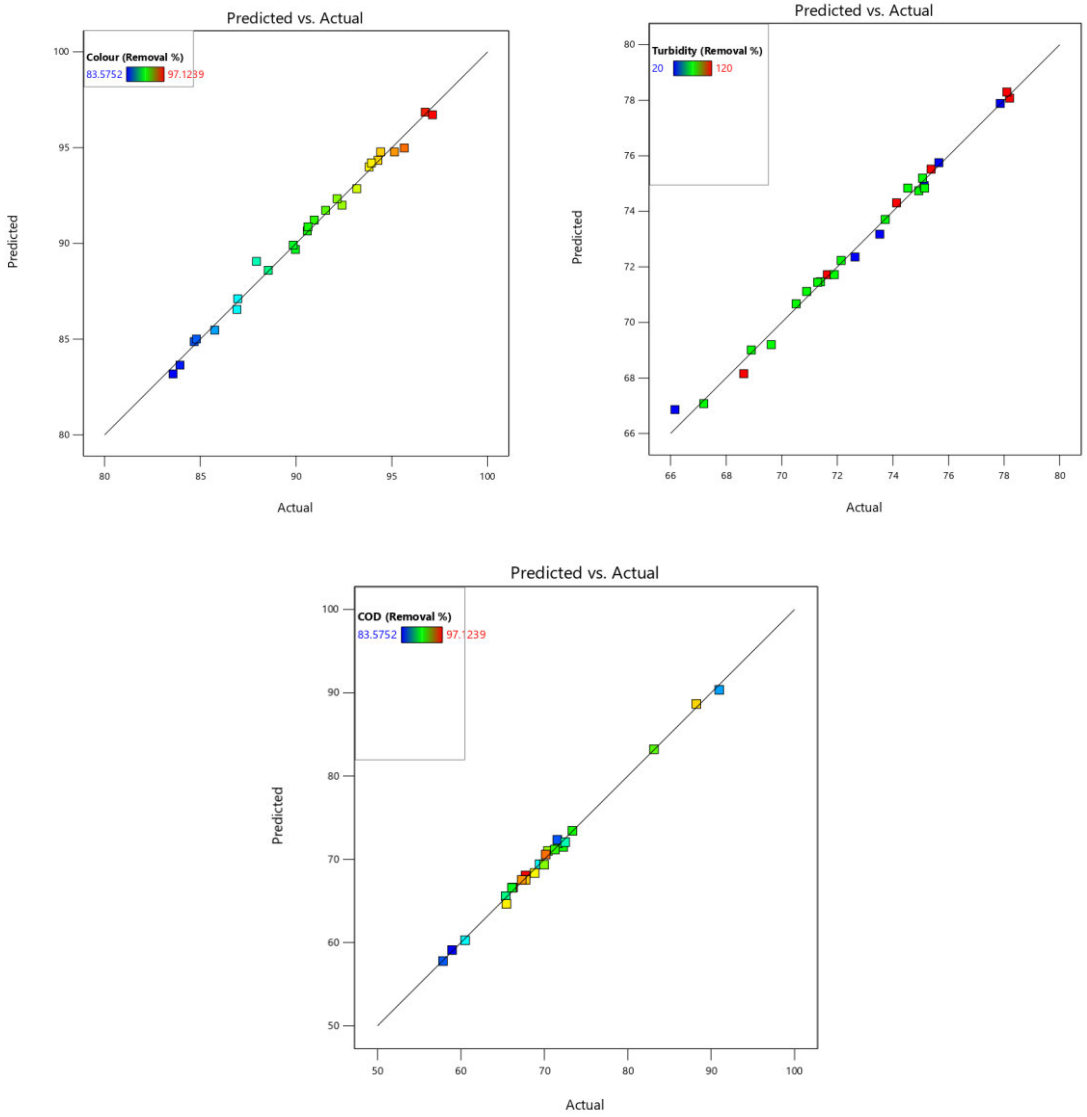

Figure 6-15: Graph showing actual vs predicted plot for (a) which represents colour, (b) representing turbidity and (c) representing COD

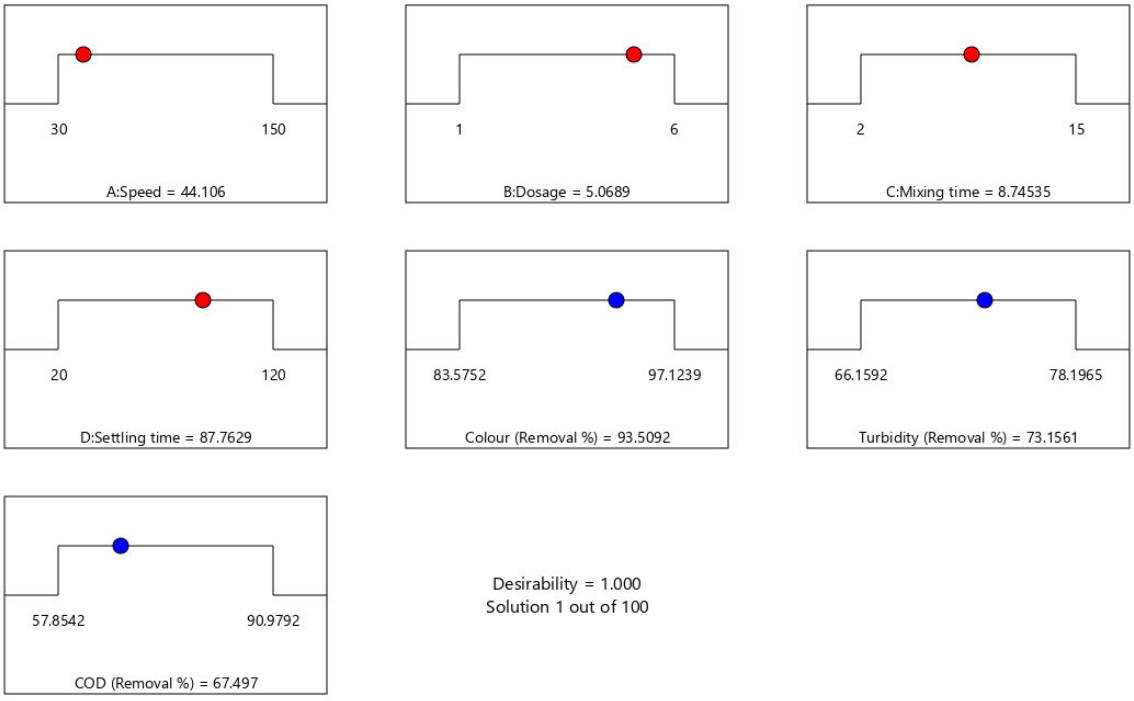

Figure 6-16: Plot showing the ramps of the optimum conditions of the coagulation process with a desirability of 100%

Table 6-10: Optimum conditions of SS for the coagulation system

Number	Speed	Dosage	Mixing time	Settling time	Colour (Removal %)	Turbidity (Removal %)	COD (Removal %)	Desirability	
1	**44.106**	**5.069**	**8.745**	**87.763**	**93.509**	**73.156**	**67.497**	**1.000**	**Selected**
2	90.000	3.500	15.000	20.000	86.554	73.178	69.413	1.000	
3	30.000	3.500	2.000	70.000	94.203	71.463	64.648	1.000	
4	90.000	6.000	15.000	70.000	92.335	70.671	69.362	1.000	
5	90.000	3.500	8.500	70.000	94.778	74.838	67.522	1.000	
6	90.000	3.500	2.000	20.000	92.858	72.356	71.709	1.000	
7	90.000	3.500	2.000	120.000	96.855	75.520	66.621	1.000	
8	90.000	6.000	8.500	120.000	94.983	68.155	70.576	1.000	
9	90.000	1.000	15.000	70.000	85.474	67.076	90.348	1.000	
10	150.000	1.000	8.500	70.000	83.646	74.742	71.953	1.000	

6.1.5 Calcined eggshell – Coagulation system optimisation

Table 6-11: Table showing the actual vs predicted results of the matrix for colour, turbidity and COD percentage removal.

Factor					Response					
Run	A:Speed	B:Dosage	C:Mixing time	D:Settling time	Colour		Turbidity		COD	
	rpm	g/L	Min	min	% Removal					
1	90	6	15	70	86.85	87.02	90.59	90.35	88.06	87.99
2	30	3.5	15	70	83.49	83.78	87.88	87.93	89.20	89.17
3	90	1	15	70	85.68	85.78	93.80	93.74	91.26	91.14
4	90	1	8.5	120	87.88	87.76	88.02	87.96	90.72	90.79
5	90	3.5	8.5	70	85.62	84.91	85.37	85.96	89.12	89.62
6	30	3.5	8.5	20	77.80	77.68	86.50	86.45	89.60	89.78
7	90	1	8.5	20	85.70	85.69	88.63	88.61	89.41	89.39
8	90	3.5	2	120	84.45	84.86	81.69	81.67	88.17	88.22
9	90	3.5	8.5	70	84.83	84.91	86.56	85.96	89.60	89.62
10	150	1	8.5	70	89.85	89.89	96.67	96.67	89.65	89.54
11	90	1	2	70	87.56	87.68	87.57	87.71	89.13	89.04
12	90	3.5	15	120	88.42	88.44	86.55	86.64	91.20	91.24
13	150	3.5	8.5	120	87.78	87.67	92.45	92.39	90.88	90.80
14	150	3.5	2	70	87.50	87.30	93.89	93.89	90.03	90.07
15	30	6	8.5	70	79.34	79.75	83.96	84.02	87.90	87.80
16	30	3.5	2	70	79.66	79.53	81.26	81.23	89.33	89.27
17	90	3.5	2	20	81.93	81.97	86.71	86.67	91.11	91.11

18	90	3.5	15	20	84.73	84.36	90.93	91.01	87.89	87.89
19	30	3.5	8.5	120	86.03	85.63	77.85	77.83	88.61	88.66
20	90	6	2	70	78.96	79.15	87.12	87.06	90.33	90.29
21	150	6	8.5	70	86.22	86.42	95.23	95.30	90.55	90.48
22	150	3.5	15	70	88.78	89.01	96.45	96.52	89.88	89.95
23	90	6	8.5	120	85.88	85.54	81.85	81.91	88.70	88.67
24	90	6	8.5	20	80.88	80.64	90.52	90.62	89.72	89.61
25	30	1	8.5	70	83.31	83.56	86.71	86.69	90.79	90.64
26	150	3.5	8.5	20	88.49	88.65	93.21	93.13	89.17	89.22

Table 6-12: ANOVA fit statistics for colour, turbidity and COD

	colour	Turbidity	COD
Std. Dev.	0.3446	0.2794	0.1626
Mean	84.91	88.38	89.62
C.V. %	0.4059	0.3161	0.1814
R^2	0.9936	0.9986	0.9850
Adjusted R^2	0.9894	0.9967	0.9751
Predicted R^2	0.9827	0.9938	0.9705
Adeq Precision	54.4773	88.7739	32.5569

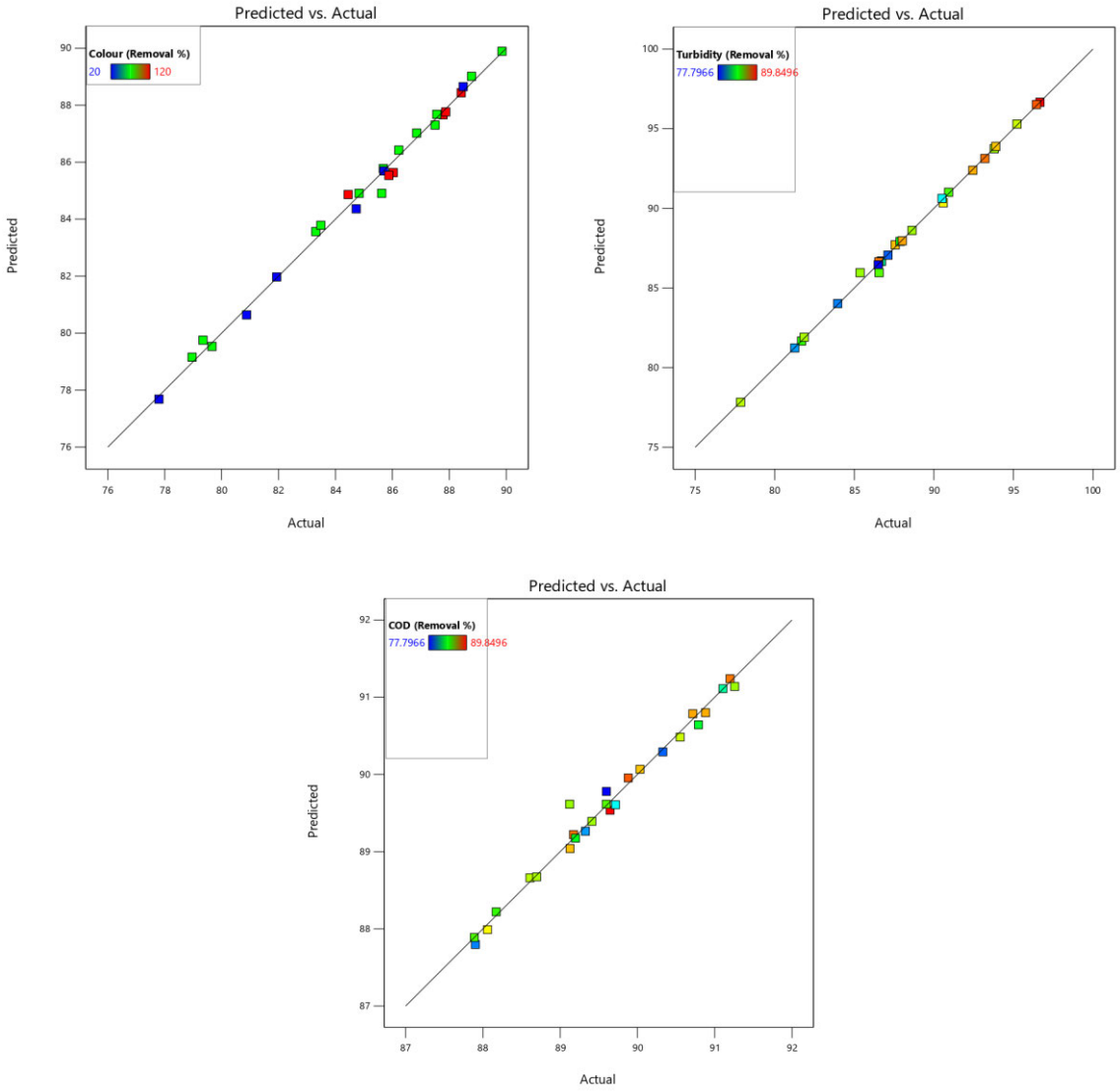

Figure 6-17: Graph showing actual vs predicted plot for (a) which represents colour, (b) representing turbidity and (c) representing COD

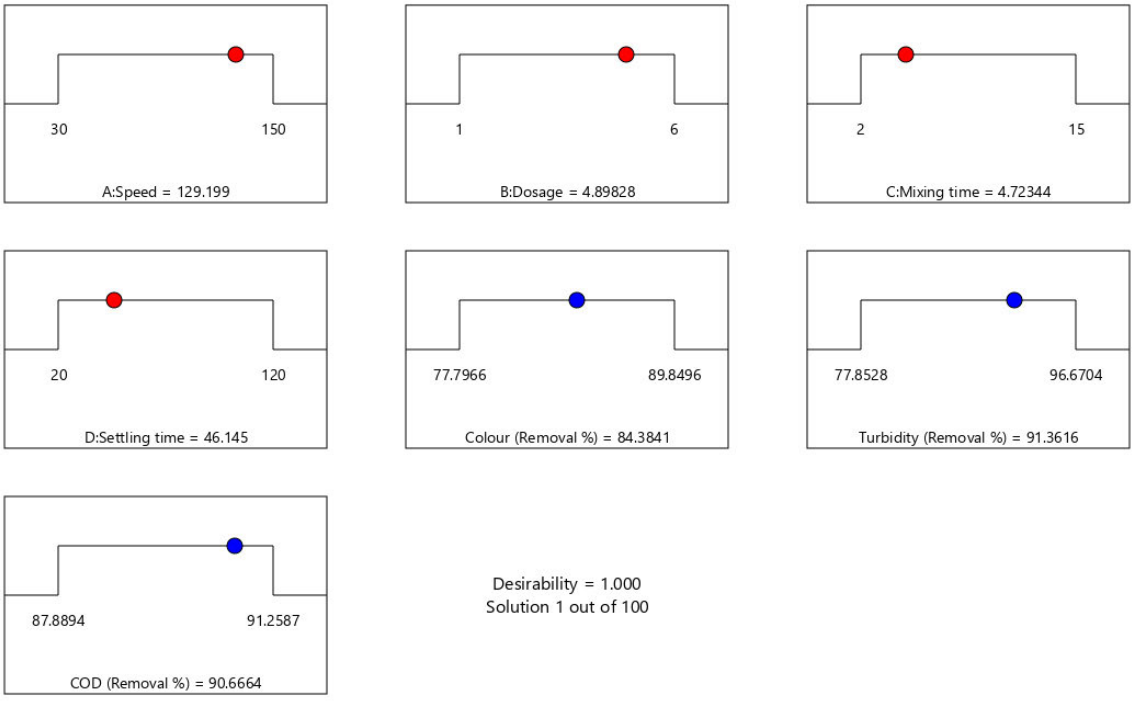

Figure 6-18: Plot showing the ramps of the optimum conditions of the coagulation process with a desirability of 100%

Table 6-13: Optimum conditions of CES for the coagulation system

Number	Speed	Dosage	Mixing time	Settling time	Colour (Removal %)	Turbidity (Removal %)	COD (Removal %)	Desirability	
1	**129.199**	**4.898**	**4.723**	**46.145**	**84.384**	**91.362**	**90.666**	**1.000**	**Selected**
2	90.000	6.000	2.000	70.000	79.154	87.063	90.292	1.000	
3	43.500	5.438	7.525	68.750	80.246	83.475	88.534	1.000	
4	90.000	1.000	8.500	20.000	85.694	88.613	89.393	1.000	
5	30.000	3.500	2.000	70.000	79.532	81.234	89.265	1.000	
6	90.000	3.500	2.000	20.000	81.971	86.667	91.112	1.000	
7	150.000	6.000	8.500	70.000	86.423	95.297	90.484	1.000	
8	90.000	1.000	8.500	120.000	87.764	87.959	90.786	1.000	
9	30.000	1.000	8.500	70.000	83.564	86.695	90.643	1.000	
10	150.000	3.500	15.000	70.000	89.013	96.517	89.954	1.000	

6.1.6 Calcined seashell – Coagulation system optimisation

Table 6-14: Table showing the actual vs predicted results of the matrix for colour, turbidity and COD percentage removal.

	Factor 1	Factor 2	Factor 3	Factor 4	Colour		Turbidity		COD	
Run	A: Speed	B: Dosage	C: Mixing time	D: Settling time	**Actual Value**	**Predicted Value**	**Actual Value**	**Predicted Value**	**Actual Value**	**Predicted Value**
1	30	3.5	8.5	20	79.66	79.35	89.50	89.61	53.58	53.76
2	30	3.5	8.5	120	80.51	80.85	91.99	92.44	50.56	50.54
3	150	3.5	8.5	20	92.09	91.83	98.05	98.00	55.06	55.22
4	90	3.5	8.5	70	87.83	86.88	97.15	97.42	52.60	52.29
5	150	6	8.5	70	95.66	95.92	99.55	99.54	58.06	57.98
6	90	6	15	70	92.37	92.48	99.49	99.63	55.56	55.39
7	90	6	2	70	83.62	83.67	97.65	97.92	60.81	61.16
8	150	3.5	2	70	88.55	88.37	96.20	95.92	62.56	62.33
9	90	3.5	15	120	84.75	84.27	95.80	95.44	55.31	55.36
10	90	1	15	70	81.36	81.39	96.21	96.34	59.21	59.00
11	30	3.5	2	70	78.08	77.93	91.83	91.72	53.50	53.28
12	90	1	8.5	20	82.49	82.70	95.16	95.21	53.25	53.39
13	90	3.5	2	20	79.68	80.19	93.22	93.24	59.17	58.90
14	150	3.5	8.5	120	92.24	92.64	97.84	98.14	54.30	54.26
15	30	6	8.5	70	81.79	82.08	94.85	94.52	52.48	52.36
16	90	1	8.5	120	85.88	86.15	98.61	98.49	54.48	54.48
17	30	1	8.5	70	78.81	78.58	90.52	90.20	54.81	54.68
18	90	3.5	8.5	70	85.93	86.88	97.69	97.42	51.98	52.29

19	90	6	8.5	20	90.58	90.20	99.25	99.30	57.19	57.27
20	90	6	8.5	120	89.40	89.07	99.11	98.99	52.07	52.01
21	90	3.5	2	120	87.57	87.37	98.78	98.62	55.58	55.66
22	90	1	2	70	84.38	84.35	96.35	96.62	55.83	56.14
23	90	3.5	15	20	88.91	89.14	98.02	97.85	56.58	56.29
24	150	1	8.5	70	89.27	89.01	99.29	99.28	54.35	54.25
25	150	3.5	15	70	92.94	92.98	99.44	99.48	54.13	54.43
26	30	3.5	15	70	79.10	79.16	89.37	89.59	57.96	58.28

Table 6-15: ANOVA fit statistics for colour, turbidity and COD

	colour	Turbidity	COD
Std. Dev.	0.5687	0.3302	0.3127
Mean	85.90	96.19	55.42
C.V. %	0.6620	0.3433	0.5643
R^2	0.9946	0.9954	0.9948
Adjusted R^2	0.9877	0.9895	0.9882
Predicted R^2	0.9736	0.9744	0.9717
Adeq Precision	41.6497	40.0452	49.6162

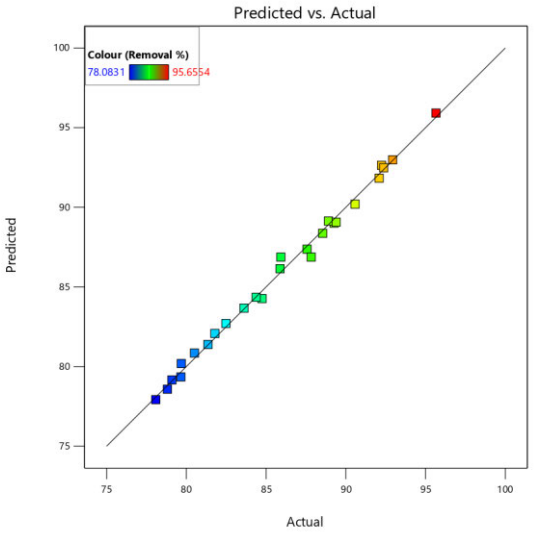

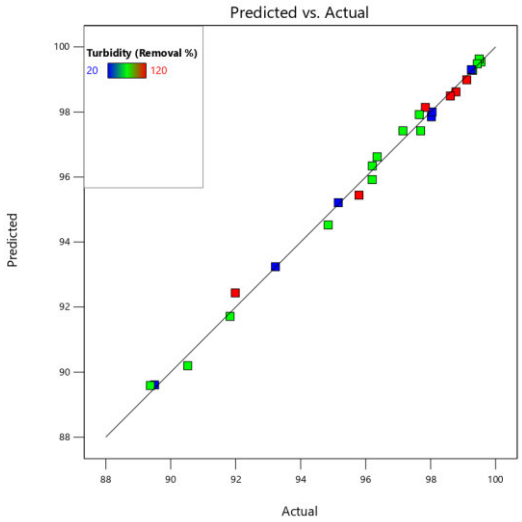

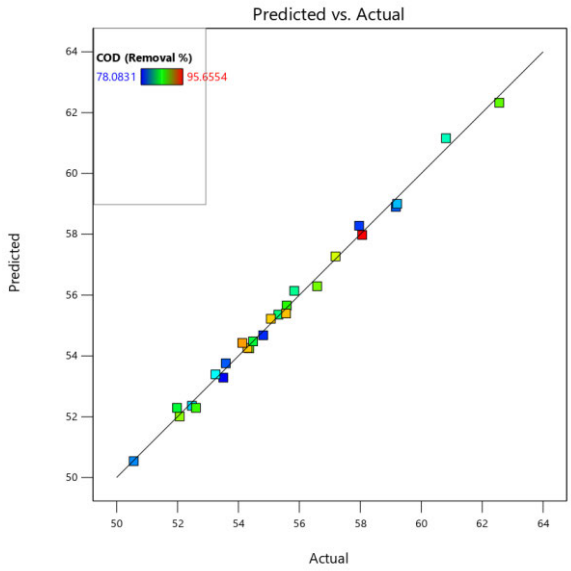

Figure 6-19: Graph showing actual vs predicted plot for (a) which represents colour, (b) representing turbidity and (c) representing COD

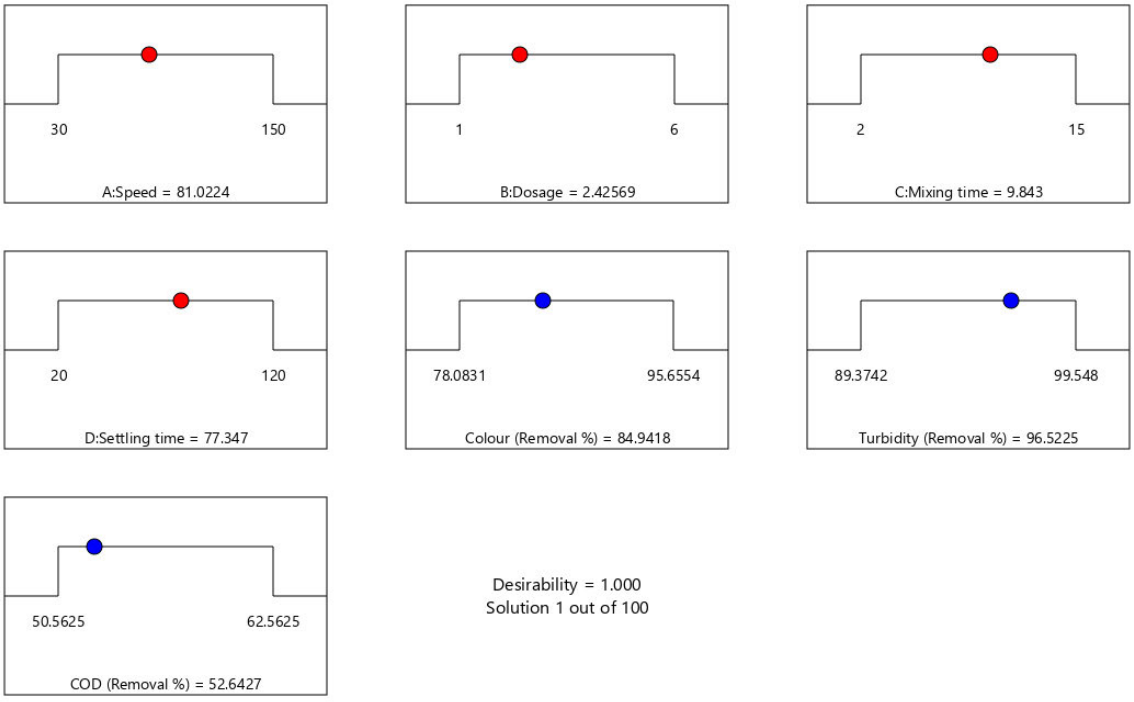

Figure 6-20: Plot showing the ramps of the optimum conditions of the coagulation process with a desirability of 100%

Table 6-16: Optimum conditions of CSS for the coagulation system

Number	Speed	Dosage	Mixing time	Settling time	Colour (Removal %)	Turbidity (Removal %)	COD (Removal %)	Desirability	

1	**81.022**	**2.426**	**9.843**	**77.347**	**84.942**	**96.523**	**52.643**	**1.000**	**Selected**
2	90.000	3.500	2.000	20.000	80.191	93.242	58.900	1.000	
3	30.000	6.000	8.500	70.000	82.080	94.525	52.361	1.000	
4	39.000	3.250	2.975	77.500	80.025	93.104	52.592	1.000	
5	90.000	3.500	15.000	120.000	84.268	95.442	55.360	1.000	
6	90.000	6.000	8.500	20.000	90.197	99.301	57.271	1.000	
7	90.000	1.000	2.000	70.000	84.352	96.621	56.140	1.000	
8	30.000	3.500	15.000	70.000	79.162	89.587	58.281	1.000	
9	30.000	3.500	8.500	20.000	79.350	89.606	53.756	1.000	
10	90.000	3.500	2.000	120.000	87.371	98.619	55.655	1.000	